Role of the Wnt/ -catenin Pathway in Liver Development and Zonation

Shen Wen, Yeh

Award date:
2012

Awarding institution:
University of Bath

Role of the Wnt/ β-catenin Pathway in Liver Development and Zonation

YEH, SHENG-WEN

A thesis submitted for the degree of Doctor of Philosophy

University of Bath

Department of Biology and Biochemistry

September, 2012

CONTENT

Content 1

List of figures and tables 10

Acknowledgements 14

Abstract 15

Abbreviations 17

Chapter 1 General Introduction 21

1.1 Liver development 22

1.2 Liver zonation 28

1.3 Wnt/β-catenin signalling pathway 34

1.4 Wnt/β-catenin signalling in liver development 38

1.4.1 The role of Wnt/β-catenin pathway in liver zonation 42

1.5 Transdifferentiation 45

1.5.1 The definition of transdifferentiation 45

1.5.2 Transdifferentiation of pancreas to liver 46

1.5.3 The Wnt pathway and hepatic transdifferentiation of pancreatic cells 52

1.6 Aims 53

Chapter 2 Materials and Methods 56

2.1 Materials 57

2.1.1 Mouse Lines 57

2.1.2 General chemicals, fixatives and buffers 57

2.1.3 Cell culture medium, reagents and exogenous factors 58

2.1.4 Markers for immunofluorescence cell staining 59

2.1.5 Primary and secondary antibodies used for staining tissue sections 60

2.1.6 Western blotting materials, reagents, primary and secondary antibodies 61

2.1.7 RNA extraction, reverse transcription (RT) and polymerase chain reaction (PCR) reagents and experimental conditions 62

2.1.8 Adenovirus (Ad) reagents, materials and kits 65

2.1.9 Other instruments.....66

2.2 Methods.....67

2.2.1 Cell culture.....67

2.2.1.1 Cell culture.....67

2.2.1.2 Cell culture maintenance.....67

2.2.1.3 Cell storage and revival.....68

2.2.1.4 Inoculation of cells.....68

2.2.2 Fractionation of liver tissue.....68

2.2.3 Western blotting.....69

2.2.4 Semi-quantitative RT-PCR.....70

2.2.5 Fluorescence microscopy and image processing.....70

2.2.6 *In situ* hybridization.....71

2.2.6.1 Mice and isolation of embryos.....71

2.2.6.2 RNA probe synthesis.....73

2.2.6.3 Tissue preparation 74

2.2.6.4 In situ hybridization on sections 74

2.2.7 Immunohistochemistry of mouse liver 75

2.2.7.1 Tissue Fixation, Embedding, and Processing 75

2.2.7.2 Immunohistochemical Analysis of Embryonic Mouse Liver 76

2.2.8 Embryonic mouse liver bud dissection 77

2.2.9 Embryonic culture of mouse liver buds 79

2.2.10 Adenoviral infections 79

2.2.10.1 Amplification of first-generation adenovirus 79

2.2.10.2 Further adenovirus amplification and dialysis 80

2.2.10.3 Rapid titre of adenovirus 81

Chapter 3 Expression profiling of hepatocyte markers and Wnt ligands and receptors during embryonic liver development 82

3.1 Background 83

3.2 Results....85

3.2.1 Expression of CPS and GS during development....85

3.2.2 Expression of β-catenin during development....90

3.2.3 Expression of Wnt pathway components during liver development....93

3.2.3.1 Wnt4....93

3.2.3.2 Wnt5a....93

3.2.3.3 Wnt5b....94

3.2.3.4 Wnt9b....94

3.2.3.5 Frizzled 1....95

3.2.3.6 Frizzled 2....95

3.2.3.7 LRP5....96

3.2.3.8 β-catenin....96

3.3 Discussion....114

Chapter 4 Conditional deletion of *Apc* during embryonic development perturbs the establishment of liver zonation 119

4.1 Background 120

4.2 Results 123

4.2.1 Effect of *Apc* deletion on zonation during development 123

4.2.2 *Apc* deletion enhances cell proliferation 124

4.2.3 Enhancement of the ductal phenotype following deletion of *Apc* 124

4.2.4 Characterization of the liver phenotype in *β–catenin*-deleted embryos 126

4.3 Discussion 135

Chapter 5 Directed differentiation of embryonic liver towards a periportal or perivenous-like phenotype by manipulating the Wnt/β-catenin pathway 139

5.1 Background 140

5.2 Results 141

5.2.1 Characterisation of the *in vitro* liver culture model 141

5.2.1.1 Characterization of the *in vitro* culture model 141

5.2.1.2 Optimization of adenoviral infection in cultured liver buds 142

5.2.1.3 Effect of modulators of the Wnt/β-catenin pathway on expression of periportal and perivenous markers in cultured embryonic liver 143

5.2.1.4 Challenges of monitoring CPS expression with Dex treated liver buds culture model 146

5.2.2 Enhanced maturation of embryonic liver in culture following treatment with ITS .. 147

5.2.2.1 Effect of ectopic Wnt1 and DKK1 on expression of CPS and GS in cultured embryonic mouse liver 148

5.2.2.2 Effect of TD114-2 and Quercetin on developing liver 148

5.2.2.3 Treatment of embryonic liver cultures with TD114-2 and Quercetin alters the expression of ammonia detoxifying enzymes 149

5.3 Discussion 168

Chapter 6 Molecular basis of the conversion of pancreatic AR42J-B13 cells to the hepatocyte phenotype 170

6.1 Background 171

6.2 Results 174

6.2.1 C/EBPβ and HNF4α are key components of the transdifferentiationof pancreatic cells to hepatocytes 174

6.2.1.1 Optimizing the infection efficiency of adenoviral vectors in pancreatic B13 cells 174

6.2.1.2 Ectopically expressed HNF4α and C/EBPβ induce morphological changes in pancreatic B13 cells 174

6.2.1.3 Ectopically expressed HNF4α and C/EBPβ induce a programme of hepatic gene expression 175

6.2.1.4 Ectopic expression of HNF4α and C/EBPβ induce hepatic protein expression 175

6.2.1.5 Analysis of time course effect of HNF4α and C/EBPβ on hepatic gene expression ・ 176

6.2.1.6 OSM does not enhance CEBPβ and HNF4α derived transdifferentiation 176

6.2.1.7 The role of histone deacetylase inhibitors in transdifferentiation.....176

6.2.2 Role of the Wnt/β-catenin signalling pathway on transdifferentiation of pancreatic cells to hepatocytes 178

6.2.2.1 Quercetin and TD114-2 179

6.2.2.2 DKK1 179

6.3 Discussion 195

Chapter 7 Final discussion and future prospects 198

Reference 203

LIST OF FIGURES AND TABLES

Figure		Page
Figure 1.1	Early stages of embryonic liver development	27
Figure 1.2	Schematic diagram of the microanatomical unit of the liver	33
Figure 1.3	Overview of canonical Wnt signalling pathway	36
Figure 2.1	Steps in the dissection of liver bud from E11.5 mouse embryos	78
Figure 3.1	Expression of GS and CPS during embryonic development	86
Figure 3.2	CPS protein starts to be expressed in liver around E13.5 days of mouse development	87
Figure 3.3	GS is expressed in liver of mouse embryos between E17.5 and E18.5	88
Figure 3.4	Regional distribution of GS and CPS in the liver of an E18.5 mouse embryo	89
Figure 3.5	Expression of β-catenin in the developing mouse liver	91
Figure 3.6	β-catenin becomes activated between E17.5 and E18.5	92
Figure 3.7	*Wnt4* expression started from E14,5 during mouse liver development	99
Figure 3.8	*Wnt5a* expressed in frontonasal region during mouse development	101
Figure 3.9	*Wnt5b* expressed throughout E11.5 to E18.5 in developing mouse liver	103
Figure 3.10	Expression of *Wnt9b* was restricted in E11.5 and E12.5 during mouse liver development	105
Figure 3.11	Expression pattern of *Fzd1* during mouse liver development	107
Figure 3.12	*Fzd2* did not express in developing mouse liver	109
Figure 3.13	*Lrp5* expressed in mouse liver during E11.5 to E13.5	111
Figure 3.14	Robust *β-catenin* expression during E11.5 to E13.5 in mouse liver	113
Figure 4.1	Changes in the expression of CPS and GS in in embryonic liver following conditional deletion of Apc.	128
Figure 4.2	Deletion of Apc at different stages of development results in a change in the expression of periportal and perivenous hepatic markers.	129
Figure 4.3	Proliferative markers are increased in *Apc*-deficient liver	130
Figure 4.4	Haematoxylin and eosin analysis in embryonic livers following β-NF induction of $AhCre^{+}Apc^{fl/fl}$.	131
Figure 4.5	Deletion of *Apc* induces changes in hepatic ductal morphogenesis.	132
Figure 4.6	Activation of Notch pathway downstream target genes in *Apc* deleted embryonic livers	133

Figure 4.7	Deletion of β-catenin results in a down-regulation in perivenous gene expression. Complementary changes in the perivenous genes in embryonic livers after β-NF induction of *AhCre*$^{+}$ *β-catenin*$^{fl/fl}$.	134
Figure 5.1	Morphological changes in mouse embryonicliver buds cultured in the presence of Dexamethasone	151
Figure 5.2	Time course of GS expression in embryonic liver buds maintained in culture	153
Figure 5.3	Cultured liver buds are amenable to adenoviral infection	154
Figure 5.4	Adenovirus infects both E-cadherin-positive and negative embryonic liver cells	155
Figure 5.5	Adenoviral infection of Wnt1 and Wnt5a induces GS expression in cultured liver buds	156
Figure 5.6	Adenoviral infection of β-catenin or treatment with TD114-2induces GS expression in cultured embryonic liver buds	157
Figure 5.7	Ectopic DKK1 expression suppressed GS in cultured embryonic liver buds	158
Figure 5.8	*GS* gene expression is associated with Wnt/β-catenin pathway manipulation	159
Figure 5.9	CPS expression is induced in embryonic liver cultures following Dex treatment	160
Figure 5.10	Dex treatment induces *Cps* expression in liver bud explants	161
Figure 5.11	Time course of *Gs* and *Cps* gene expression in ITS-treated liver cultures	162
Figure 5.12	Adenoviral expression of Wnt1 and DKK1 induces complementary changes in Cps and Gs in ITS-treated liver buds	163
Figure 5.13	Morphological changes in mouse embryonic liver buds culture with TD114-2.	164
Figure 5.14	Morphological changes in liver buds following culture with Quercetin	165
Figure 5.15	Quercetin and TD114-2 induce complementary changes in periportal and perivenous genes in cultured embryonic liver buds	167
Figure 6.1	Morphological changes in pancreatic cells B13 following infection Ad-C/EBPβ and/or Ad-HNF4α	181
Figure 6.2	Expression of C/EBPβ and HNF4α in B13 cells following adenoviral infection	182
Figure 6.3	Ectopic expression of C/EBPβ and HNF4α induces hepatic transdifferentiation of pancreatic B13 cells	183
Figure 6.4	C/EBPβ and HNF4α induces AFP protein expression in B13 cells	184
Figure 6.5	Albumin protein was induce in B13 cells after ectopic C/EBPβ and HNF4α	185

Figure 6.6	C/EBPβ and HNF4α induce E-cadherin protein expression in B13 cells	186
Figure 6.7	Ectopic C/EBPβ and HNF4α induce Transferrin protein expression in B13 cells	187
Figure 6.8	Ectopic C/EBPβ and HNF4α induce CPS protein expression in B13 cells	188
Figure 6.9	Time course of expression of hepatocyte markers following adenoviral infection of C/EBPβ and HNF4α	189
Figure 6.10	OSM did not enhance C/EBPβ and HNF4α –induced hepatic transdifferentiation of pancreatic B13 cells	190
Figure 6.11	C/EBPβ and HNF4α directed transdifferentiation of pancreatic B13 cells to hepatocytes was not altered by the addition of inhibitors of histone deacetylase	191
Figure 6.12	Inhibition of Tcf/Lef activity alone does not stimulate transdifferentiation	192
Figure 6.13	Quercetin and TD114-2 do not stimulate transdifferentiation of pancreatic B13 cells to hepatocyte-like cells	193
Figure 6.14	Ectopic expression of DKK1 does not stimulate hepatic transdifferentiation of pancreatic B13 cells	194

Table		Page
Table 1-1	Reactions of the urea cycle	30
Table 1-2	Summary of the Wnt ligands, receptors and antagonists	37
Table 2-1	List if reagents used for immunostaining	58
Table 2-2	Composition of medium used for cell culture	58
Table 2-3	List of primary antibodies used for immunofluorescence cell staining	59
Table 2-4	List of secondary antibodies used for immunofluorescence cell staining	60
Table 2-5	List of primary antibodies used for immunohistochemistry staining	60
Table 2-6	List of chemicals used for western blotting	61
Table 2-7	List of primary antibodies used for western blotting	62
Table 2-8	List of chemicals used for RNA extraction and RT-PCR	62
Table 2-9	List of PCR primers	64
Table 2-10	List of adenoviral vectors used for gene transduction	65
Table 2-11	List of other general instruments	66
Table 2-12	Riboprobes for *in situ* hybridization	73
Table 3-1	Target mRNAs for *in situ* hybridization	84
Table 3-2	Summary of results of *in situ* hybridization	117
Table 4-1	Study design of β-NF injection induced *Apc* deletion in embryonic mouse liver	122
Table 4-2	The proteins involved in each type of metabolic zonation	122

ACKNOWLEDGEMENTS

I would like to express my gratitude to all those who gave me the possibility to complete this thesis. I want to thank the Department of Biology and Biochemistry for giving me permission to commence this thesis, to do the necessary research work and to use departmental facilities.

I am deeply indebted to my supervisor Professor David Tosh whose help, stimulating suggestions and encouragement helped me in all the time of research and writing of this report. I have furthermore to thank Dr. Zoë Burke for sharing valuable ideas and suggestions to my experiments.

I want to thank all members in Lab. 0.62 for all their help, support, interest, valuable hints, coffee, tea and dipped biscuits. I also wish to say “Thank you, Gaby. I know you can hear me” and share this thesis with her. I would also like to thank my dear family and friends for their thoughtfulness and encouragement.

ABSTRACT

Understanding normal liver development is critical for the production of cell therapies for treating liver disease and also for the construction of *in vitro* liver models. During the progress of the research described in this thesis I specifically addressed the role of the Wnt/β-catenin pathway in liver development and also the effect of ectopic expression of liver-enriched transcription factors on the conversion of pancreatic cells to hepatocyte-like cells.

The Wnt pathway is known to play a critical role in the maintenance of the zonation of ammonia metabolizing enzymes in the adult liver. Herein we determined the spatiotemporal role of the Wnt/β-catenin pathway in the development of zonation in embryonic mouse liver. We initially examined the expression of Wnt ligands (Wnt4, Wnt5a, Wnt5b and Wnt9), receptors (Frizzled1, Frizzled2 and LRP5) and two hepatic zonation markers, the periportal marker and urea cycle enzyme carbamoylphosphate synthetase (CPS) and the perivenous enzyme Glutamine synthetase (GS) at different stages of liver development by *in situ* hybridization, immunohistochemistry and western blotting. We observed temporal changes in the Wnt signalling molecules. In addition, we found that CPS became expressed between E14.5 and E15.5 and gradually the number of cells expressing the enzyme increased during development. Nuclear β-catenin and GS were expressed between E17.5 and E18.5 of liver development in a complementary fashion to the CPS-expressing cells.

In order to examine the effect of activating the Wnt/β-catenin pathway during liver development, conditional deletion of *Apc* was induced at different time points during liver development and the expression of periportal and perivenous hepatocyte and ductal markers determined by PCR and immunohistochemical techniques. Conditional loss of *Apc* resulted in the expression of nuclear

β-catenin throughout the developing liver. This was accompanied by a reduction in the expression of CPS and up-regulation of GS expression. When Apc loss was induced at around E16.5 and liver samples were collected at E18.5, we also observed an upregulation of the ductal phenotype.

To extend these studies we examined the direct role of the Wnt/β-catenin pathway on development of liver zonation regulation by infecting *in vitro* cultures of embryonic mouse livers with adenoviral vectors expressing Wnt1 and Wnt5a. The results demonstrated that ectopic expression of Wnt1 and Wnt5a enhances the perivenous phenotype.

Transdifferentiation is the conversion of one differentiated cell type to another and a number of *in vitro* models have been developed for converting pancreatic cells to hepatocytes, including culturing the rat pancreatic amphicrine call line AR42J-B13 (B13) with synthetic glucocorticoid dexamethasone (Dex). CCAAT-enhancer binding proteins (C/EBP)-β has been identified as part of the molecular basis of the switch however it did not cause the same degree of morphological flattening as Dex. To test the role of hepatic nuclear factor (HNF4)-α in Dex induced transdifferentiation, we co-expressed C/EBPβ and HNF4α in B13 cells by using adenoviral infection. The results showed that ectopic expressed HNF4α and C/EBPβ could induce the expression of hepatic genes and morphological changes of B13 cells reminiscent of hepatocytes.

ABBREVIATIONS

ALB	Albumin
AFP	Alpha-fetoprotein
APC	Adenomatous polyposis coli
AhCre	Acryl Hydrocarbon receptor
Ad	Adenovirus
BCL9	B cell lymphocyte 9
BOP	N-nitrosobis(2-oxopropyl)amine
BEC	Biliary epithelial cells
C/EBP	CCAAT/enhancer binding protein
CPS	Carbamoylphosphate synthetase I
CaMKII	Calcium/calmodulin-dependent kinase II
CBP	CREB binding protein
CK	cytokeratin
Cre	Causes recombination
CMV	cytomegalovirus
Cx	Connexin
DKK	Dickkopf
DAB	3,3’-diaminobenzidine
DAPI	4,6-diamidino-2-phenylindole dihydrochloride
DEPC	diethylpyrocarbonate
DMSO	dimethylsulfoxide

DNA	Deoxyribonucleic acid
DMEM	Dulbecco’s modified Eagle’s medium
DTT	dithiothreitol
Dsh	Dishevelled
Daam1	Dishevelled-associated activator of morphogenesis 1
Dex	dexamethasone
EDTA	ethylenediaminetetraacetic acid
EGF	epidermal growth factor
eGFP	enhanced green fluorescent protein
FBS	foetal bovine serum
FGF	fibroblast growth factor
Fox	forkhead box
GATA	GATA-binding protein
Gck	Glucokinase
GFP	green fluorescent protein
GSK3β	glycogen synthetase kinase 3β
GLP-1	glucagon-like peptide-1
HEPES	4-(2-Hydroxyethyl)piperazine-1-ethanesulfonic acid
Hes1	hairy and enhancer of split 1
HMG	high mobility group
HRP	horse radish peroxidase
HDAC	Histone deacetylase
HNF	hepatocyte nuclear factor

IRES	internal ribosome entry site
JNK	Jun N-terminal kinase
Jag1	jagged 1
Kras	Kirsten rat sarcoma
KGF	Keratinocyte growth factor
LAP	liver activating protein
LIP	liver inhibitory protein
LEF	Lymphocyte enhancer factor
LRP	lipoprotein receptor-related protein
LoxP	locus of X-over P1
MOI	multiplicity of infection
NBT/BCIP	nitro-blue tetrazolium and 5-bromo-4-chloro-3'-indolyphosphate
Ngn3	neurogenin 3
NICD	Notch intracellular domain
NFAT	Nuclear factor of activated T cells
NLK	Nema-like kinase
PBS	phosphate-buffered saline
PBS-T	phosphate-buffered saline-Tween 20
PCNA	proliferating cell nuclear antigen
PCR	polymerase chain reaction
Pdx1	Pancreatic and duodenal homeobox 1
PKC	Protein kinase C

PCP	planar cell polarity
PLC	Phospholipase C
Prt	Prometheus
PVDF	polyvinylidene fluoride
RNA	ribonucleic acid
RSV	Rous sarcoma virus
RT-PCR	reverse transcriptase-polymerase chain reaction
sFRPs	secreted Frizzled-related proteins
SDS	sodium dodecyl sulphate
siRNA	short interference ribonucleic acid
Sox	SRY-box containing gene
SSC	Saline sodium citrate
TCF	T-cell factor
TCDD	2,3,7,8-tetrachlorodibenzo-p-dioxin
TGF	transforming growth factor
TSA	trichostatin A
UGT	UDP- glucuronosyltransferase
Wntless	Wls

CHAPTER 1 GENERAL INTRODUCTION

1.1 Liver development

The liver is the largest gland in the body and exhibits both endocrine and exocrine properties. The endocrine functions include the secretion of several hormones including insulin-like growth factor I and II, angiotensinogen and thrombopoietin, while the major exocrine secretion of the liver is in the form of bile. The liver is also responsible for detoxification and metabolism of drugs and toxins and their subsequent elimination and the regulation of intermediary metabolism through the co-ordinated regulation of carbohydrate, fat and protein metabolism (Haubrich et al., 1995; Zakim and Dannenberg, 1990).

The principal functional cell type of the liver is the parenchymal hepatocyte, which accounts for 78% of volume in the rat liver (Blouin et al., 1977). The hepatocyte is a polarized epithelial cell with apical and basolateral surfaces. The basolateral surface faces onto the sinusoids. Sinusoids are the blood vessels that supply the hepatocytes and are lined by endothelial cells. The hepatocyte does not have a basement membrane instead there is a space between the basolateral surface of the hepatocyte and the sinusoidal endothelial cell. Moreover, the basement membranelike extracellular matrix (ECM) underlying sinusoidal endothelial cells have a low-density structure that minimally impedes sinusoid-hepatocyte exchange (Hahn et al., 1980; Kmiec, 2001). This arrangement facilitates the endocrine-like function of the liver, which is to condition the venous blood, received from the digestive tract, through secretion of plasma proteins and removal of toxic products. The apical surface of the hepatocyte forms the bile canaliculus, the smallest branch of the biliary tree. Tight junction proteins, including occludin, claudin and ZO-1, seal the apical domains of two adjacent hepatocytes, helping to create the bile canaliculus (Vinken et al., 2006). Biliary epithelial cells

(cholangiocytes), sinusoidal endothelial cells, hepatic stellate cells (Ito cells), Kupffer cells, and pit cells (liver-specific natural killer cells) represent the majority of non-hepatocyte (non-parenchymal) cell types in the liver. Hepatocytes and biliary epithelial cells originate from a common precursor, the hepatoblast that derives from the definitive endoderm (Douarin, 1975).

The parenchymal cells of the liver derive from the anterior portion of definitive endoderm which emerges from the primitive streak to displace the extra embryonic endoderm of the yolk sac at around mouse embryonic day 7 (Tremblay and Zaret, 2005).

Prior to specification (at mouse embryonic day (E) 8.25, 3-4 somite stage), there are three distinct fated domains of hepatic progenitor cells that are located in the medial and bilateral regions of the foregut (Figure 1.1A) (Tremblay and Zaret, 2005). Hepatic differentiation begins in the ventral foregut endoderm immediately after the endothelium interacts with cardiac mesoderm, around the 6 somite stage of embryogenesis (E8-8.5) [Figure 1.1B (a)]. During foregut closure, the medial and lateral domains come together (Figure 1.1A, green arrows) as the hepatic endoderm is specified. The progenitor cells within these regions converge to lie adjacent to the developing heart and in close position to regions of lateral plate mesoderm that will ultimately generate the mesothelial cells of proepicardium and septum transversum (LeDouarin, 1975(Medlock and Haar, 1983) The newly specified cells then proliferate within the epithelial layer, while morphogenetic extension of the foregut pulls the hepatic endoderm away from the heart region, towards to the midgut [Figure 1.1B (b)]. It is at this time that a family of transcription factors, the Foxas (previously known as hepatocyte nuclear factor (HNF) 3) (Dufort et al., 1998), specifies the endoderm to express hepatic genes. Foxa proteins are considered to function as ‘pioneer proteins’ in that they attach early on during development to silent (hypoacetylated) chromatin (Zaret, 1999). This enables competence that will allow the

attachment of other liver-specific transcription factors and the subsequent induction of hepatic pattern of gene expression (Cirillo et al., 2002). A subclass of GATA zinc-finger transcription factors (GATA4) also has a pioneer role in liver-specific gene expression (Bossard and Zaret, 1998). The presence of both Foxa and GATA persists up to E11.5 acting together as potentiators of hepatic fate by generating a receptive chromatin structure that surrounds 'hepatic' enhancers (Cirillo et,al, 2002). The change in chromatin structure allows the enhancers to be occupied by other transcription activators such as CCAAT/enhancer-binding protein (C/EBP) and nuclear factor 1 (NF1) subsequently activating the albumin promoter (Block et al., 2003; Cirillo et al., 2002).

Around embryonic day 9 (10–12 somite stage), the liver epithelial cells proliferate and migrate in a cord-like fashion into the mesenchyme of septum transversum, and at this stage of development the liver bud can be seen as an outgrowth of hepatoblasts (Perez-Pomares et al., 2004)[Figure 1.1B (C)]. The hepatoblasts in the liver bud are bipotential, giving rise to both hepatocytes and bile duct epithelial cells (BEC). The septum transversum mesenchyme contributes endothelial cells and stellate cells that form and line the sinusoids (Gouysse et al., 2002). The hepatic vasculature develops as the liver bud grows. Vasculogenic endothelial cells and nascent vessels are critical for liver morphogenesis and will ultimately help establish the cellular architecture that is important for normal liver function (Matsumoto et al., 2001). By embryonic day 10.5, the liver is the main site of haematopoietic and ultimately well over 50% of the liver mass by mid-gestation is made-up of haematopoietic cells (Shiojiri and Sugiyama, 2004).

Studies indicated that fibroblast growth factor 1 (FGF1) and FGF2, by themselves, could initiate hepatic development of the ventral endoderm (Jung et al., 1999). In addition to FGFs, bone morphogenic proteins (BMPs, members of the TGF-β superfamily) also contribute to the induction

of hepatogenesis. BMPs are produced at high levels in the septum transversum, suggesting that these mesenchymal cells are also required for the commitment of foregut endoderm to a hepatic fate (Rossi et al., 2001). Recent studies demonstrated that BMPs, TGF-β signalling formed dynamic inductive network regulated the formation of pancreas and liver progenitors (Wandzioch and Zaret, 2009). Flexibility in hepatic programming, in that the prospective lateral hepatic progenitors receive FGF signalling prior to that for BMP, whereas the prospective medial hepatic progenitors receive BMP signalling prior to that for FGF has been suggested. Regardless of this marked difference, descendants of both progenitor cell types activate *Afp* and *Hnf4* in the nascent liver bud (Wandzioch and Zaret, 2009).

During the perinatal period, numerous changes take place in the liver. Haematopoiesis , which is a major function of the fetal liver, declines dramatically as haematopoietic stem cells migrate to the bone marrow (Johnson and Moore, 1975). Hepatoblasts, which are highly proliferative in the fetal period, become quiescent. As expected, many cell cycle regulated genes are silenced during this period. In addition, a number of liver-enriched genes such as *Afp and H19* are silenced at birth (Spear et al., 2006). In contrast, many enzymes, including those involved in intermediary metabolism and detoxification must be induced (Callikan and Girard, 1979). The lobular architecture of the liver is established during the perinatal period, along with zonal control of gene expression (Notenboom et al., 1996).

The hematopoietic system is established at specific sites in the embryo through a succession of developmental programs that result in the generation of distinct precursor colony-forming cells (CFC) that in turn produce all the differentiated blood cells that enter the circulation. The first hematopoietic cells in the mouse embryo arise in blood islands that form from extraembryonic

mesoderm at the neural plate stage of development at embryonic day 7.5 (E7.5) (Haar and Ackerman, 1971). These primitive erythroblasts derived from the yolk sac represent the predominant mature blood cells in the early circulation and differ from erythrocytes derived later from the fetal liver and bone marrow. Primitive erythroblasts are large, nucleated cells that synthesize embryonic globins (Barker, 1968; Steiner and Vogel, 1973). Definitive erythropoiesis is established in the liver beginning at 28-32 somite pairs (E9.5)(Houssaint, 1981), and results in the generation of small, enucleate erythrocytes that synthesize the adult forms of globin. In contrast to the yolk sac's restricted hematopoiesis, fetal liver hematopoiesis is multilineage and includes the differentiation of definitive erythroid, myeloid, megakaryocyte and lymphoid cells (Moore and Metcalf, 1970). Guo and colleagues found that E11.5-E14.5 corresponds to a fetal liver hematopoietic expansion phase with distinct molecular features, including the expression of KRAB (Kruppel-associated box)-containing zinc finger proteins which are known to affect bone marrow hematopoiesis (Guo et al., 2009). Late in fetal life, hematopoietic activity initiates in the bone marrow which, shortly after birth, becomes the predominant site of blood cell production for the duration of postnatal life. Previous studies indicated an important role of Wnt signalling in regulating hematopoiesis during mammalian development (Staal and Clevers, 2005). Expression of Fz5, Wnt5a and Wnt10b has been found in both mouse embryonic yolk sac and fetal liver. Mice homozygous for a null mutation of Fz5 die at E10.75 due to defect of yolk sac angiogenesis and reduced proliferation of endothelial cells in the yolk sac can be observed at earlier stages (Ishikawa et al., 2001). Wnt10b was also found to be expressed by murine fetal liver hematopoietic progenitors (Austin et al., 1997). The progenitor cell populations can be expanded greatly in vitro by adding of Wnt1-, Wnt5a- or Wnt10b-conditioned media.

A

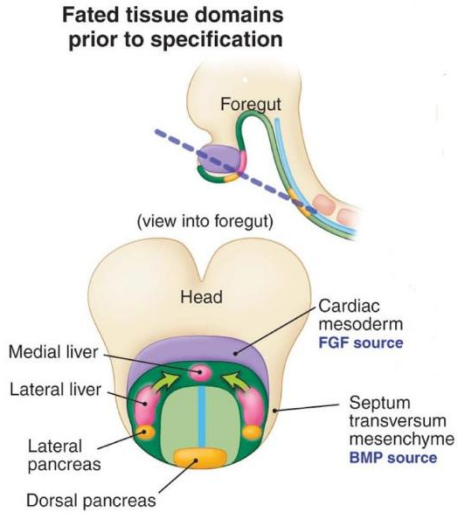

B

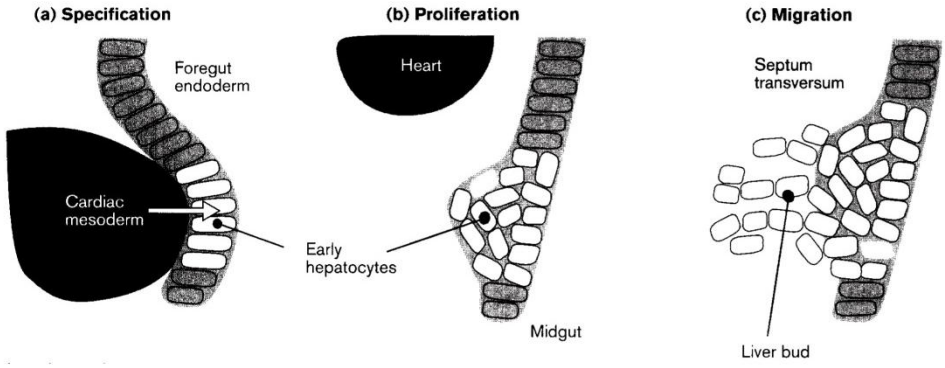

Figure 1.1 Early stages of embryonic liver development

A. Fate map of cell domains before tissue induction (mouse embryos at 3-4 somites stage or E8.25). Green arrows indicate movement of lateral progenitor regions toward the ventral-medial region.

B. Formation of the liver bud. (a) In about 6 somites stage embryo, cardiac mesoderm induces (arrow) the foregut endoderm to activate liver specific genes (white blocks). (b) As the mesoderm is pulled towards the midgut during gut closure, the early hepatocytes begin to proliferate within endoderm layer. (c) The early hepatocytes migrate into a region of loose mesenchyme (referred to as the septum transversum). The early hepatocytes then coalesce around the sinusoids in the mesenchyme, forming the liver organ (Zaret, 1998; Zaret and Grompe, 2008).

1.2 Liver zonation

Establishment of the lobular liver architecture during the perinatal period is accompanied by zonal gene regulation. This compartmentalization of function is determined by the position of hepatocytes within the lobule, the microanatomical organization of the smallest functional unit of the liver (Braeuning et al., 2006; Jungermann and Katz, 1989). The unit is divided into three zones: the periportal zone, which surrounds the afferent vessel and portal triad and receives blood rich in oxygen and nutrients, the intermediate zone, which surrounds the periportal zone and finally the outer, perivenous zone (Figure 1.2). The expression of key rate-limiting enzymes are heterogeneously distributed across the lobule with some liver enzymes bring more highly expressed in periportal regions whereas other enzymes are preferentially expressed in pericentral regions. For example, the activities of key rate-limiting enzymes for some pathways e.g. gluconeogenesis (glucose-6-phosphatase) are higher in the periportal zone whereas the activities of other enzymes e.g. glycolytic (glucokinase) enzymes are higher in the perivenous zone (Katz et al., 1977). Consequently, most of the major hepatic functions exhibit differences in activity within the periportal and perivenous zones. For example, metabolism of drugs and xenobiotics also display well defined zonation (Lindros, 1997), The cytochrome P450 system is responsible for the conversion of xenobiotics into more readily excretable products. This involves monooxygenation followed by conjugation with either glucuronic acid or sulfuric acid. Monooxygenation mainly occurs in the perivenous zone, with glucuronidation as the major conjugation reaction in these cells, whereas sulfotransferase which are involved in sulfation showed heterogeneous expression in periportal and perivenous hepatocytes (Buhler et al., 1992; Lindros, 1997; Tosh et al., 1996). Other zonated processes include: lipid metabolism, with lipogenesis occurring perivenously and fatty-acid

degradation periportally (Braeuning et al., 2006); Cyp7a1-mediated synthesis of bile acids derived from cholesterol, showing clear perivenous zonation (Berkowitz et al., 1995); and the metabolism of several amino acids, the catabolism of histidine and serine being mostly periportal, and glutamine synthesis (associated with ammonia detoxification) being perivenous.

While the gradients of function mentioned above are pronounced, perhaps the most striking example of zonation is observed in the enzymes and pathways of ammonia detoxification. The liver contains two systems for the removal of ammonia: the urea cycle and the enzyme glutamine synthetase (GS).

The urea cycle (Table 1-1) is a cycle of biochemical reactions occurring in many animals that produces urea $CO(NH_2)_2$ from ammonia (NH_3). This cycle was one of the first metabolic cycles to be discovered by Hans Krebs and Kurt Henseleit in 1932. In mammals, the urea cycle takes place only in the liver. The urea cycle consists of five reactions - two mitochondrial and three cytosolic. The cycle converts two amino groups, one from $NH4^+$ and one from Aspartate, and a carbon atom from HCO_3^-, into the relatively nontoxic excretion product, urea, at the cost of four "high-energy" phosphate bonds (3 ATP molecules are hydrolyzed to 2 ADP molecules and one AMP molecule). Ornithine (Orn) is the carrier for the carbon and nitrogen atoms.

Carbamoylphosphate synthetase I (CPS) is the rate-limiting enzyme in the urea cycle, a well-studied example of periportal expression (Dingemanse et al., 1996). The combined capacity of the urea cycle and glutamine synthetase (GS) systems allows the liver to effectively regulate blood ammonia level within narrow limits. Glutamine synthetase catalyses the ATP-dependent formation of glutamine from glutamate and ammonia: Glutamate + ATP + NH_3 → Glutamine + ADP + phosphate + H_2O

Table 1-1 Reactions of the urea cycle

Step	Reactant	Product	Catalyzed by	Location
1	$2ATP + HCO_3^- + NH_4^+$	Carbamoyl phosphate + 2ADP + Pi	CPS1	mitochondria
2	Carbamoyl phosphate + Ornithine	Citrulline + Pi	OTC	mitochondria
3	Citrulline + Aspartate + ATP	Argininosuccinate + AMP + PPi	ASS	cytosol
4	Argininosuccinate	Arginin + Fumarate	ASL	cytosol
5	Arginin + H_2O	Ornithine + Urea	ARG1	cytosol

Enzymes in the urea cycle: Carbamoylphosphate synthetase (CPS1), Ornithine transcarbamoylase (OTC), Argininosuccinate synthetase (ASS), Argininosuccinate lyase (ASL) and Arginase 1 (ARG1)

As blood ammonia levels in the blood accumulate (e.g. during hyperammonemic conditions arising from diseases such as liver failure and inborn errors of the urea cycle) the levels in the brain also increase reaching toxic levels (Cooper and Plum, 1987). Ammonia is a metabolite which is mostly produced within the gut during protein digestion and deamination. The urea cycle within the liver regulates the concentration of ammonia in the systemic circulation maintaining blood ammonia levels in the 50–100 μM range. Therefore, reduced hepatic capacity for ammonia removal leads to hyperammonemia which is a metabolic disturbance characterised by an excess of ammonia in the blood may lead to increased levels of brain ammonia and consequently a spectrum of central nervous system dysfunction and encephalopathy including impaired memory, shortened attention span, sleep-wake inversions, brain oedema, intracranial hypertension, seizures, ataxia and coma. During liver failure, brain ammonia concentrations can reach 1-5mM. Many deaths of patients with liver failure occur due to neurological complications such as brain oedema, increased intracranial pressure and brain stem herniation. These symptoms have been demonstrated to be related to

arterial ammonia concentrations in both clinical (Bernal et al., 2007; Bhatia and Mihas, 2006) and animal studies (Jover et al., 2006; Sen et al., 2006).

Several models have been proposed to account for zonal regulation in the adult liver. The differentiation model proposes that expression of genes is dependent on the developmental status of the hepatocyte (Sigal et al., 1992). This model suggests that liver is organized with three compartments: a slow cycling stem cell compartment; an amplification compartment with cells rapidly proliferating in response to regenerative stimuli; and a terminal differentiated cell compartment. The developmental status of cells along the portocentral axis dictates the gene expression, and is based on evidence that putative hepatic stem cells exist in portal triads and those hepatocytes adjacent to the portal triads are the least differentiated, whereas hepatocytes around the central veins are terminally differentiated. The various compartments positioned in a polarized organization are associated with a gradient in the chemistry of extracellular matrix, gene expression, pharmacological and toxicological response. A support of the differentiation model is the Streaming Liver Hypothesis (Zajicek et al., 1985). Here, the hepatic stem cells become more differentiated as they migrate from the portal region towards the central veins. While there is evidence that hepatic stem cells exist in the portal regions, strong experimental data argues that neither the developmental nor streaming models can account for all zonal gene regulation (Bralet et al., 1994). It has also been suggested that cell-cell or cell-matrix interactions could account for zonal patterns of expression (Kuo and Darnell, 1991). For example, by observation of GS mRNA expression during the regeneration after surgical removal of two-third of the liver and the treatment with carbon tetrachloride which specifically kills pericentral hepatocytes, only hepatocytes resumed contact with pericentral veins were the high level of GS transcription restored. Therefore interactions between

central vein endothelial cells and pericentral hepatocytes were suggested to be account for GS expression. While this model might explain expression of GS, it is hard to envisage how this mechanism could account for other zonal gene expression. It has also been proposed that the directional flow of blood along the sinusoids in a portocentral direction could govern zonal gene expression (Jungermann and Kietzmann, 1996). Blood enters the portal triad rich in oxygen, nutrients and hormones. The concentration of these substances changes as blood flows towards the central veins. Although blood-borne molecules may account for zonal regulation these have not yet been firmly identified, this remains the most widely accepted model to account for position-dependent gene expression. As pointed out by Lamers and colleagues (Christoffels et al., 1999), gradual changes in regulatory molecules could account for both gradient (gradual) and compartment (well-defined) patterns of expression, depending on how the extracellular stimuli are integrated into the transcriptional machinery that lead to zonal control. Recently, a role of Wnt/β-catenin signalling pathway in maintenance of hepatic zonation in adult mice has been established (Benhamouche et al, 2006; Burke et al, 2009). Further details of the role of the Wnt/β-catenin signalling pathway in maintenance of hepatic zonation will be discussed in 1.4.1.

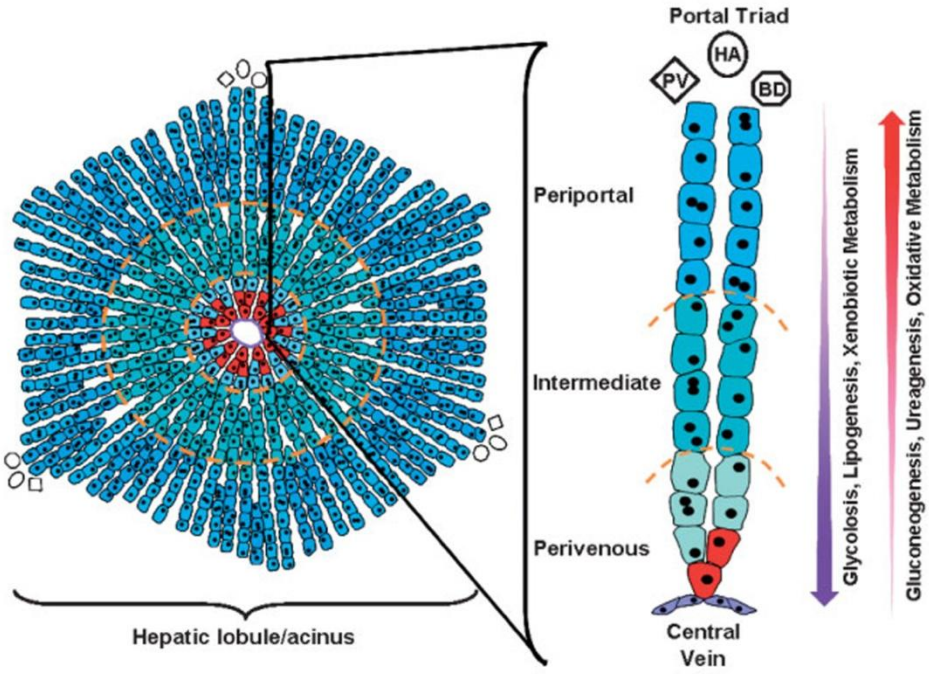

Figure 1.2 Schematic diagram of the microanatomical unit of the liver

Each liver acinus assumes a roughly hexagonal shape with hepatocytes radiating out from the central vein. This architecture is repeated throughout the liver plate with portal triads [composed of a branch of the hepatic artery (HA), portal vein (PV) and bile duct (BD)] placed at regular intervals between the acinii. Along the portovenous axis, hepatocytes can be divided into three zones: periportal, intermediate and perivenous. Gradients in metabolic pathways such as gluconeogenesis, glycolysis, xenobiotic metabolism, lipogenesis and ammonia metabolism are observed along this axis. Cells of the proximal perivenous zone express glutamine synthetase (red) while the remaining hepatocytes along the tract express carbamoylphosphate synthetase (blue). Figure was adapted from (Burke et al., 2006b)

1.3 Wnt/β-catenin signalling pathway

The Wnt signalling pathway plays a central role in embryonic development, maintenance of adult stem cells (e.g. intestinal stem cells) and the progression of human tumours of multiple tissues, including the brain, breast, colon, skin, and liver (Cadigan and Nusse, 1997). In the liver, β-catenin appears to be an active player in hepatoblastomas, benign liver neoplasms, hepatocellular carcinoma, and cholangiocarcinomas (Thompson and Monga, 2007).

The *Wnt* genes encode a large family of secreted glycoproteins, homologous to wingless in *Drosophila*, that signal at the cell surface via at least two receptors: Frizzled, a seven-pass transmembrane domain-containing serpentine protein and the Low-density-lipoprotein-related protein (LRP) receptor (Table 1-2). Transduction of the Wnt signal is mediated through three distinct pathways: the canonical Wnt pathway dependent upon activation of β-catenin, the Wnt/Ca^{2+} pathway and the Wnt/PCP (planar cell polarity) pathway (Kikuchi et al., 2006). The Wnt glycoproteins are produced by the neighbouring cells and secreted in a process that involves components, such as a multiprotein retromer complex and the multispanning transmembrane protein Wntless (Wls). The secreted Wnt ligands bind to the receptors of the seven-membrane-spanning Frizzled family and single-spanning LRP family. Secreted factors such as secreted Frizzled-related proteins (sFRPs) bind to Wnts and block the interaction with Frizzled receptors. Also Dickkopf (DKK) antagonizes Wnt signalling by blocking the LRP receptors. In the canonical Wnt pathway (Figure 1.3), the Wnt-Frizzled-LRP complex leads to the recruitment and phosphorylation of the cytoplasmic protein Dishevelled, a key transducer of the Wnt signal. Subsequently, glycogen synthase kinase 3β (GSK3β) and Axin, two proteins that form part of a complex with the tumour suppressor protein

adenomatous polyposis coli (APC) that normally directs the phosphorylation and ubiquitination of β-catenin, are inhibited and degraded. In the absence of the APC protein complex, free cytoplasmic β-catenin is un-phosphorylated on threonine 41 and serines 33, 37, and 45 by a protein complex comprised of glycogen synthase kinase 3 β (GSK3β) and CK (casein kinase)(Rubinfeld et al., 1996; Yost et al., 1996), and can then accumulate and enter the nucleus, where it forms a transcriptionally active complex with T cell factor (TCF)/Lymohocyte enhancer factor (LEF) family of transcription factors. The transcriptional complex can then replace Groucho from chromatin, and interacting with other coactivators like CREB binding protein (CBP), B cell lymphocyte 9 (BCL9), and Pygopus. Signalling through this pathway is very much dependent upon the level of β-catenin within the cell (Miller et al., 1999). The three pathways branch at the level of Dishevelled (Dsh) protein. In the non-canonical jun N-terminal kinase (JNK) pathway, Dsh (via Dishevelled-associated activator of morphogenesis 1 (Daam1)), is connected to downstream effectors, such as Rho, and regulates cytoskeletal organization and cell polarity. The Wnt/Ca^{2+} pathway leads to the release of intracellular calcium, and involves activation of Phospholipase C (PLC) and protein kinase C (PKC). Ca^{2+} is also important as it can activate Calmodulin-dependent protein kinase C (CaMKII), and Nemo-like kinase (NLK), which suppresses canonical Wnt signalling (Grigoryan et al., 2008).

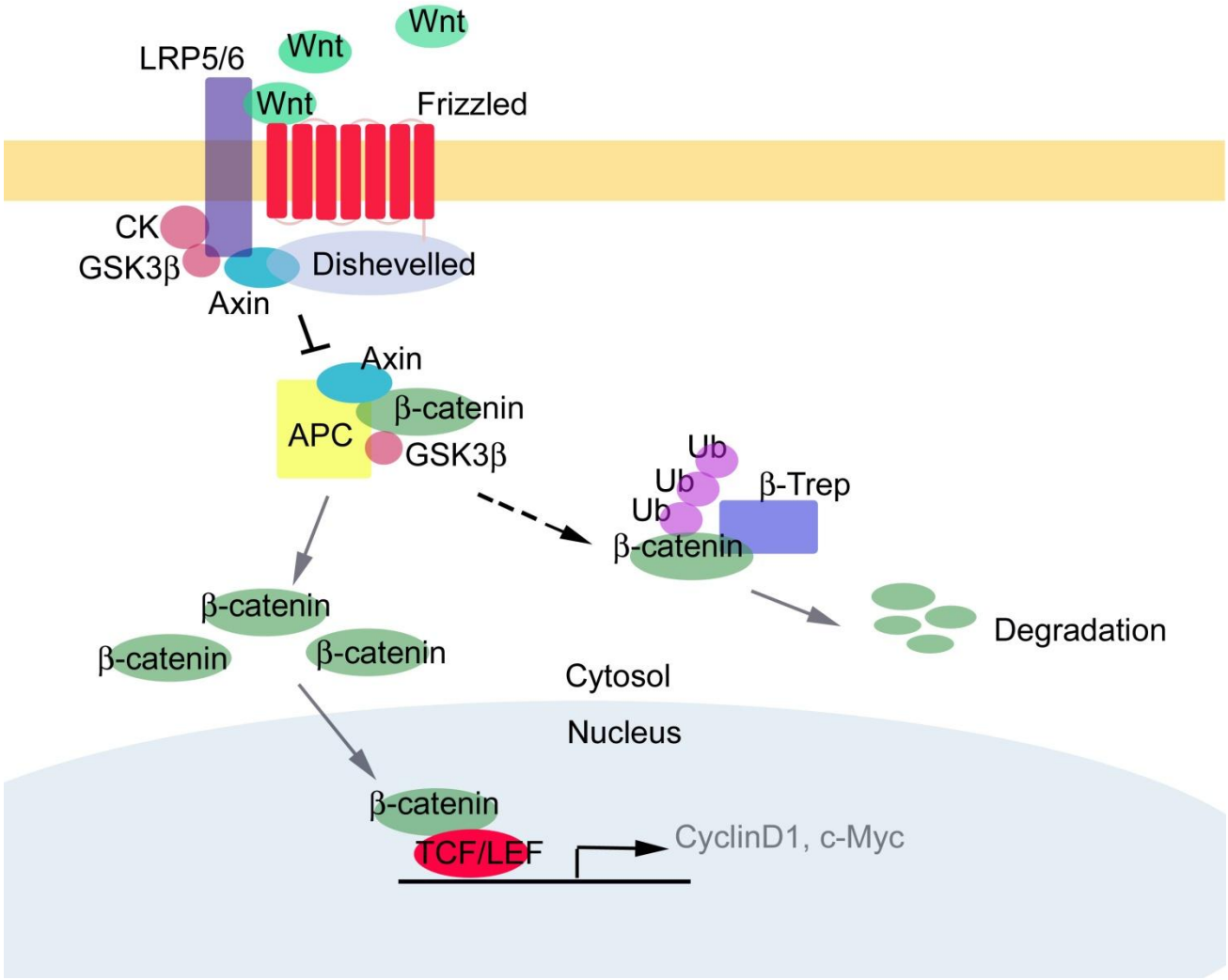

Figure 1.3 Overview of canonical Wnt signalling pathway

Table 1-2 Summary of the Wnt ligands, receptors and antagonists

Ligands	Pathway	**Receptors**	Pathways	**Antagonists**
Wnt1	Canonical	**Fzd1**	Canonical	**Sfrp1**
Wnt2		**Fzd2**	Noncanonical	**Sfrp2**
Wnt2b	Noncanonical	**Fzd3**	Noncanonical	**Sfrp3/Frzb**
Wnt3	Canonical	**Fzd4**	Noncanonical	**Sfrp4**
Wn3a	Canonical	**Fzd5**	Canonical	**Sfrp5**
Wnt4	Canonical Noncanonical	**Fzd6**	Noncanonical	**Wisp1**
Wnt5a	Noncanonical	**Fzd7**	Canonical	**Wisp2**
Wnt5b	Noncanonical	**Fzd8**		**Wisp3**
Wnt6	Canonical Noncanonical	**Fzd9**	Canonical	**Dkk1**
Wnt7a	(Maybe Wnt/PCP)	**Fzd10**		**Dnn2**
Wnt7b		**Fzd11**		**Dkk3**
Wnt8a	Canonical			**Dkk4**
Wnt8b	Canonical	**LRP5**	Canonical Noncanonical	**Wif1**
Wnt9a		**LRP6**	Canonical Noncanonical	
Wnt9b				
Wnt10a				
Wnt10b				
Wnt16	Noncanonical			

1.4 Wnt/β-catenin signalling in liver development

The Wnt signalling pathway may play a key role during liver development. Ober and co-workers recently demonstrated the requirement for mesodermally-derived Wnt signalling to direct liver specification in the zebrafish embryo (Ober et al., 2006). An analysis of the zebrafish mutant *Prometheus* points to a previously unknown role for Wnts during liver specification. *Prometheus* (*prt*) mutant was generated by Ober et al (Ober et al, 2006) used a forward genetics approach involving N-ethyl-N-nitrosourea (ENU) mutagenesis of the transgenic zebrafish line Tg(gutGFP)s854. In this line, green fluorescent protein (GFP) is used as a reporter and is expressed throughout the developing endoderm. The *prt* mutants exhibit defective hepatic fate specification and the liver is either absent or strongly reduced. This is accompanied by reduced or no expression of the early hepatoblast markers *hhex* (*haematopoietic ally expressed homeobox*) and *prox1* (*prospero-related homeobox 1*). These genes normally mark the early phase of liver formation. Positional cloning revealed that the prt gene encodes a novel *Wnt2b* homologue, named *Wnt2bb*. This is the first example of genetic evidence to show the role for Wnt signalling in liver formation.

The expression of the *secreted frizzled-related protein 5 (sfrp5)* gene, which encodes a Wnt inhibitor, is expressed in the mouse foregut endoderm (Finley et al., 2003) suggesting that inhibition of the Wnt pathway may be required during hepatic specification. Further experiments demonstrated that interactions between Wnt11 and the Sfrp5 protein can coordinate cell fate and morphogenesis during *Xenopus* foregut development. Depletion of *Sfrp5* results in reduced foregut gene expression, hypoplastic liver and ventral pancreatic buds. It is possible that finely executed waves of inhibition

and activation of Wnt signalling may mediate the various stages of endoderm patterning, such as liver development, or that convergence of other pathways known to operate during this time, such as BMP signalling, may act to enhance the Wnt pathway, as BMP2 enhances Wnt2b expression in keratinocytes (Yang et al., 2006). Interestingly, FGF8 and BMP4 are essential for hepatic induction and differentiation and both are known targets of Wnt signalling (Kawakami et al., 2001). Whether these factors act downstream or in a feedback loop with an earlier temporal specifying Wnt signal in the mouse liver remain to be elucidated. The role for Wnt/β-catenin pathway in developing liver has been further studied recently. Livers from mouse embryos cultured with β-catenin antisense oligonucleotides showed a decrease in proliferation and a simultaneous increase in apoptosis, two vital processes in liver development (Tan et al, 2006). This correlated well with a study that found that overexpression of β-catenin in developing chicken livers leads to a three-fold increase in liver size (Suksaweang et al., 2004). This effect on cell proliferation might be mediated by downstream targets such as cyclin D1 that regulates G1/S transition in cell cycle, which is also know downstream target of β-catenin. Thus, β-catenin is likely playing an important role during early liver development in hepatocyte expansion via its transcriptional co-activator role.

It has also been shown that the temporal expression of β-catenin during mouse liver development with high levels at E10-E14 along with its nuclear location in hepatoblasts, which correlated with increased cell proliferation. Microarray, Northern blotting, and protein analyses showed peak expression of β-catenin during early liver development at E10-E12, followed by a decrease and a complete loss of normal β-catenin after E16 through the remaining prenatal period. At the early stages, β-catenin localized to the cytoplasm and nuclei of resident cells in addition to its normal membranous localization, which was seen at all later stages and in adult liver. Decreases in β-catenin

levels at E14 onward coincided with its decreased gene expression and increased degradation (Micsenyi et al., 2004). This membranous localization and functional complex with its partners E-cadherin and Met might be a hallmark of acquisition of hepatocytic maturation and polarity. Indeed, antisense ablation of β-catenin promoted a more immature cell type that continued to coexpress stem cell and mature hepatocyte markers (Monga et al., 2003). Additionally, studies using Matrigel in primary hepatocyte cultures showed an increase in membranous complexes as a part of the differentiation process (Monga et al., 2006). This indicates that hepatocyte maturation might be a function of the cell-cell adhesion properties of β-catenin with some contribution from its transcriptional coactivator function. The latter function might be associated with the function of β-catenin in regulating expression of genes involved in hepatocyte maturation, such as the cytochrome P450s, shown recently to be tentative targets of the Wnt/ β-catenin pathway in liver (Sekine et al., 2006).

β-catenin has also been shown to play a role in biliary specification during liver development. β-catenin antisense ablation in E10 liver cultures led to an absence of cytokeratin kinase-positive biliary cells (Monga et al, 2003). Conversely, growth in Wnt3a-conditioned media showed survival and proliferation of predominantly Cytokeratin 19-positive cells as compared with the control media or Wnt3a-conditioned media containing soluble Frizzled-related protein-1 (sFRP1), a Wnt inhibitor (Hussain et al, 2004). Thus, β-catenin appears to play multiple important roles during hepatic morphogenesis based on in vitro and limited in vivo analysis, although whether such observations would hold true during in vivo gene targeting approaches for β-catenin or upstream effectors remains to be seen.

In order to further investigate the role for Wnt/β-catenin signalling in the embryonic liver Decaens et al applied conditional deletion strategy using *Cre* recombinase under the control of Cre/locus of X-over P1 (loxP) system to perform adenomatous polyposis coli (*Apc*) deletion in hepatoblasts (Decaens et al., 2008). The *Cre* recombinase was under the control of a chimeric α-fetoprotein-albumin enhancer/promoter. The loss of *Apc* and accumulation of β-catenin protein were detected in clusters of cells from E11.5 in $Apc^{-/-hb}$ livers and led to embryonic lethality between E16.5 and E18.5. Because β-catenin has been shown to regulate proliferation and survival of resident cells in ex vivo experiment for liver development (Micsenyi et al, 2004), liver hypoplasia due to severe impairment of proliferation as shown by the lack of Ki67 staining was an unexpected consequence of activation of the β-catenin pathway in the liver. However by using qPCR the authors confirmed that some genes with a positive impact on proliferation, such as Ki-ras (v-Ki-ras2 Kirsten rat sarcoma viral oncogene homolog (*Kras2*)), were preferentially down-regulated, whereas growth arrest-associated genes were up-regulated in $Apc^{-/-hb}$ livers. Apc loss in the hepatoblast also showed both repression of the expression of hepatoblast markers and blockage of differentiation toward the hepatocyte lineage. A significant increase in the expression of cytokeratin genes cytokeratin-19 and cytokeratin-7, two hepatoblasts and cholangiocytes markers, were observed in both E12.5 and E14.5 $Apc^{-/-hb}$ livers by qPCR. However, no staining in $Apc^{-/-hb}$ cell clusters and bile ducts with antibodies directed against cytokeratin-19 and cytokeratin-7 were observed. This implicated *Apc* deletion leaded to a partial commitment of $Apc^{-/-hb}$ hepatoblasts to biliary lineage. While whole embryonic E14.5 $Apc^{-/-hb}$ livers labelled with cell tracker were transplanted into the livers of adult recipient mice, new bile ducts with embryonic origin stained with anti- cytokeratin-19 antibody were identified in the vicinity of adult portal spaces. According to these data, the activation of β-catenin signalling in

hepatoblasts induces premature, mislocalized, and incomplete differentiation of these cells toward the biliary lineage.

In contrast to the studies described above, Tan et al deleted *β-catenin* in the developing hepatoblasts utilizing Foxa3-Cre and *floxed-β-catenin* transgenic mice from E8 to E8.5 (Tan et al., 2008). Deletion of *β-catenin* in developing livers resulted in significantly underdeveloped livers after E12 with lethality occurring at around the E17 stage of development. Histology revealed an overall deficient hepatocyte compartment due to increased cell death due to oxidative stress and apoptosis, and diminished expansion secondary to decreased cyclin-D1 and impaired proliferation. A paucity of primitive bile ducts was also observed. While no intrinsic defect in haematopoietic was observed, distorted hepatic architecture and deficient hepatocyte compartments resulted in defective endothelial cell organization was suggested to account for the overall foetal pallor.

1.4.1 The role of Wnt/β-catenin pathway in liver zonation

It has been demonstrated that liver tumours in mice carrying activating mutations in *β-catenin* exhibit altered zonal gene expression (Hailfinger et al., 2006). That is, tumours carrying *β-catenin* mutations express GS throughout the lesion, whereas Ha-ras tumours are negative for GS but express E-cadherin (a marker typical of a periportal phenotype). It is the observation, such as this, from liver tumours, that first hinted β-catenin may be required for mediating the expression of zone-specific genes. Benhamouche and colleagues have established a role for the Wnt pathway in regulating the zonation of ammonia detoxification along the portovenous axis (Benhamouche et al., 2006). Initially the authors demonstrated complementary expression of active β-catenin and APC proteins in wild-type liver where localization is restricted to the perivenous and periportal regions, respectively.

Based on this observation, it was proposed that, APC, acting by repressing the nuclear translocation of β-catenin, may be responsible for mediating zonation of the urea cycle. To test this hypothesis, hepatic *Apc* inactivation transgenic mice were generated. Liver-specific inactivation of the *Apc* gene was achieved by crossing conditional mutant mice for *Apc* with TTR-CreTam mice. In this line, the transthyretin promoter drives liver-specific expression of a tamoxifen (Tam)-inducible Cre recombinase. Injection of the resulting $Apc^{lox/lox}$ mice with a single dose of tamoxifen generates Apc^{koliv} animals, in which the *Apc* gene is inactivated only in the liver. Hepatic Apc conditional deletion leads to a complete disappearance of the APC protein by 7 days postinjection and subsequent lethality of mice due to the development of severe hepatomegaly, hyperammonaemia and hyperglutaminaemia. The mice displayed profound changes in liver gene expression. Apc^{koliv} mice exhibit a conversion of hepatocytes from a periportal to a perivenous phenotype with GS expression extending from the central vein to the portal triad throughout the liver. Additional genes and proteins (glutamate transporter-1, ornithine aminotransferase, leucocyte cell-derived chemotaxin-2, Axin2 and Rnase4) normally only expressed in perivenous hepatocytes were also upregulated following loss of APC. Concomitant loss of periportal-specific markers such as CPS, Glutaminase2, Arginase1 and PEPCK1 was also observed in the Apc^{ko} mice. To further validate a role for the Wnt pathway in regulating zonation, Benhamouche et al infected wild-type mice with an adenoviral vector expressing the Wnt antagonist, Dickkopf 1 (DKK1). Inhibiting Wnt signalling led to a decrease in perivenous gene expression pattern and an increase in periportal markers, indicating that, while activation of β-catenin is required for inducing a perivenous phenotype, inhibition of Wnt signalling mediates a periportal program of gene expression. However, in a small number of cells located in the proximal perivenous region, closest to the central vein, DKK1 is unable to overcome Wnt activation resulting in continued expression of GS.

Recently, using conditional deletion of *Apc*, *β-catenin*, and *c-Myc* induced in the livers of mice our lab extended these observations to explore the role of 3 key components (Apc, β-catenin, and c-Myc) of the Wnt pathway in the liver zonation of ammonia metabolizing enzymes (Burke et al., 2009). Conditional loss of *Apc* resulted in the expression of nuclear β-catenin and GS in most hepatocytes irrespective of zone. Deletion of *β-catenin* induced a loss of GS and a complementary increase in expression of CPS irrespective of whether Apc was present or not. However, deletion of *c-Myc* did not perturb the pattern of zonation. These results demonstrated that critically metabolic zonation is β-catenin dependent but c-Myc independent. The subtle change in the zonation of the CPS and GS-expressing cells requires finely regulation of gradient distribution of β-catenin /APC. Therefore additional components of the Wnt/ β-catenin pathway may be involved in maintaining the perivenous phenotype.

The timing of β-catenin expression may make it difficult to determine the mechanisms responsible for induction of metabolic zonation during liver development. CPS -expressing cells first appear at E13 and, with the exception of the area immediately around the hepatic veins, fill the entire lobe by E16. GS-expressing cells are detected at E17, in the small population of cells negative for CPS, thus recapitulating the zonation observed in adult liver (Spijkers et al., 2001). It has been proposed that maturation of periportal cells is required to induce the expression of a perivenous gene program during liver development. Interestingly, β-catenin levels peak between E12 and E14, around the time when CPS expression is induced, but become undetectable by E18 (Micsenyi et al., 2004). If Wnt signalling is required for setting up periportal and perivenous gene expression programs during development, as well as maintaining them in adult liver, one might expect β-catenin to be present at least in the region of the hepatic veins around E17 when GS-positive cells first appear. However,

β-catenin levels remain undetectable until after birth suggesting that alternative signalling pathways operate to direct the development of the perivenous cell phenotype or more complicated mechanism underlying remained elucidated.

1.5 Transdifferentiation

1.5.1 The definition of transdifferentiation

Transdifferentiation is the conversion of one differentiated cell type to another and may occur either directly (without an intervening cell division) or indirectly. Transdifferentiation challenges our preconceived ideas about the nature of the differentiated state. It was generally accepted that the terminally differentiated state was fixed, but it is now clear that differentiation can sometimes be reversed or altered (Eberhard et al., 2010; Shen and Tosh, 2010; Slack, 1986; Slack and Tosh, 2001; Tosh and Slack, 2002). Transdifferentiation is a subset of a wider class of cell type interconversions referred to as metaplasias. Examples of transdifferentiation have been documented during development (e.g. in the epithelial cell switch from stratified squamous to columnar during oesophagus development and from pseudostratified to squamous during the female reproductive system development (Cunha, 1976) (Yu et al., 2005) and in the adult (e.g. the appearance of hepatocyte in the pancreas) (reviewed by Tosh and Slack, 2002)

Cells that have the potential to interconvert by transdifferentiation generally arise from adjacent regions in the developing embryo (Slack and Tosh, 2001; Tosh and Slack, 2002). For example, the

liver and pancreas arise from adjacent regions of the developing endoderm and are able to interconvert in later life (Shen et al., 2000). The conversion of one cellular phenotype to another may either occur through a process of dedifferentiation and then redifferentiation or directly without an intermediate stage of dedifferentiation. The change in cell fate may be brought about by changing the local microenvironment (e.g. through the alteration of external factors) which causes a change in the expression of key (master switch genes). Master switch genes can determine which part of the body is formed by each region of the embryo. In normal development, particular combinations of these genes are activated in each region through the action of inducing signals. Each combination encodes a particular state of developmental commitment. The protein products of the homeotic genes are transcription factors, and their function is to regulate the next level of genes in the hierarchy, which eventually leads to individual tissue types. Transdifferentiation can therefore be brought about by introducing key master switch genes into cells.

1.5.2 Transdifferentiation of pancreas to liver

The appearance of hepatocytes in the pancreas is one well-documented example of transdifferentiation. Hepatocytes appear in the pancreas of hamsters or rats in response to various experimental treatments - for example, treatment of rats with a copper-deficient diet (Rao et al., 1988) (Rao et al., 1989), or after transplantation of pancreatic epithelial cells (Dabeva et al., 1997), and in transgenic mice that overexpress keratinocyte growth factor in the pancreatic islets (Krakowski et al., 1999). The reverse transdifferentiation (liver to pancreatic exocrine cell) is induced in the livers of rats after treatment with polychlorinated biphenyls (Rao et al., 1986). This ability to interconvert presumably reflects the close developmental relationship between the pancreas and liver: they both

arise from the foregut endoderm (Zaret and Grompe, 2008). Their development is controlled by signals from adjacent structures of ectodermal and mesodermal origin, the notochord and aorta (reviewed by (Wells and Melton, 1999)). I will now review in more detail the models for the conversion of pancreatic cells to hepatocytes. The liver, lungs, and ventral pancreas derive from the ventral foregut adjacent to cardiac mesoderm and in opposition to the notochord. Liver specification from ventral foregut by cues from adjacent cardiac mesoderm has been shown in chick (Le Douarin, 1968) and mouse (Gualdi et al., 1996). The pancreas develops from the dorsal and ventral domain of the foregut. The interaction of endoderm with notochord and other transcription factors including FGF2, activin-β-B which can repress endodermal expressed sonic hedgehog (shh) and induction of Pdx1 are necessary for proper dorsal pancreas formation and for expression of pancreatic genes (Hebrok et al., 1998). Retinoic acid (RA) however may play a role in ventral pancreatic development (Wells and Melton, 1999). The ventral component of the pancreas derives from the endoderm that is immediately adjacent and lateral to presumptive hepatic endoderm. Although communication between liver and ventral pancreas has not been characterized, it is possible that interaction between these adjacent structures plays a role in subsequent morphogenesis.

Transdifferentiation of pancreatic cells to hepatocytes has been established in both *in vivo* and *in vitro* models. *In vivo* studies have been based on treatment with carcinogens or feeding rodents a modified diet. One of the most reliable methods for inducing hepatocytes in the rat pancreas is the copper-depletion-repletion protocol (Rao et al.1988). A highly reproducible *in vivo* model in which hepatocytes are induced in the pancreas of adult rats maintained on copper-deficient diet containing a relatively non-toxic copper-chelating agent for 7-9 weeks was described by Rao et al, 1988. This dietary manipulation resulted in almost complete loss of pancreatic acinar cells at the end of

copper-depletion regimen. Northern blot analysis of total RNA obtained from the pancreas of these rats revealed the expression of albumin mRNA. Albumin protein was also demonstrated in these pancreatic hepatocytes by immunofluorescence. In hamsters, treatment with peroxisomal proliferators ciprofibrate, 2,3,7,8-tetrachlorodibenzo-p-dioxin (TCDD) (Rao et al. 1988) or N-nitrosobis(2-oxopropyl)amine (BOP) (Scarpelli and Rao, 1981) all induce the appearance of hepatocytes in the pancreas. Moreover, a study of hepatocellular carcinoma in the pancreas has revealed that hepatic differentiation may arise from any of the three pancreatic cells (endocrine, acinar and ductal cells) when investigating human cases (Paner et al., 2002). Keratinocyte growth factor (KGF) under the control of insulin promoter can also induce hepatocytes in pancreas (Krakowski et al., 1999). Cadmium, a toxin heavy metal, can also induce hepatocytic transdifferentiation in rat pancreas (Waalkes et al., 1992). Dabeva et al. (1997) demonstrated that epithelial progenitor cells from the pancreas differentiate into hepatocytes and express liver-specific proteins when transplanted into the liver (Dabeva et al., 1997). After transplanting genetically lacZ-labelled pancreatic duct epithelial cells (previously embedded into collagen matrix) into isogenic Fischer-344 rats, Chen et al. (1995) found that ductal pancreatic cells resembled hepatocytes in different degrees of differentiation (Chen et al., 1995). Less than 5% of lacZ-labelled cells formed ductular structures. The hepatocyte-like cells from the subcutaneous implantation site expressed mixed phenotypes of both hepatocyte and ductal cell, including the expression of α-fetoprotein, tyrosine amino-transferase, gamma-glutamyl transpeptidase, carbonic anhydrase II, and cytokeratin 19. In contrast, the hepatocyte-like cells colonizing the mesentery showed the phenotype of mature hepatocytes, including abundant glycogen storage and a lack of α-fetoprotein and carbonic anhydrase II expression. Neither acinar cell nor endocrine differentiation was seen (Chen et al,

1995). These findings demonstrate that pancreatic ductal cells can be the progenitor cell for transdifferentiated hepatocytes.

Two in vitro models have been developed for converting pancreatic cells to hepatocytes, the pancreatic amphicrine call line AR42J-B13 (Shen et al. 2000) and cultured mouse embryonic pancreas (Percival and Slack, 1999). These models allow the close observation of the cells during transdifferentiation and the ability to trace the cell lineage during their conversion to a hepatic fate. The AR42J cells are derived from rat pancreatic tumour (Longnecker, 1994). This cell line probably represents a progenitor population that under certain circumstances may generate other cell pancreatic cell types. AR42J cells can be converted to endocrine producing insulin cells after treatment with activin A and β-cellulin (Mashima et al., 1996). AR42J-B13 (B13) cells, a subclone derived from the parent AR42J cell line, were induced to form insulin-producing cells after treatment with glucagon-like peptide-1 (GLP-1) can generate glucagon secreting α-cells (Zhou et al., 1999). Shen et al. (2000) have shown that culturing pancreatic B13 cells with the synthetic glucocorticoid dexamethasone (Dex) for 2 weeks can induce the transdifferentiation into hepatocytes. The nascent hepatocytes loose expression of the pancreatic marker amylase and start to express hepatocyte markers such as glucose-6-phosphatase, transferrin (TFN) and albumin. The change in gene expression is accompanied by a change in the morphology of the cells. Indeed following Dex treatment, the B13 cells enlarge and flatten onto the substratum. More recently, Lardon et al. (2004) demonstrated that treating with Dex can induce adult rat pancreatic acinar calls maintained in culture to convert to hepatocyte-like cells (Lardon et al., 2004).

The glucocorticoid receptor is a ligand activated transcriptional regulator (Glass and Rosenfeld, 2000) that acts to induce hepatic transdifferentiation as addition of RU486 to the cultures inhibits the

Dex-induced transdifferentiation of B13 cells to hepatocyte-like cells (Shen et al. 2000). Our lab has also identified the molecular basis of the switch, which involves induction of the transcription factor CCAAT/enhancer-binding protein (C/EBP)β. Transfection of *C/EBP*β into AR42J-B13 cells induced transdifferentiation, whereas introduction of the dominant-negative form of C/EBPβ (termed liver-inhibitory protein or LIP) inhibited the transdifferentiation. Further evidence for a role for C/EBPβ in liver development is indicated by the fact that this factor is bound to the albumin enhancer in embryonic hepatocytes at embryonic day 12.5 (Bossard et al., 1997). The function of C/EBPβ (and the C/EBP family in general) in liver development awaits further clarification as the family shows a certain degree of redundancy. Messenger RNAs of C/EBPα, C/EBPβ, and C/EBPδ are expressed by mature hepatocytes in primary cell culture from young adult rats (Borlak et al., 2002; Borlak and Thum, 2001). These results are consistent with the theory that variations in C/EBP expression and function help regulate hepatocyte terminal differentiation (Diehl et al., 1994). In liver and intestine C/EBPα mRNA expression is coordinately induced just prior to birth (Birkenmeier et al., 1989). The role of C/EBPα in the developmental expression of a subset of genes governing essential metabolic processes had been elucidated with a mutant mouse model that lacks C/EBPα. The mutation resulted in the failure of the liver and white and brown adipose tissue to develop normal metabolic functions in the perinatal period, including hepatic glycogen synthesis and gluconeogenesis and the synthesis and deposition of triglyceride in adipose tissue (Tosh et al., 1996). Both C/EBPβ and C/EBPδ can transactivate hepatocyte growth factor (HGF). Partial hepatectomy, which is known to activate HGF gene expression in the liver, increased C/EBP (especially C/EBPβ) binding activity to this region of the HGF promoter (Jiang and Zarnegar, 1997). The importance of the role of both C/EBPα and β in hepatocyte differentiation has also been described previously (Diehl et al., 1994).

Shen et al (2003) showed that when treating mouse embryonic pancreatic cultures with Dex, the transcription actor C/EBBβ is induced in the epithelium and Pdx-1 is reduced (Shen et al., 2003). Burke et al (2006) demonstrated in B13 cells, the induction of C/EBPβ mRNA after only 8 hours of treatment with Dex (Burke et al., 2006a). The induction of C/EBPβ was followed by the up-regulation of other liver-enriched transcription factors, including C/EBPα, Hepatocyte Nuclear Factor 4 α (HNF4α) and retinoid X receptor α (RXRα). Unlike C/EBPβ (which revealed a strong nuclear staining), C/EBPα nuclear expression was weaker and restricted to more mature cells. It has been shown that during the transdifferentiation of B13 cells to hepatocytes, HNF4α accumulates in the nuclei at a stage following induction of C/EBPβ suggesting that HNF4α may be downstream of C/EBPβ (Shen et al. 2000). HNF4α is a protein that is abundant in both adult and fetal liver as well as the intestine (reviewed by Shen et al. 2003). Several studies have shown the importance of HNF4α in regulation of liver differentiation and regeneration (Li et al., 2000; Nagy et al., 1994). A knockout study in the fetal livers of mice revealed that as a consequence of HNF4α removal, some genes essential for liver function are absent e.g. HNF1α and the pregnane X receptor (PXR) (Li et al., 2000). The retinoid X receptor α (RXRα) is involved in the regulation of hepatic metabolism. RXRα regulates cholesterol, fatty acid, bile acid, steroid and xenobiotic metabolism (Wan et al., 2000). Burke et al. (2006) reported that after 9 days of treating B13 cells with Dex, RXRα localizes to nucleus of the hepatocytes suggesting prolonged Dex-treatment induces a mature liver phenotype. Although transfection of C/EBPβ caused a similar hepatic transdifferentiation programme to treatment of Dex, it did not cause the same degree of morphological flattening suggesting that additional factors may be required to produce a more differentiated hepatic phenotype from pancreatic cells.

The question arises whether the hepatocytes induced from pancreatic B13 cells are *bone fide* liver cells. The hepatocytes express liver genes involved in phase I and II detoxification pathways, ammonia detoxification and glucose metabolism. In addition, the ability of the hepatocytes to respond to xenobiotics was tested (Burke and Tosh 2006; Tosh et al. 2002). The hepatocytes were found to express significantly higher levels of detoxifying enzyme catalase when treated with the peroxisomal proliferator ciprofibrate in comparison to B13 cells treated with Dex alone (Burke et al. 2006). The hepatocytes also possess the ability to replicate hepatotropic hepatitis B virus (Wang et al., 2005). Furthermore, the hepatic phenotype of the cells is stable even after 14 days of Dex withdrawal with some of the hepatocytes still expressing liver markers such as TFN or albumin following Dex removal (Tosh et al. 2002).

1.5.3 The Wnt pathway and hepatic transdifferentiation of pancreatic cells

In 2010, Wright and colleagues investigated the role of the Wnt signalling pathway in the transdifferentiation of pancreatic B13 cells to hepatocytes (Wallace et al., 2010). The authors suggested that transient suppression of Wnt signalling is pivotal to the glucocorticoid-dependent transdifferentiation of B13 cells. They found that glucocorticoid treatment would result in a transient loss of constitutive WNT3a expression, phosphorylation and depletion of β-catenin, loss of β-catenin nuclear localisation, and significant reduction in TCF/LEF transcriptional activity before overt changes in phenotype into hepatocyte-like cells (the authors referred to the hepatocytes as B-13/H cells). A return to higher TCF/LEF transcriptional activity correlated with the re-expression of WNT3a in B-13/H cells. β-catenin knockdown alone substituted for and enhanced

glucocorticoid-dependent transdifferentiation. Similarly, overexpression of a mutantβ-catenin (pt-Xβ-cat) protein that blocked glucocorticoid-dependent suppression of TCF/LEF activity resulted in inhibition of transdifferentiation. A small-molecule activator of TCF/LEF transcription factors blocked glucocorticoid-dependent effects, as observed with pt-Xβ-cat expression. Quercetin (a TCF/LEF inhibitor) did not promote transdifferentiation into B-13/H cells, but did potentiate glucocorticoid-mediated transdifferentiation. Later a serine/threonine protein kinase (serum and glucocorticoid regulated kinase 1 (SGK1) which was markedly induced in the B-13/H cells was shown to direct phosphorylate β-catenin (Wallace et al, 2010). These data demonstrate that the transdifferentiation of B13 cells into hepatocyte-like cells in response to glucocorticoid may be dependent on the repression of constitutively active WNT signalling.

1.6 Aims

To determine the expression of Wnt ligands, receptors and co-receptors in developing mouse liver.

To date, the expression of members of the Wnt signalling family including ligands, receptors and effectors are not well characterised during normal mouse development. Indeed the data so far is limited to RT-PCR results (Bi et al., 2009). The main concerns with the RT-PCR data are that it reflects expression at the whole organ rather than at the cellular level and the technique suffers from relatively poor sensitivity. Here we aim to determine the expression of members of the Wnt signalling family by a combination of *in situ* hybridization, immunostaining and western blotting to reveal the comprehensive expression pattern during mouse liver development.

To determine the role of the Wnt/β-catenin pathway in liver development

While we know quite a lot about the role of the Wnt/β-catenin signalling pathway in liver development and in the maintenance of zonation in the adult liver we do not know whether the Wnt/β-catenin pathway is also critical for the induction of metabolic zonation in the developing mouse liver. To address this shortfall, we will determine the effects of β-catenin activation and deletion in mouse liver development (and more specifically metabolic zonation) by conditional deletion of either *Apc* or *β-catenin*.

To test whether exogenous application of Wnt/β-catenin components is able to promote a periportal or a perivenous phenotype in cultured mouse embryonic liver buds.

Previous studies have shown that the Wnt/β-catenin pathway controls the perivenous and periportal programs of gene expression (Benhamouche et al, 2006; Burke et al, 2009). Our goal is to use our understanding of the role of the Wnt/β-catenin pathway to promote a periportal or perivenous-like phenotype in cultures of embryonic mouse liver.

To dissect the molecular mechanisms underlying glucocorticoid-induced transdifferentiation of pancreatic cells to hepatocytes

An *in vitro* model of transdifferentiation has been developed for converting pancreatic cells to hepatocytes based on the addition of the synthetic glucocorticoid Dexamethasone to the pancreatic cell line AR42J-B13 (B13) (Shen et al. 2000). While the induction of C/EBPβ is known to be an

early event in the Dex-induced transdifferentiation, the role of the liver-enriched transcription factor HNF4α is not well understood. This constitutes the last aim of the project.

CHAPTER 2 MATERIALS AND METHODS

2.1 Materials

2.1.1 Mouse Lines

AhCre^{+}Apc$^{fl/fl}$ mice were designed as previously described (Shibata, 1997). To investigate the phenotype of conditional deletion of Apc and β-catenin, mice bearing a loxP-flanked Apc or β-catenin allele were crossed onto a novel inducible cre transgenic background, which uses the Cyp1A promoter to deliver inducible cre expression in the liver (Sansom et al, 2004). In this transgenic line (Ahcre), cre expression is inducible from a cytochrome P450 promoter element that is transcriptionally up-regulated in response to lipophilic xenobiotics such as β-napthoflavone. Extensive recombination showed in liver, intestine, pancreas, gallbladder, esophagus, and stomach in response to β-napthoflavone treatment (Sansom et al, 2004). The Ahcre model provides a simple route for introducing specific gene mutations into many of the epithelia of the gastrointestinal tract of the mouse. It has been used to show that β-catenin is required for the maintenance of intestinal cell proliferation and is implicated in goblet cell differentiation and enterocyte-matrix attachment (Ireland et al, 2004). Outbred male mice from 6 to 12 weeks of age were segregated for the C57BJ and S129 genomes. The loxP flanked alleles used was *AhCre*. Timed pregnancies were performed and the age of the embryos was determined by the day a vaginal plug was detected, which was assigned as day 0.5 (E0.5). To induce recombination, pregnant mice were given intraperitoneal injections of β-napthoflavone (β-NF) (80 mg/kg) at the times indicated. Mice were humanely killed by a Schedule 1 procedure. All experiments were performed under the UK Home Office guidelines.

2.1.2 General chemicals, fixatives and buffers

Table 2-1 List if reagents used for immunostaining

Chemical, fixatives and buffer	Components	Supplier
Acetone:Methanol (Ac:Me)	1 volume acetone: 1 volume methanol	Fisher Scientific
Blocking buffer (BB)	2% (v/v) BB made in phosphate buffered saline (PBS) from 10% BB. A 10% (w/v) working stock of blocking powder was prepared by dissolving the BB in maleic acid buffer [100mM Maleic acid, 150 mM NaCl, pH7.5]	Roche
Bovine serum albumin (BSA)	1% (w/v) of BSA in PBS	Sigma, UK
Citrate buffer	1% (v/v) Citrate buffer	Lab vision
Ethylene-diaminetetraacetic acid (EDTA)	1%(v/v) EDTA buffer	Lab vision
Gel mount		Biomedia
Paraformaldehyde (PFA)	4% (w/v) PFA in PBS, pH 7.4	Fisher Scientific
PBS	0.95% (w/v) PBS	Autogen Bioclear
Triton x-100	0.1% (v/v) Triton X-100 in PBS	Sigma, UK
Optimal Cutting Temperature compound (OCT)		BBC Biochemical,

2.1.3 Cell culture medium, reagents and exogenous factors

Table 2-2 Composition of medium used for cell culture

Culture medium	Supplier
Dulbecco's Modified Eagle's Medium (DMEM)	Sigma, UK
Basel Medium Essential (BME)	Sigma, UK

Minimum Essential Medium Eagle		Sigma, UK
Reagent	Final concentration	Supplier
Fetal Bovine Serum (FBS)	10 % (v/v)	Sigma, UK
Gentamycin	20μg/ml	Gibco Invitrogen
L-Glutamine	2mM	Sigma, UK
Penicillin-streptomycin	100 units/ml, 100μg/ml	Sigma, UK
Trypsin- EDTA		Gibco Invitrogen
Dexamethasone (Dex)	1μM final (stock solution of 1mM of Dex made up in 100% Ethanol)	Sigma, UK
Quercetin		Sigma, UK
Insulin-Transferrin-Selenium (ITS)		Sigma, UK

2.1.4 Markers for immunofluorescence cell staining

Table 2-3 List of primary antibodies used for immunofluorescence cell staining

Primary antibodies	Species	Fixation	Dilution	Antigen retrieval	Supplier
Anti-amylase	Rabbit	PFA	1:100		Sigma, UK
Anti-Albumin	Rabbit	PFA	1:200		Abcam
Anti-a-fetoprotein (AFP)	Rabbit	PFA	1:200		Abcam
Anti-C/EBP ・	Mouse	PFA	1:100		Santa Cruz
Anti-Green fluorescent protein (GFP)	Rabbit	PFA	1:200		Abcam
Anti-CPS	Rabbit	Methanol	1:200	EDTA	Abcam
Anti-Glutamine synthetase (GS)	Mouse	PFA	1:300	Citrate	BD Tansduction
Anti-SRY	Rabbit	PFA	1:100	EDTA	Chemicon

(sex-determining region Y)-box 9 (Sox9)					

Table 2-4 List of secondary antibodies used for immunofluorescence cell staining

Secondary antibodies	Species	Conjugate	Dilution	Supplier
Anti-mouse	Horse	Fluorescein isothiocyanate (FITC)	1:200	Vector
Anti-mouse	Horse	Texas-red	1:200	Vector
Anti-rabbit	Goat	FITC	1:200	Vector
Anti-rabbit	Goat	Texas-red	1:200	Vecor

2.1.5 Primary and secondary antibodies used for staining tissue sections

Table 2-5 List of primary antibodies used for immunohistochemistry staining

Primary antibodies	Species	Fixation	Dilution factor	Antigen retrieva;	Supplier
GS	Mouse	PFA or Formalin	1:200	Citrate	BD Transduction
CPS	Rabbit	Methanol or Formalin	1:200	EDTA	Abcam
β-catenin	Mouse	PFA or Formalin	1:50	EDTA	BD Transduction
Sox9	Rabbit	PFA or Formalin	1:200	EDTA	Chemicon

2.1.6 Western blotting materials, reagents, primary and secondary antibodies

Table 2-6 List of chemicals used for western blotting

Materials and regents	Components and suppliers
PBS-Tween (PBST)	0.1%(v/v) Tween-20 (Sigma, UK) in PBS
Blocking solution	5% (w/v) Marvel (non-fat milk) in PBST
Enhanced chemiluminescence (ECL)	Amersham
Extra thick filter paper	Bio-Rad
Lysis buffer	0.5M Tris-HCl (Fisher Scientific) pH6.8
Precision Plus Protein Rainbow Standard Ladder	Bio-Rad
Protease inhibitor cocktail (Catalog number P8340), Components including AEBSF, 104mM; Aprotinin, 80μM; Bestatin, 4mM; E-64, 1.4 mM; Leupeptin, 2mM; Pepstatin A, 1.5mM	Sigma, UK
Bio-Rad Protein Assay Dye Reagent Concentrate (Catalog number 500-0006)	Bio-Rad, UK
Running buffer	25mM(w/v) Tris (Fisher), 192mM(w/v) Glycine (Fisher), 0.1% Sodium dodecyl sulphate (SDS) (Sigma, UK)
2x Sample buffer	0.125M Tris-HCl pH6.8, 4% SDS, 20% Glycerol, 0.02% Bromophenol blue pH6.8, 0.2M Dithiothreitol (DTT) (Sigma, UK)
Transfer buffer	25mM Tris, 193mM Glycine, 20% Methanol
Tris-HCl Criterion Precast Gel	Bio-Rad

Table 2-7 List of primary antibodies used for western blotting

Primary antibodies	Species	Dilution	Supplier	Secondary antibodies		
				Dilution	Species/Conjugate	Supplier
β-catenin	Mouse	1:5000	Transduction	1:2000	Goat- Horse radish peroxidase (HRP)	Vector
CPS	Rabbit	1:2000	Abcam	1:2000	Goat-HRP	Vector
GS	Mouse	1:2000	Transduction	1:2000	Goat-HRP	Vector
GAPDH	Mouse	1:10000	Chemicon	1:2000	Goat-HRP	Vector
LaminB1	Goat	1:1000	Santa Cruz	1:2000	Donkey-HRP	Santa Cruz

All antibodies were diluted in 3% marvel in PBST.

2.1.7 RNA extraction, reverse transcription (RT) and polymerase chain reaction (PCR) reagents and experimental conditions

Table 2-8 List of chemicals used for RNA extraction and RT-PCR

Reagent	Supplier
RNA extraction	
Chloroform	Fisher Scientific
75% Ethanol	Fisher Scientific
Isopropanol	Fisher Scientific
Tri reagent	Sigma, UK
RT	
10mM dNTP Mix	Invitrogen
0.1M DTT	Invitrogen
Oligo(dT)12-18 oligonucleotides	Invitrogen
SuperScript ll Reverse Transcriptase 10000U	Invitrogen
10X RT buffer	Invitrogen
PCR	

100 bp DNA ladder	Geneflow
1kb DNA ladder	Geneflow
ReddyMix Master mix	ABgene

Table 2-9 List of PCR primers

Primers	Forward	Reverse
Rat-Albumin	GCCCTACCCACAAAGCCTCAG	AGCCCCTTCATATCACAGAGCA
Rat-AFP	AACAAGTATGGATTCTCAGG	ATTGATGCTCTCTTTGTCTG
Rat-β-actin	TCCGTAAAGACCTCTATGCC	AAAGCCATGCCAAATGTCTC
Rat-CPS	CGTCCAAGATTCCTTGGTGT	ATGGAAGAGAGGCTGGGATT
Rat-CK7	ACTTGCTGGCACCTCTGAGT	GCTGCTCTTGGCTGACTTCT
Rat-CK19	GAGCTGGAGGTGAAGATTCG	TCAAACTTGGTCCGGAAGTC
Rat-Cx43	TCTTCATGCTGGTGGTGTC	TAACCAGCTTGTACCCAGG
Rat-Sox9	CAAGACTCTGGGCAAGCTCTG	TCTGCTTGCCCATTCTTCAC
Mouse-CyclinD1	GGATGCTGGAGGTCTGCGA	AGAGGCCACGAACATGCAAG
Mouse-Glutaminase 2	AACCCAGTGGTCTGCGCTAT	ACAATGGCACCAGCATTGAC
Mouse-Glt1	ATGTCCACGACCATCATTGC	ACCTCGTCGTTCTTCTTCCC
Mouse-Arginase I	GGTTCTGGGAGGCCTATCTT	TTATGGTTACCCTCCCGTTG
Mouse-ASS	TGGATACAGTGGCGAACAAA	AGCAGGGACCATCCTTTACC
Mouse-ASL	CAGGTTGAGAGCCACTCCTT3	CAAGCTCACCTTTTGCTGGT
Mouse-RNase4	GAACGGCCAGATGAACTGTCA	CTGGTTCTTGCCCTGTATCTA
Mouse-RHBG	GTGTGGGCTTTACCTTCCTCG	CGCAGAAGTCAGCGTTGAT
Mouse-PEPCK	TGGCTACGTCCCTAAGGAA	GGTCCTCCAGATACTTGTCGA
Mouse-GS	TTTATCTTGCATCGGGTGTG	TTGATGTTGGAGGTTTCGTG
Mouse-CPS	GAGTGGGTCTGCCATGAAC	TGGACATTGAATGGCCCAAG
Mouse-β-actin	TGCTCTAGACTTCGAGCAGGAGAT	TCATCGTACTCCTGCTTGCTGATC
Mouse-GAPDH	TTGTCAGCAATGCATCCTGCACCA	GTCTCCTGTGACTTCAACAGCAAC
Mouse-β-catenin	GCAACCCTGAGGAAGAAGAT	TTAGCTCCTTCCTGAGGAG
Mouse-Cytokeratin7	GCAGGATGTGGTGGAAGATT	CGTGAAGGGTCTTGAGGAAG
Mouse-Cytokeratin19	ACCCTCCCGAGATTACAACC	AGAGTCAGCTCATCCAGCAC
Mouse-Connexin43	GAGGGAAGTACCCAACAGCA	CCC AGGAGCAGGATTCTGA
Mouse-Sox9	CGCCTTGAAGATAGCATTAGGA	CAAGAACAAGCCAGCCGTCA

Mouse- Hes1	AGCACAGAAAGTCATCAAAGCC	TTCATGCACTCGCTGAAGCC
Mouse- Hey1	GCCGACGAGACCGAATCAAT	GCTGGGATGCGTAGTTGTTG
Mouse-manic fringe	CGTGATGTGTATGTGGGCAAG	TCAGGGCGCTGCCAGCAG

2.1.8 Adenovirus (Ad) reagents, materials and kits

Table 2-10 List of adenoviral vectors used for gene transduction

Adenovirus construct	Constructed by	Titre (iu/ml)
Ad-CMV-Null	Gift from Harry Heimberg, Brussels	$6.7x10^{7}$
Ad-RSV-GFP	Gift from Emma Regradsoe, Oxford	$8.6x10^{10}$
Ad-β-catenin		$4.2x10^{11}$
Ad-Wnt1-HA		$3.03x10^{10}$
Ad-Wnt5a-HA		$1.6x10^{12}$
Ad-DKK1		$4.6x10^{11}$
Ad-CMV-LAP	Gift from Dr. Hiroshi Sakaue, Japan (Schroeder-Gloeckler JM et al. 2007)	$7x10^{9}$
Ad-HNF4α		$6x10^{10}$
Ad-C/EBPα		
Ad-HNF1α		$7.3x10^{9}$

2.1.9 Other instruments

Table 2-11 List of other general instruments

Instrument	Supplier
NanoPhotometer Pearl	Geneflow, UK
L-80 ultracentrifuge	Beckman, UK
DMRB microscope	Leica, UK
DM*IRB* inverted microscope	Leica, UK
MSE Mistral 1000 centrifuge.	ISTCP

2.2 Methods

2.2.1 Cell culture

2.2.1.1 Cell culture

The AR42J-B13 (B13) cell line (provided by Dr. Itaru Kojima, Maebashi Japan) was maintained in complete media composed with DMEM supplemented with 10% FBS, 1% penicillin/streptomycin and 2% L-glutamine as described previously (Shen et al. 2000). The B13 cells were treated with 1μM Dex every other day.

2.2.1.2 *Cell culture maintenance*

B13 cells were cultured in complete media in 75cm^2 tissue culture flasks and passaged when cells were approximately 90% confluent. To passage the cells the media was removed and 10ml of PBS was added to remove excess serum from the cells. The PBS was then decanted off and 3ml of Trypsin-EDTA solution was added and the cells incubated at 37℃ in 95% air / 5% CO_2 for 3-5min. The flask was gently tapped until the cells were dislodged and then the cell suspension was added to a 12ml centrifuge tube containing 9ml of complete medium. The supernatant was then removed and the cells were resuspended in 1ml of complete medium. Approximately 100μl of cell stock was inoculated in a new 75cm^2 tissue culture flask containing 12ml of complete medium and incubated at 37℃ in 95% air / 5% CO_2 for future experiment.

2.2.1.3 Cell storage and revival

Unused cell stock was spun down at 1000 rpm for 4 min using MSE Mistral 1000 centrifuge. The supernatant was decanted off and 1ml of freezing medium (10% Dimethyl sulphoxide (DMSO) in FBS) was added to the 12ml centrifuge tube and mixed with the cells. The suspension was then transferred to a 2ml cryogenic vial and stored in a -20℃ freezer for 1hr before transferring to -80℃ freezer. The next day, vials were transferred to liquid nitrogen.

2.2.1.4 Inoculation of cells

Approximately 2µl of cell stock was added to 2ml of complete medium and seeded into a 35mm tissue culture dish. For immunostaining, the cells were plated into dishes containing sterile glass coverslips at a confluence of 10-15%. Cells were allowed to attach for 24hrs at 37℃ in an atmosphere of 95% air / 5% CO_2.

2.2.2 Fractionation of liver tissue

Liver tissue was lysed and homogenized in 500µl of cytosolic extraction buffer (10mM KCl, 20mM HEPES, 1mM EDTA, 10% Glycerol, pH7.9). The lysate was rotated at 4°C for 30min at 10 rpm and then homogenized by passing through a 27G needle using a 1ml syringe. The nuclear pellet was prepared by centrifugation at 3000 x g for 5 min at 4°C. The supernatant (which preserves the soluble cytoplasmic contents) was transferred to a freshly labelled eppendorf and the pellet contains mitochondria and ER-golgi membrane and intact nuclei. The pellet was then washed twice by 500µl of cytosolic extraction buffer and then dissolved in 50µl nuclear extraction buffer (10mM KCl,

20mM HEPES, 400mM NaCl, 1mM EDTA, 20% Glycerol, pH7.9) and rotated at 4°C at 10rpm for 60min. The lysate were then centrifuged again at 16300 x g for 15 min at 4°C and the supernatant (which preserves the soluble nuclear extract) was then transferred to a freshly labelled eppendorf and stored at -80°C. The recovered insoluble pellet contains cytoskeletal, membrane and chromatin-bound proteins.

2.2.3 Western blotting

Protein extracts were prepared from liver samples by a cycle of rapid freeze–thawing in lysis buffer (0.5 mol/l Tris-HCl [pH.6.8] containing a 1:100 dilution of protease inhibitor cocktail (Sigma, UK). Samples were centrifuged at 14,000 rpm for 10 min at 4°C to remove cellular debris and quantified using the Bio-Rad (Hercules, California) protein assay reagent. Protein extracts were denatured by mixing with a 2 x SDS-PAGE loading buffer containing 0.125 mol/l Tris-HCl pH 6.8, 4% SDS, 20%, glycerol, 0.2 mol/l DTT, 0.02% bromophenol blue and heated to 100°C for 5 min. We separated 10μg of protein on a 5% or 10% Criterion precast Tris-HCl polyacrylamide gel (Bio-Rad) and then transferred the protein onto a BioTraceNT nitrocellulose membrane (Pall Corporation, Pensacola, Fla). The membrane was blocked using 5% (w/v) Marvel in 0.1% (v/v) PBS-Tween and subsequently probed with primary antibody. Briefly, antibodies were obtained and diluted as follows: anti-mouse β-catenin (1:5000, Transduction), anti-mouse GS (1:15000, Transduction), anti-rabbit CPS (1:15000, Abcam) (Table 2-7). Anti-mouse glyceraldehyde- 3-phosphate dehydrogenase (GAPDH; 1:2000; Ambion) and anti-goat-Lamin B1 (1:2000, Santa Cruz) were used as loading control. Secondary antibodies were obtained and diluted as follows: peroxidase labeled anti-rabbit or anti-mouse both at 1:2000 (Amersham Biosciences, Bucks, UK). The signal was

detected with the ECL TM Western blotting analysis system (Amersham) and developed on Hyperfilm (Amersham). Experiments were repeated at least 3 times and typical results are shown.

2.2.4 Semi-quantitative RT-PCR

Total RNA was isolated from the cells or tissues using TRI reagent (Sigma, Poole, UK). Digestion with RQ1 RNase-free DNase (Promega, Southampton, UK) was performed to eliminate any contaminating genomic DNA. The concentration of extracted RNA was measured on a Beckman Spectrophotometer. Messenger RNA was isolated from total RNA by using SuperScript First-Strand Synthesis System for RT-PCR (Invitrogen Life Technologies). Messenger RNA (mRNA) was first isolated by incubation of Oligo(dT)12–18 oligonucleotides from 2μg extracted total RNA; complementary DNA (cDNA) was prepared by SuperScript II reverse transcriptase treatment. cDNA samples were incubated with 2 units of RNase H at 37^{o}C for 20 min to remove the RNA–cDNA hybridised residues. Polymerase chain reactions containing the mixture of the same concentration of cDNA, 1.1 X ReddyMix™ PCR Master Mix (ABgene, Surrey, UK) and 50 ng primers (listed in Table 2-9.) were processed in a DNA thermal cycler using the following conditions: denaturation at 94°C for 1 min, amplification at 56°C for 1 min and elongation at 72°C for 1 min for the indicated cycles. The samples were analyzed by electrophoresis using a 1.0% agarose gel and a 1 kb ladder (Invitrogen Life Technologies). Experiments were repeated at least 3 times and typical results are shown.

2.2.5 Fluorescence microscopy and image processing

For immunofluorescent staining, cells were cultured on noncoated glass coverslips, rinsed with PBS, fixed with 4% paraformaldehyde (PFA) in PBS for 30 min or ice cold Acetone/Methanol (1:1) for 5 min. For PFA fixed cells, cells were then permeabilised with 0.1% (vol/vol) Triton X-100 in PBS for 30 min, and incubated in 2% blocking buffer (Roche, East Sussex, UK), then incubated sequentially with primary antibodies for overnight at 4℃ and secondary antibodies for 2 hours at room temperature. After incubation of secondary antibodies, cells were washed 3 times with PBS buffer and counterstained with 4'6'-diamidinp-2-phenylindole (0.1μg/ml DAPI), and then mounted in mounting medium. Alternatively, for staining of liver buds cultures, the buds were fixed with MEMFA (10% formaldehyde, 0.1M Mops, pH7.4, EGTA 2mM, $MgSO_4$ 1mM) for 20 min at room temperature. They were then washed in PBS and stored in PBS at 4℃ for up to a few days. Prior to immunostaining, the cultures were treated with 1% Triton X-100 in PBS and then blocked as described above. The details and working dilution of antibodies has been listed in Table 2-3 and Table2-4.

Specimens were observed using Leica DMRB fluorescent microscope. Images were then collated into figures in Adobe Photoshop 7.0. Experiments were repeated at least 3 times and typical results are shown.

2.2.6 *In situ* hybridization

2.2.6.1 Mice and isolation of embryos

Animal husbandry and embryo isolation were carried out in accordance with Home Office regulations. Stage specific embryos were isolated from timed matings of CD1 mice, based on the observation of a copulatory plug representing embryonic day 0.5 (E0.5).

2.2.6.2 RNA probe synthesis

Digoxigenin (DIG)-labelled antisense and sense riboprobes were transcribed via the T7/SP6 RNA transcription system (Roche Diagnostics) according to the manufacturer's guidelines. The RNA probe sizes were as described as Table 3. *In situ* hybridization experiments were performed at least six times. For each experiment, at least four embryos from each developmental stage were used. Typical results are shown.

Table 2-12. Riboprobes for *in situ* hybridization

RNA probe	Corresponding cDNA region (bp)	Length (bp)
Fzd1	3151-3560	409
Fzd2	902-1300	398
Lrp5	600-1120	520
Wnt4	269-462	193
Wnt5a	820-1318	498
Wnt5b	1534-1774	240
Wnt9b	535-735	200
β–catenin	361-1021	660

2.2.6.3 Tissue preparation

Embryos were dissected and washed several times in sterile PBS. Following fixation in 4% PFA at 4ºC for overnight all embryos were washed three times in sterile PBS and processed for cryosectioning. The embryos were then preserved overnight in 30% sucrose in PBS, embedded in Optimal Cutting Temperature compound (OCT) media and stored at -80ºC.

2.2.6.4 In situ hybridization on sections

For *in situ* hybridization, cryosections (14μm) were obtained using a Leica CM1850 cryostat. Sections were fixed for 10min in 4% PFA and then washed 3 times in PBS for 3min each. The sections were then treated with 1 μg/ml proteinase K in 50 mM Tris pH 7.5, 5mM EDTA for 2-6 min according to the embryonic stage (2min for E10.5, 3min for E11.5, 4min for E12.5, 5min for E13.5 and 6min for E14.5-E18.5). Following proteinase K treatment, the sections were fixed again in 4% PFA for 10 min and then washed 3 min in PBS. The sections were washed a total of three times in PBS. Sections were acetylated in a buffer containing 1.36% triethanolamine, 0.18% HCl and 0.25% acetic anhydride for 10min and washed three times in PBS for 5 min each. Prehybridization was carried out in a 5 x saline sodium citrate (SSC) buffer humidified chamber at room temperature for 2hrs in hybridization buffer containing 50% formamide, 5 x SSC (pH4.5), 50μg/ml yeast RNA, 1% SDS and 50μg/ml heparin. Probes were diluted to 0.5μg/ml in hybridization buffer, heated to 80ºC for 5min and cooled for 5 min at room temperature. Hybridization was carried out overnight at 72ºC in a 50% formamide/5 x SSC humidified chamber. Posthybridization, the sections were washed as follows; 3 hours at 72ºC in 0.2x SSC for 3 hours, three times for 5 min each in 0.2 x SSC at room temperature and once in a solution (which we refer to as solution 1) containing 0.1M Tris (pH7.5),

0.15M NaCl and 0.24mg/ml levamisole for 5 min. Sections were blocked for 1hr in blocking solution containing 2% heat inactivated fetal calf serum and 2 % blocking reagent (Roche) in maleic acid buffer (100mM maleic acid and 150mM NaCl, pH7.5) and incubated overnight with an anti-DIG alkaline phosphatase antibody (1:5000 dilution in blocking solution) at 4ºC in a humidified chamber. Excess antibody was removed by washing three times for 5 min each in solution 1 and sections equilibrated by washing three times 10 min each in a solution (solution 2) containing 0.1M Tris pH9.5, 0.1M NaCl, 50mM $MgCl_2$, 1% Tween-20. Sections were then incubated with nitro-blue tetrazolium and 5-bromo-4-chloro-3'-indolyphosphate (NBT/BCIP) substrate (diluted to 20 μl/ml in solution 2) for 6hrs to 3 days. The reaction was stopped with 50mM Tris pH8.0, 5mM EDTA and the sections mounted in gel mount prior to photography. Experiments were repeated at least 6 times and typical results are shown.

2.2.7 Immunohistochemistry of mouse liver

2.2.7.1 Tissue Fixation, Embedding, and Processing

Embryonic livers were fixed by incubation overnight in 4% paraformaldehyde or 10% formalin (Sigma, St Louis, Mo) at 4°C depending on the antibody to be used. After fixation, tissue samples were processed sequentially through the following: PBS, NaCl, 50% ethanol, 70% ethanol, 90% ethanal, 100% ethanol, 100% ethanol, Histoclear, wax, wax and wax for one hour each in the Leica TP 1020 tissue processor. The tissue was embedded in paraffin wax at a Leica EG 1160 embedding station and sectioned using a Leica RM 2155 microtome into 4μm ribbons that were mounted on Fisherbrand microscope slides.

2.2.7.2 Immunohistochemical Analysis of Embryonic Mouse Liver

Samples were dehydrated through an increasing ethanol series, embedded in paraffin wax and sectioned at 5μm. Immunostaining for GS, CPS, Sox9 and phospho-histone3 was carried out as follows. Sections were dewaxed and rehydrated through a decreasing series of ethanol (100%, 100%, 95%, 90%, 70%, and 50%). Sections were rinsed in distilled water (dH_2O), washed twice in phosphate-buffered saline (PBS) for 5min each and permeabilized with 0.5% triton X-100 for 30min. High temperature antigen retrieval was performed in citrate (for GS) or EDTA (for Sox9 and CPS) buffer for 30min at 90°C and sections were allowed to cool to room temperature for 30min. After two 5-minute washes in PBS, endogenous peroxidases were quenched with the DAKO Envision peroxidase block (Glostrup, Denmark) for 10min. Sections were washed in PBS and blocked for 30min in 2% blocking buffer Roche (Mannheim, Germany) before addition of the following antibodies: anti-mouse GS (1:400; Transduction Laboratories, San Diego, California), anti-rabbit CPS (1:100, Abcam), anti-rabbit Sox9 (1:100; Millipore) and anti-rabbit-phosphohistone H3 (1:100, Upstate) in 2% blocking buffer overnight at 4°C. Excess primary antibody was removed by washing 3 times in PBS for 10min each. Sections stained for GS, Sox9 and phosphohistone H3 were incubated with the DAKO Envision peroxidase-labeled anti-mouse or rabbit secondary antibody polymer for 30min. The DAB substrate-chromogen mixture was added to the sections and allowed to develop within 10min. The reaction was terminated in dH_2O and the sections counterstained with haematoxylin where appropriate. Immunostaining for β-catenin (1:50; Transduction Laboratories) was carried out as previously described (Sansom et al., 2004). Sections stained for CPS were incubated with fluorescence conjugated secondary antibody after washed out excessive primary antibodies, Alexa Fluor 546 goat anti-rabbit IgG (Invitrogen) for 60min and then washed 3 times in

PBS for 10min each. The slides were then mounted with Mowiol. Specimens were observed using a Leica DMRB microscope. Image collection from the Leica was made with a Spot camera and images collated into figures in Photoshop. Experiments were repeated at least 3 times and typical results are shown.

2.2.8 Embryonic mouse liver bud dissection

Embryos were obtained from female CD1 mice (University of Bath, UK) 11.5 days postcoitum. The pregnant female mice were killed by cervical dislocation and the uteri were removed from the uterus. The uteri were transferred to a 100mm Petri dishes containing ice-cold phosphate buffered saline (PBS) where individual embryos were separated using surgical scissors (see Figure 2-1). The embryos were removed from their deciduas using fine forceps. The embryos were then transferred to a 60mm Petri dishes containing Minimum Essential Medium with Hank's salt (Sigma) and supplemented with 10%FBS, penicillin (100U/ml), streptomycin (100μg/ml), 2mM L-glutamine and gentamycin (20μg/ml). Using a tungsten needle, the liver buds were removed from its location. The liver buds were collected for tissue culture in 35mm culture dishes containing Basal Medium Essential (BME) medium supplemented with 10%FBS, penicillin (100U/ml), streptomycin (100μg/ml) and 2mM L-glutamine.

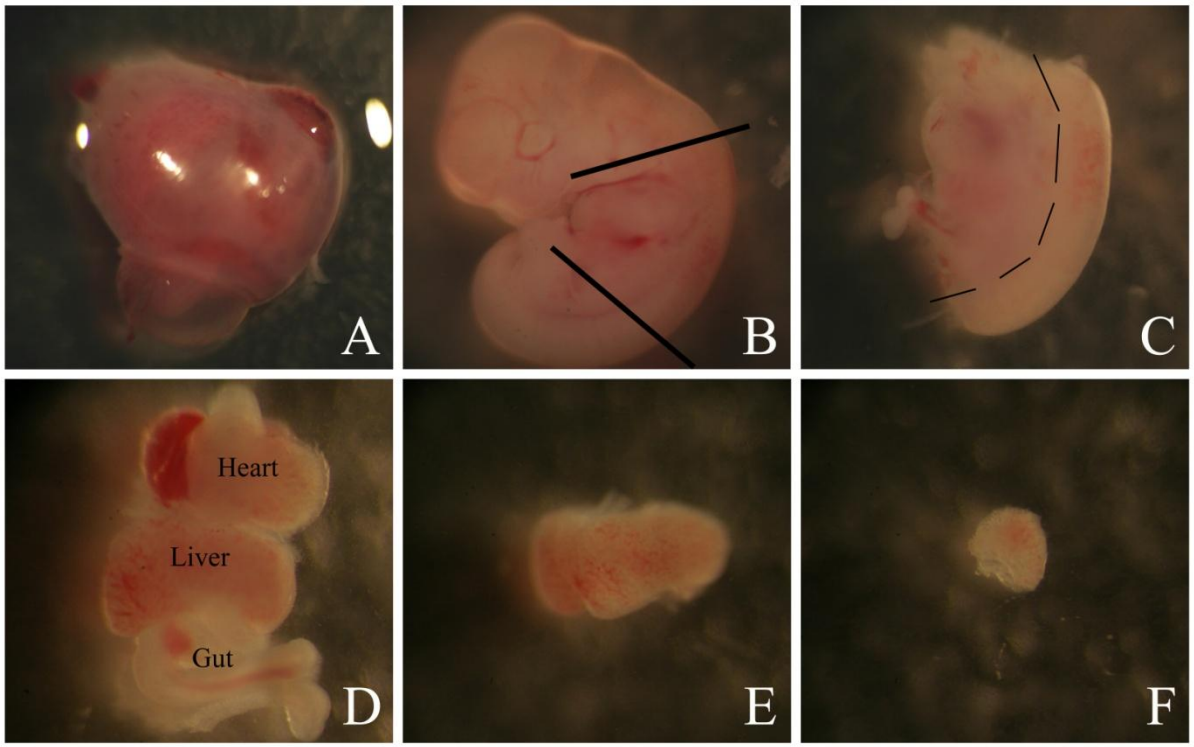

Figure 2.1 Steps in the dissection of liver bud from E11.5 mouse embryos

A. Separated uteri in 60mm Petri dish containing PBS.

B. E11.5 mouse embryo isolated from uteri.

C. Decapitation and dissect out tail (alone the black lines) and four limbs

D. Opening up the embryo (alone the dashed line) and removal of the internal viscera

E. Separation of the liver bud from the stomach

F. The bud was chopped into small pieces suitable for plating

2.2.9 Embryonic culture of mouse liver buds

Cultures were set up as described in Burke et al (2010) with minor modification. The liver buds were isolated from E11.5 mouse embryos as described above. To set up cultures, the coverslips were placed in 35 mm petri plates containing BME medium with Earle's salt, 20% foetal bovine serum and 50ug/ml gentamycin. A plastic cloning ring of 3 mm internal diameter was placed over a fibronectin-coated area, and cut pieces of liver were dropped into the centre. To ensure spreading during culture, the buds were turned if necessary with fine needle so that the cut surface lay in contact with the fibronectin. Cultures were maintained for up to 7 days at 37℃ in 95% air / 5% CO_2, with a change of medium every day. The cloning ring was removed at the second day of culture.

2.2.10 Adenoviral infections

2.2.10.1 Amplification of first-generation adenovirus

Adenoviral vectors were amplified in Human embryonic kidney (HEK) 293 cells grown in DMEM supplemented with 10% gamma irradiated FBS, penicillin (100U/ml), and 2mM L-glutamine. To amplify the virus, 3x T225 flasks were seeded with HEK 293 cells. When the cells reached 70% confluency, the media was replaced with 35ml of fresh DMEM and different dilutions of viral pre-stock (125µl, 12.5µl and 2µl) was added to each flask to ascertain the optimal volume. After 24hrs the cells should show small signs of cytopathic effect (CPE). A high CPE is not desirable and is caused by adding too much virus. After 48hrs the 50% cells should detach from the flask. If no effect is seen then the volume of virus added is not enough. The cells infected with optimal virus volume were harvested by shaking the flask to detach the remaining cells. The cells were pipetted

into 50ml Falcon tubes and centrifuged at 1000rpm for 4min. The supernatant was discarded and the pellet resuspended in 1ml of DMEM supplemented with 10% gamma irradiated FBS, penicillin (100U/ml), and 2mM L-glutamine. To lyse the cells, the cells were frozen on dry ice and thawed rapidly at 37℃ in water bath while shaking vigorously. The freeze/thaw cycle was repeated three times to release the virus. The pre-stock was then stored in -80℃.

2.2.10.2 Further adenovirus amplification and dialysis

Eight T225 flasks of HEK 293 cells at 70% confluency were infected with the previously determined volume of pre-stock. The cells were harvested 2-4 days later and centrifuged at 402 x *g* for 10min in 4 x 50ml Falcon tubes. The supernatant was discarded and the pellets were resuspended in 5ml of 100mM Tris-HCl. The cells were freeze/thawed rapidly four times and centrifuged at 402 x *g* for 5min. The supernatant was collected in 10ml syringes to estimate the volume and mixed with 0.6 volume of CsCl-saturated 100mM Tris-HCl. The virus supernatant was mixed and placed into Beckman 342412 centrifuge tubes. The tubes were filled to the neck and sealed so that no air bubbles were present. The tubes were then spun at 65000rpm for 24hrs at 22℃ in an ultracentrifuge (Beckman Vti90 rotor was used). After the tubes were removed, a white band of virus was visible approximately half way down the tube. To collect the virus, the bands were extracted using a 25G needle attached to a 2ml syringe inserted just below the band. The collected virus was then transferred to a new Beckman centrifuge tube and filled with balance solution (one volume of 100mM Tris-HCl pH8.0 with 0.6 volume of CsCl-saturated Tris-HCl). The tube was then sealed and spun again at 65000rpm overnight at 22℃ in the ultracentrifuge. The virus band was extracted again in 0.8-1.1ml and injected into a gamma irradiated Slide-A-Lyzer dialysis cassette (Pierce) with most of the air bubbles removed. The cassette was attached to a float and incubated while being stirred in

one litre of cold dialysis buffer (10mM Tris-HCl pH7.5 and 1mM $MgCl_2$) for 1hr. The buffer was then replaced with fresh buffer and the cassette was left for another hour. The virus was then extracted and passed through a 0.22μm filter into a Falcon tube. The virus was then aliquoted into sterile eppendorf tubes, frozen on dry ice and stored at -80℃.

2.2.10.3 Rapid titre of adenovirus

To titre the virus, a 12-well plate was seeded with HEK 293 cells. When the cells were 90% confluent the purified virus was diluted in the medium (10^2, 10^3, 10^4, 10^5, 10^6 and 10^7 dilutions) and 100μl of each dilution was added to each well with one well left uninfected to as a negative control. The infected cells were incubated for 48hrs at 37℃. Later, the cells were fixed with ice-cold methanol and incubated at 4℃. After 10min the fixed cells were washed with 3x PBS and blocked by adding 1ml of 2% blocking buffer to each well and left for 30min. The mouse anti-hexon primary antibody was diluted 1:1000 in 2% blocking buffer and 0.5ml was added to each well after blocking. The cells were incubated with antibody for 1hr. The secondary HRP conjugated rat anti-mouse antibody was then diluted 1:500 in 2% blocking buffer and 0.5ml was added after washing 3xPBS. The cells were left to incubate for 1hr. Later, 3,3'-Diaminobenzidine (DAB) solution was prepared as recommended by the manufacturer (Vector Laboratories). The cells were washed again 3xPBS after removing the secondary antibody and 0.5ml of the DAB solution was added to each well. Infected cells were stained with 2-3min. The cells were viewed under the Stereomicroscope (DTX-10) and the reaction stopped by rinsing the cells with water. The cells were counted in 6 fields viewed under the 20x objective. The titre was then estimated as follows: average number of infected cells per field x573/0.1 x dilution factor.

CHAPTER 3 EXPRESSION PROFILING OF HEPATOCYTE MARKERS AND WNT LIGANDS AND RECEPTORS DURING EMBRYONIC LIVER DEVELOPMENT

3.1 Background

Metabolic zonation in the adult liver has been studied extensively (Gebhardt, 1992). However, the molecular mechanism(s) responsible for the induction of zonation during embryonic liver development remains less well understood. The detoxification of ammonia is heterogeneously distributed across the liver lobule, The liver contains two systems for the detoxification of ammonia the urea cycle and glutamine synthetase. The enzymes of the urea cycle and glutamine synthetase have a reciprocal distribution pattern in the liver. In adult liver, carbamoylphosphate synthetase (CPS), (the rate-limiting enzyme in the urea cycle), is present in the periportal, intermediate and first few layers of the perivenous zone. CPS is absent in the very last downstream perivenous hepatocytes, in which glutamine synthetase (GS) is expressed. We wished to determine the expression patterns of GS and CPS during development of the mouse embryonic liver, using a combination of immunostaining and western blotting techniques.

The Wnt/β-catenin pathway is an evolutionarily conserved signalling cascade that plays a key role in development and adult tissue homeostasis and is aberrantly activated in many tumours. For example, the APC gene was among the first tumour suppressors to be cloned. A germline APC mutation is the genetic cause of a hereditary cancer syndrome termed Familiar Adenomatous Polyposis (FAP) (Kinzler et al., 1991; Nishisho et al., 1991). FAP patients inherit one defective APC allele and as a consequence develop large numbers of colonic adenomas, or polyps, in early adulthood. Loss of both APC alleles occurs in the large majority of sporadic colorectal cancers (Kinzler and Vogelstein, 1996). Loss-of-function mutations in Axin have also been found in hepatocellular carcinomas, whereas oncogenic β-catenin mutations occur in a wide variety of solid tumours (Reya and Clevers,

2005). In liver, the Wnt/β-catenin pathway has been found to play a key role in metabolic zonation of adult liver, regeneration and hepatocellular carcinogenesis (reviewed in Thompson and Monga, 2007). Although β-catenin is central to liver biology, its upstream effectors remain obscure. Classically, there are 19 Wnt and 10 Frizzled genes in the mouse genome. One previous study identified 11 Wnts and 9 Frizzleds that are normally expressed in the adult mouse liver (Zeng et al., 2007). However the expression of individual Wnt or Frizzled genes during liver development is not known. As the first step towards understanding the role of the Wnt/β-catenin pathway in liver development, we determined the expression profile of members of the Wnt pathway (listed in Table 3-1) using *in situ* hybridization from mouse embryonic day 11.5 (E11.5) to E18.5.

Table 3-1 Target mRNAs for *in situ* hybridization

Receptors	Ligands	Effector
Fzd1	Wnt4	β-catenin
Fzd2	Wnt5a	
Lrp5	Wnt5b	
	Wnt9b	

3.2 Results

3.2.1 Expression of CPS and GS during development

In order to investigate the role of the Wnt/β-catenin signalling pathway in the development of zonation, we also analysed the expression of two key genes that are heterogeneously distributed across the liver lobule and are involved in ammonia detoxification: the periportal marker, Carbamoylphosphate synthetase (CPS) and the perivenous marker, Glutamine synthetase (GS). We used mouse livers dissected from E12.5 to E18.5. Western blotting and immunostaining techniques were applied to determine the spatio-temporal expression of the CPS and GS proteins.

Total protein was extracted from mouse embryonic livers at E12.5, 13.5, 14.5, 15.5, 16.5, 17.5 and 18.5 and probed for CPS and GS expression (Figure 3.1). In agreement with previous studies (Notenboom et al., 1997), CPS became expressed between E13.5 and E14.5 and gradually increased thereafter. GS only became expressed between E17.5 and E18.5.

To determine when the normal embryonic zonal expression pattern was established, we used immunostaining to determine the localisation of CPS and GS and in developing mouse embryos. We found that a few cells expressed CPS at E13.5 and E14.5 (Figure 3.2) but then the numbers increased and gradually the normal expression pattern became apparent with most hepatocytes expressing CPS in periportal, intermediate and the first few layers of the perivenous zone by E17.5. In contract, GS expression was restricted to a few cell layers around the central vein at E17.5-18.5 (Figure 3.3).

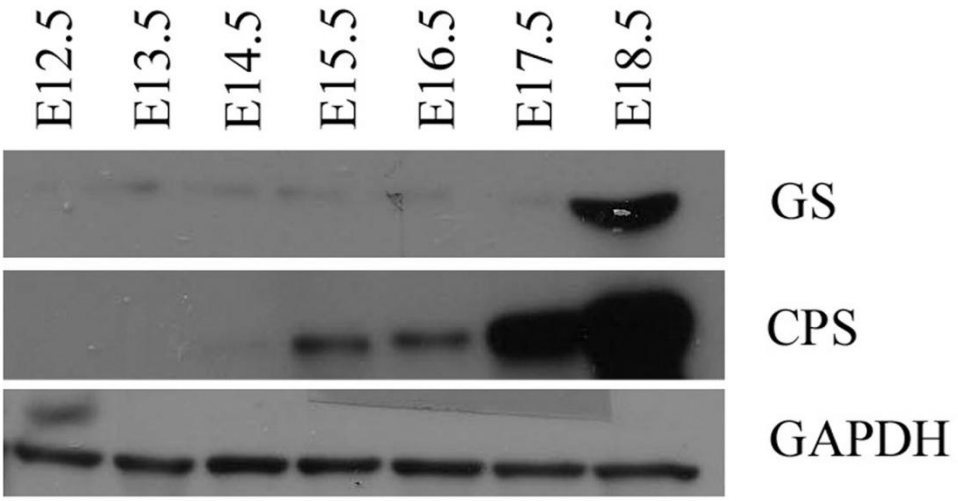

Figure 3.1 Expression of GS and CPS during embryonic development

Cell extracts were prepared from embryonic livers from E12.5 to E18.5. 10μg of protein from each sample was separated by electrophoresis on a 10% Tris-HCl gel and blotted onto PVDF membrane. Blots were probed with primary antibodies against GS, CPS or GAPDH and then with HRP-conjugated secondary antibodies. The signal was detected by ECL chemiluminescence.

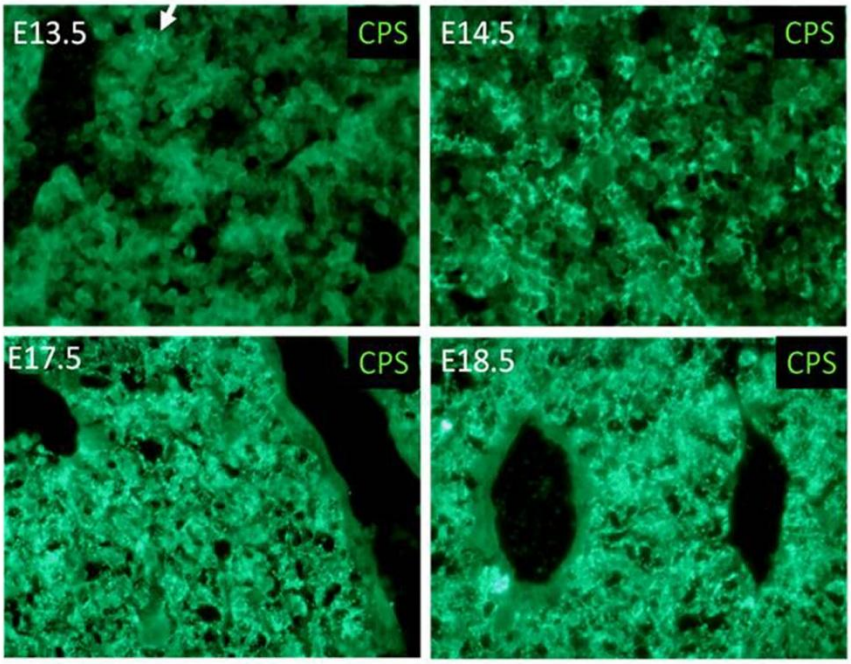

Figure 3.2 CPS protein starts to be expressed in liver around E13.5 days of mouse development

OCT-embedded cryosections of embryonic livers were immunostained with anti-CPS and FITC conjugated secondary antibody. Only a few cells express CPS in the E13.5 liver (arrows) (Magnification X 400).

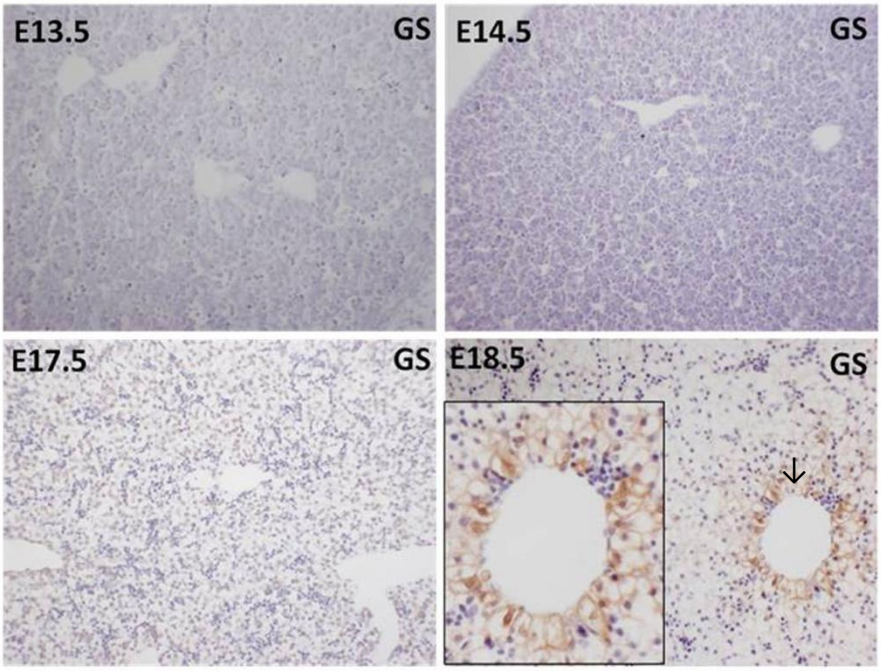

Figure 3.3 GS is expressed in liver of mouse embryos between E17.5 and E18.5

Paraffin-embedded sections of embryonic livers were immunostained with anti-GS and horseradish peroxidise conjugated secondary antibody. The signal was detected by DAB staining. Haemotoxylin was used as a nuclear counterstain (Magnification X 200). Magnified image of E18.5 (arrowed) is at left lower corner (X 400).

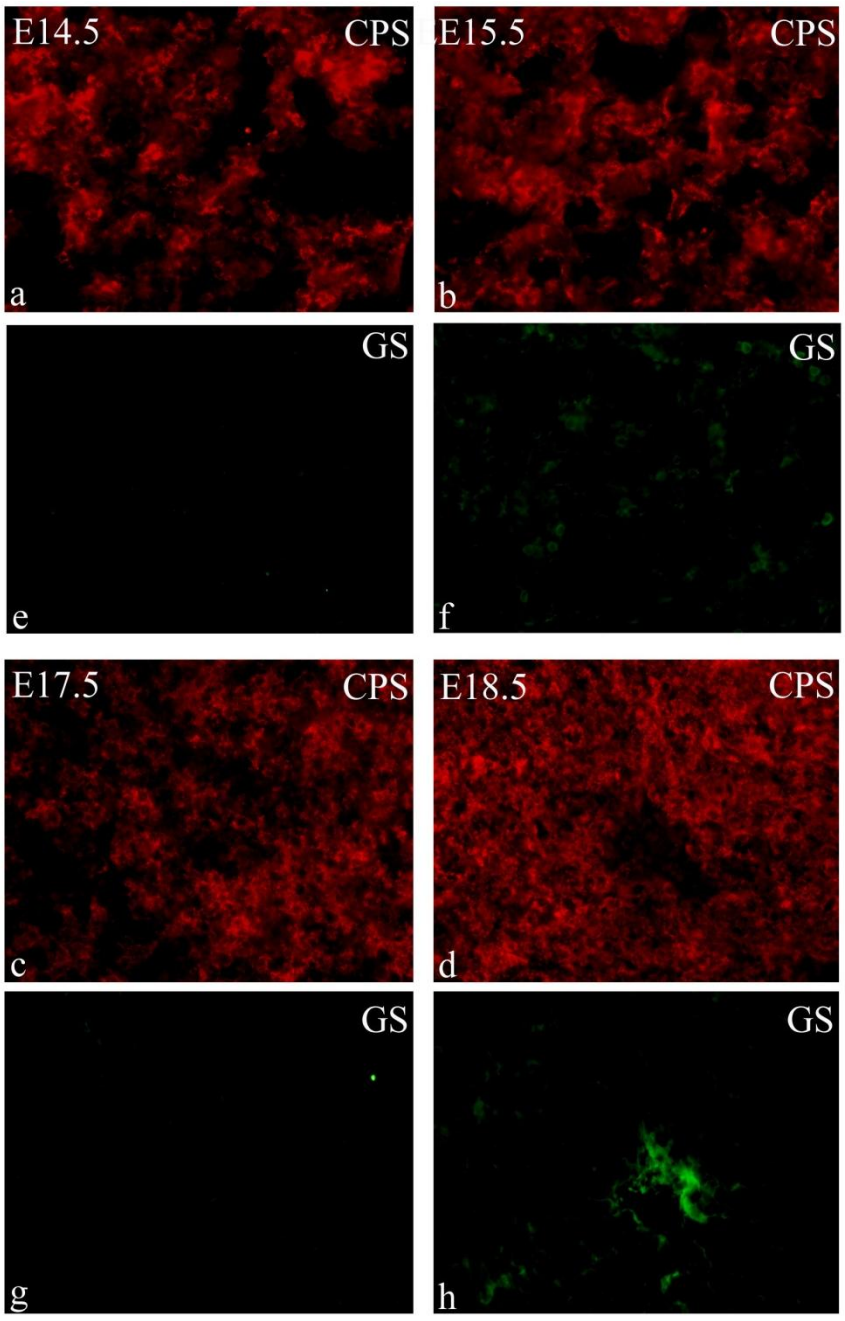

Figure 3.4 Regional distributions of GS and CPS in the liver of an E18.5 mouse embryo

OCT-embedded cryosections of embryonic livers from E14.5 (a and e), E15.5 (b and f), E17.5 (c and g) and E18.5 (d and h) were immunostained with both anti-CPS (red) and anti-GS (green) antibodies. GS positive cells (g) were located complementary to CPS positive cells (d) in E18.5. (Magnification X 400)

3.2.2 Expression of β-catenin during development

To determine the expression of activated β-catenin versus total β-catenin, we probed cytosolic and nuclear fractions using an antibody raised to the total (phosphorylated and dephosphorylated) of β-catenin (Figure 3.5). Nuclear β-catenin was transiently expressed at E12.5 and then gradually decreased. Although we found evidence of small amount of nuclear β-catenin between E14.5 to E16.5, the highest levels were observed between E17.5 and E18.5 correlating with the peak of GS expression.

Immunohistochemical analysis was performed to determine the localisation of β-catenin during mouse liver development (Figure 3.6). Paraffin-embedded embryonic livers from E14.5 to E18.5 were sectioned and probe to β-catenin antibody. Nuclear β-catenin was barely detectable at E14.5 and E15.5. However, in agreement with the western blotting data (Figure 3.5), a robust nuclear β-catenin signal was detectable between E17.5 and E18.5 of mouse liver development.

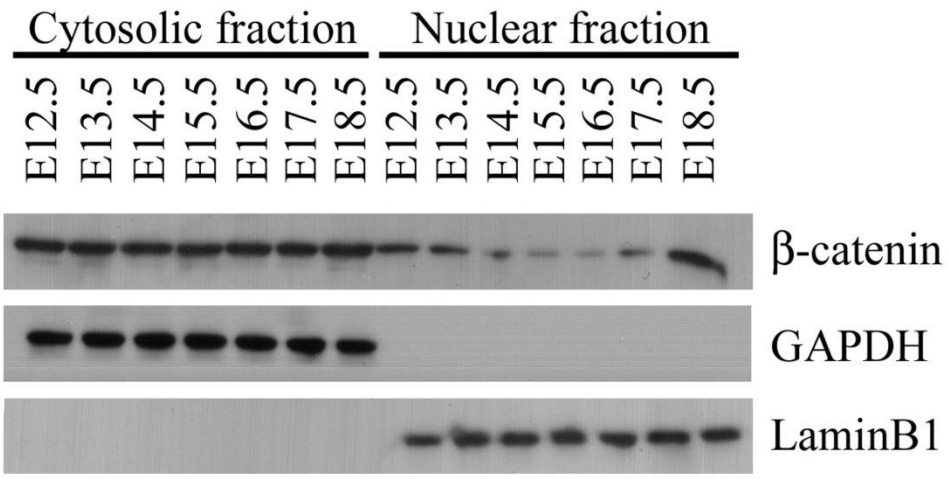

Figure 3.5 Expression of β-catenin in the developing mouse liver

Nuclear and cytosolic extracts were prepared from embryonic livers from E12.5 to E18.5. 10ug of protein sample was separated by electrophoresis on 10% Tris-HCl gel and blotted onto PVDF membrane. Blots were probed with primary antibodies against β-catenin, the nuclear protein LaminB1 or the cytosolic protein, GAPDH and then with HRP-conjugated secondary antibodies. The signal was detected by ECL chemiluminescence. Some weak nuclear β-catenin expression was detected from E12.5 to E16.5. At E18.5, β-catenin was strongly expressed in the nuclear fraction.

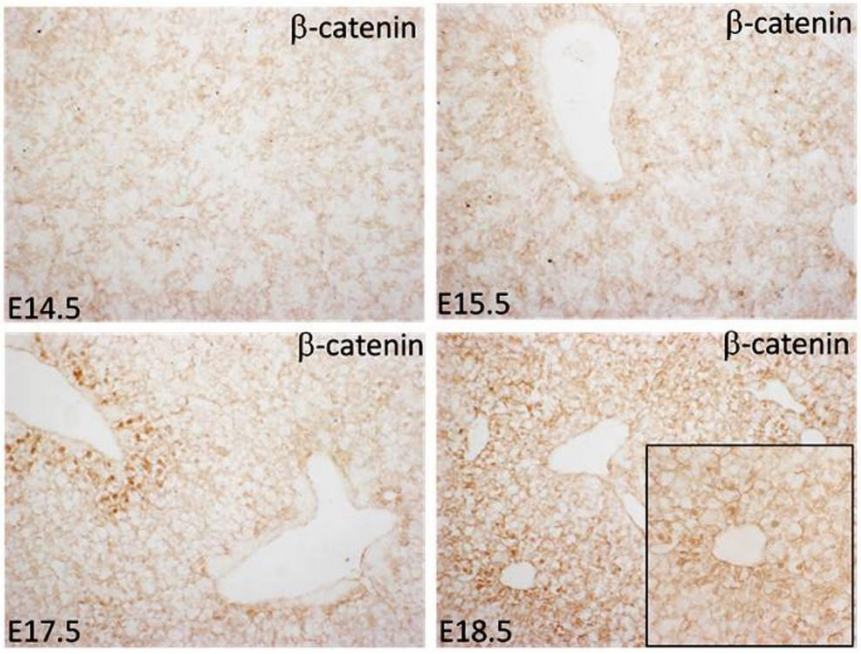

Figure 3.6 β-catenin becomes activated between E17.5 and E18.5

Paraffin-embedded sections of embryonic livers from E14.5, E15.5, E17.5 and E18.5 were immunostained with anti-β-catenin and HRP-conjugated secondary antibody. β-catenin remains membrane bound form since E14.5. Nuclear β-catenin became abundant between E17.5 and E18.5. (Magnification X 200). Magnified image of E18.5 is at right lower corner (X 400).

3.2.3 Expression of Wnt pathway components during liver development

3.2.3.1 Wnt4

Wnt4 was not expressed during early liver development from E11.5 to E12.5 (Figure 3.7 I-J). Bi et al previously noted the expression by RT-PCR at E12.5 (Bi et al, 2009). In contrast, we found expression of *Wnt4* from E14.5 in the embryonic liver and the signal remained strong until E18.5 (Figure 3.7 K-N). We also observed expression in the mucosal lining of stomach and duodenum from E14.5 to E18.5, and lung, kidney and pancreatic primordium expression from E13.5 to E15.5. This was in accordance with previous studies conducted by RT-PCR on the digestive tract (Lickert et al., 2001) and whole-mount *in situ* hybridization during kidney ontogeny (Merkel et al., 2007), respectively.

3.2.3.2 Wnt5a

We did not detect *Wnt5a* expression in the mouse embryonic liver throughout E11.5 to E18.5. This was in agreement with the previous RT-PCR results (Bi et al, 2009). However, at stage E11.5, we found *Wnt5a* expressed in the medial and lateral nasal process, the primordium of the primary palate and the ventral extremity of lower jaw (Figure 3.8 H). The expression of *Wnt5a* was maintained in these tissues until stage E13.5 (Figure 3.8 I-J). This is the first time the localization of *Wnt5a* transcripts was closely observed during mouse development. The observation was consistent with the previous study of chicken craniofacial development which showed *Wnt5a* expression in maxillary, mandibular prominence, lateral nasal prominences and lateral edges of the frontonasal mass by

whole-mount *in situ* hybridization (Geetha-Loganathan et al., 2009). We also observed *Wnt5a* expression in the tips of branchial arch and lower limbs from E11.5 to E13.5.

3.2.3.3 Wnt5b

Wnt5b expression has not been shown in the mouse embryonic liver to date. In this study we clearly observed *Wnt5b* expression in the hepatic bud from E11.5 to E18.5 (Figure 3.9 H-N). We also found *Wnt5b* expression in the branchial arch, the mucosa of duodenum and stomach, heart and lung bud at E11.5 and E12.5; lung, mucosal lining of stomach, duodenum and metanephros at E13.5; lung, duodenum, pancreatic primordium and metanephros at E14.5 and E15.5; intestine, gastric mucosa and pancreas at E17.5 and E18.5. However previous RT-PCR results showed the absence of *Wnt5b* mRNA expression in mouse embryonic liver (Bi et al, 2009). This difference could be due to higher sensitivity of the *in situ* hybridization. This gastro-intestinal pattern of *Wnt5b* gene expression confirmed previous studies with RT-PCR on mouse embryonic digestive tract (Lickert et al., 2001) (Heller et al., 2002).

3.2.3.4 Wnt9b

We first observed *Wnt9b* expression at stage E11.5 in the hepatic buds and other tissues including the branchial arch, lung bud, mucosa of duodenum and stomach. The signal remained in these tissues until E12.5 (Figure 3.10 H-I). By stage E13.5, the *Wnt9b* expression gradually reduced and became undetectable in the liver and other tissues (Figure 3.10 J). This was in contrast with previous RT-PCR experiment showing expression through whole embryonic stages from E12.5 till E18.5 (Bi et al, 2009).

3.2.3.5 Frizzled 1

We detected *Fzd1* mRNA expression in the hepatic buds from E11.5 until E18.5 (Figure 3.11 H-N). This was in accordance with the previous results demonstrated by RT-PCR in mouse embryonic liver (Bi et al, 2009). We observed *Fzd1* expression in other tissues including mucosa of duodenum and stomach, lung bud, main bronchus and heart at E11.5; lung bud, stomach and duodenum at E12.5; lung, mucosal lining of stomach, duodenum and metanephros (the definitive kidney) at E13.5 and E14.5; intestine, gastric mucosa and pancreas at E17.5 and E18.5. The expressions of the receptor in these tissues has not been reported previously but suggested a role for the Wnt/β-catenin pathway in the development of these tissues. To date, this is the first comprehensive expression pattern for *Fzd1* to be conducted.

3.2.3.6 Frizzled 2

We did not observe *Fzd2* signal at any of the early stages of mouse development (i.e. from E11.5 to E13.5). *Fzd2* first appeared at stage E14.5 in the lung, kidney, duodenum and pancreatic primordium. *Fzd2* expression persisted in these tissues up to stage E15.5 (Figure 3.12 K and L). At E17.5 and E18.5, we were still able to observe *Fzd2* expression in the intestine tissue. However, *Fzd2* signal was clearly excluded from the liver through E11.5 to E18.5. The gastro-intestinal expression was consistent with previous RT-PCR observations suggesting *Fzd2* is broadly expressed in mouse foregut mesenchyme (Heller et al., 2002).

3.2.3.7 LRP5

We first observed *Lrp5* expression at stage E11.5 in the hepatic buds and the signal remained until stage E13.5 (Figure 3.13 H-J). However, the *Lrp5* expression was gradually lost from the liver after E14.5 (Figure 3.13 K-N). We also found *Lrp5* in many tissues other than liver including the mucosa of the stomach and duodenum, the ventricular and atrial chambers of the heart, the midgut loop, branchial arch and lung bud at E11.5; lung bud, stomach and duodenum at E12.5; lung, mucosal lining of stomach, duodenum and metanephros at E13.5; lung, metanephros, adrenal gland and duodenum at E14.5; lung, kidney, adrenal gland, duodenum and pancreatic primordium at E15.5. Bi et al showed *Lrp5* mRNA equally expressed throughout all embryonic stages from E12.5 to E18.5 (Bi et al, 2009). However, *in situ* hybridization is more sensitive than PCR and our results demonstrate that *Lrp5* expression decreased after E14.5.

3.2.3.8 β-catenin

β-catenin expression was first observed in the hepatic bud at E11.5 (Figure 3.14 H). By stage E14.5, *β-catenin* was strongly expressed in the liver. However, the signal was gradually lost from the liver by stage E17.5. Previous data demonstrated peak expression of *β-catenin* during early liver development at E10-E12, followed by a decrease and a complete loss of normal *β-catenin* after E16 through the remaining prenatal period (Micsenyi et al, 2004). We also observed *β-catenin* expression in the cystic primordium (gall bladder), mucosa of stomach and duodenum, midgut loop, branchial arch, lung bud, main bronchus at E11.5; lung bud, stomach and duodenum at E12.5; lung, mucosal lining of stomach, duodenum and metanephros at E13.5; lung, cortical region of metanephros, pancreatic primordium and duodenum at E14.5; lung, cortical region of kidney, adrenal gland,

duodenum and pancreatic primordium at E15.5; intestine, gastric mucosa and pancreas at E17.5 and E18.5.

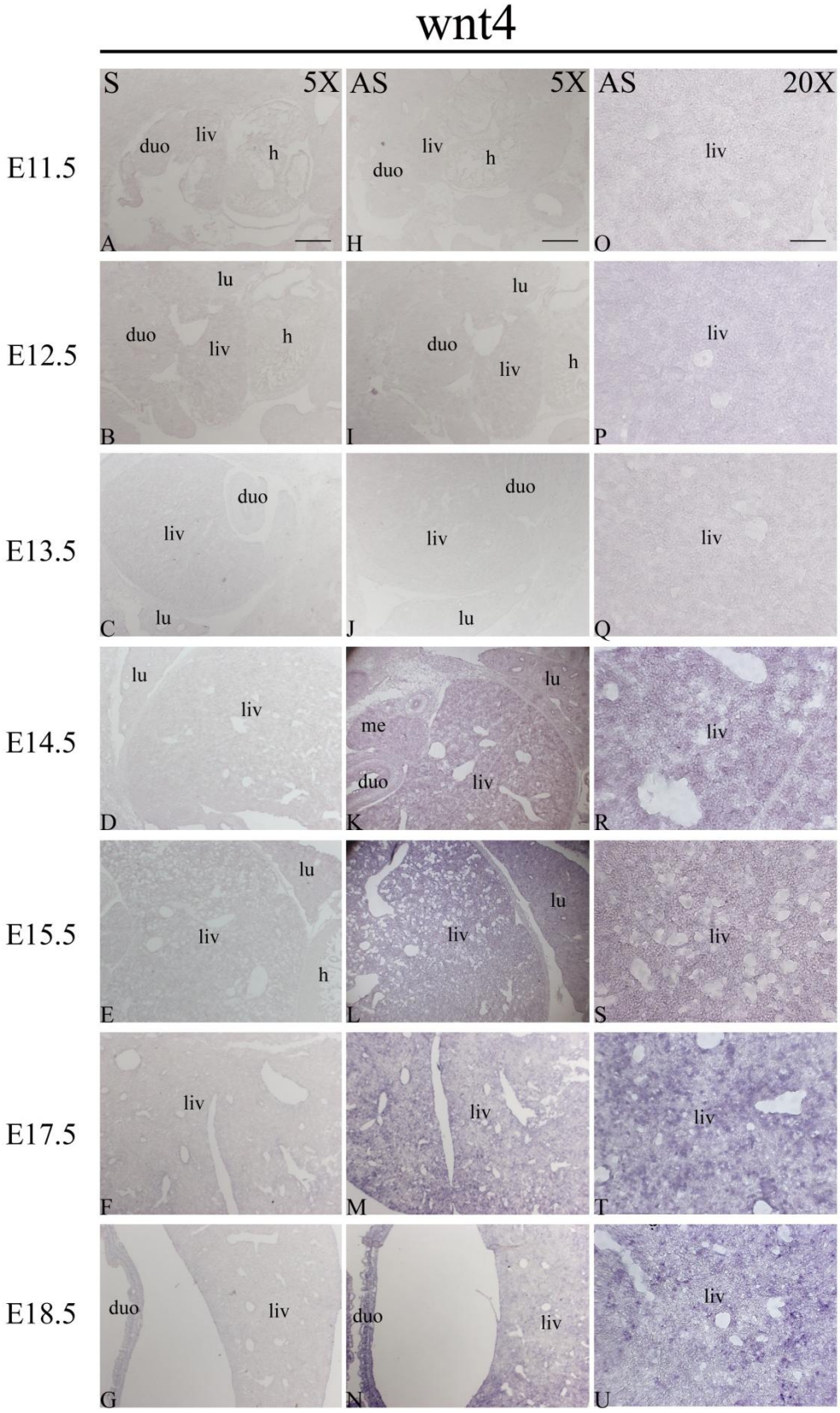
wnt4
S
5X
AS
5X
AS
20X
E11.5
E12.5
E13.5
E14.5
E15.5
E17.5
E18.5
duo
liv
h
lu
me
A
H
O
B
I
P
C
J
Q
D
K
R
E
L
S
F
M
T
G
N
U

Figure 3.7 *Wnt4* expression started from E14.5 during mouse liver development

Sections were hybridized with sense (A-G) and anti-sense probes (H-N). *Wnt4* was expressed in embryonic liver from E14.5 and remained strongly expressed until E18.5. Annotations as follows: h, heart; liv, liver; lu, lung; duo, duodenum; me, metanephros. O-U are higher magnification of livers from H-N. Scale bars in A and H represent 350 μm; in O represents 87 μm.

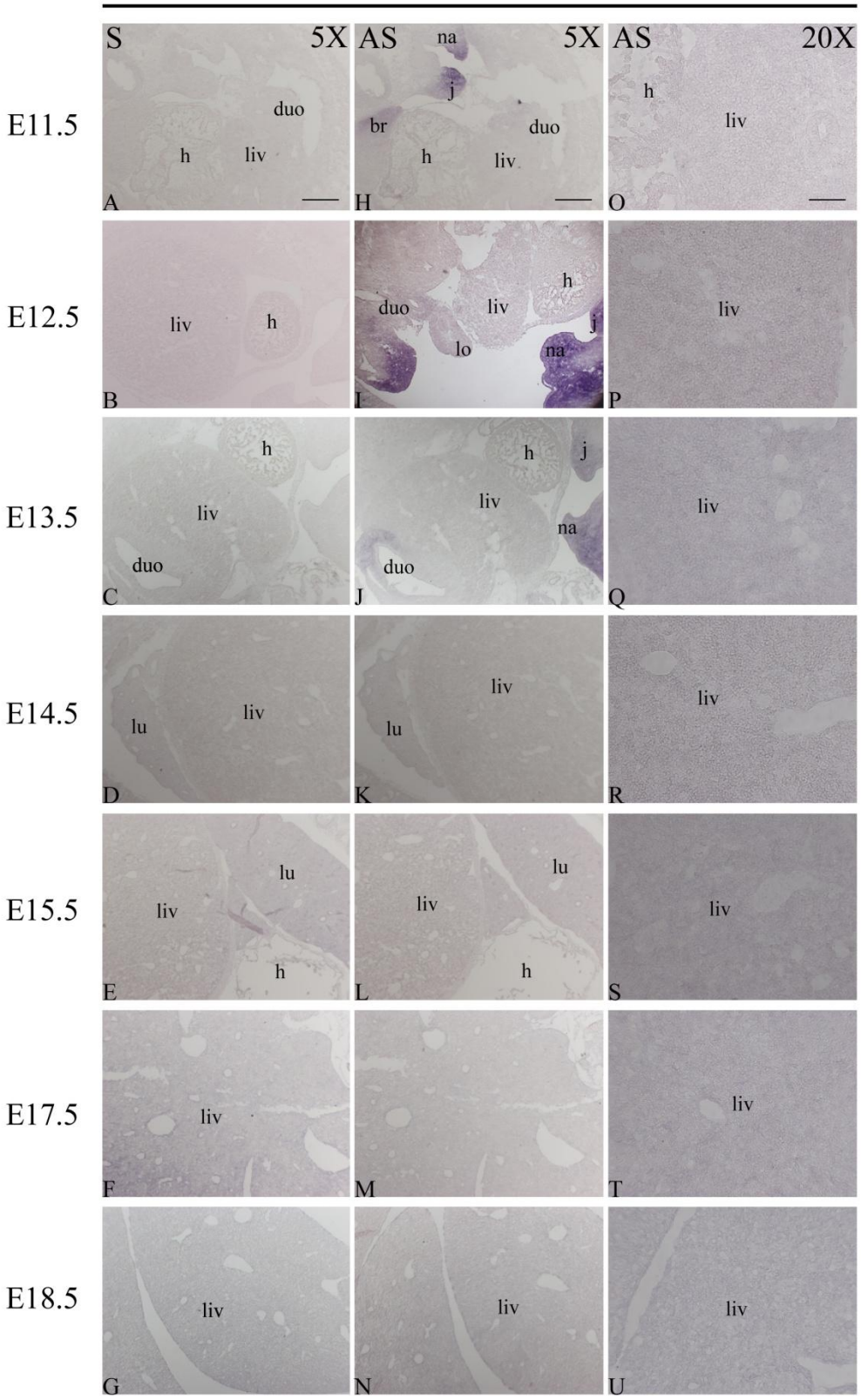
wnt5a
S
5X
AS
na
5X
AS
20X
E11.5
duo
h
liv
A
br
j
duo
h
liv
H
h
liv
O
E12.5
liv
h
B
duo
liv
h
j
lo
na
I
liv
P
E13.5
h
liv
duo
C
h
j
liv
na
duo
J
liv
Q
E14.5
lu
liv
D
liv
lu
K
liv
R
E15.5
lu
liv
h
E
lu
liv
h
L
liv
S
E17.5
liv
F
M
liv
T
E18.5
liv
G
liv
N
liv
U

Figure 3.8 *Wnt5a* is expressed in frontonasal region during mouse development

Sections were hybridized with sense (A-G) and anti-sense probes (H-N). We did not detect any *Wnt5a* expression in mouse embryonic liver. However, the maxillary expression of *Wnt5a* was observed from E11.5 to E13.5 in a variety of tissues. Annotations as follows: h, heart; liv, liver; lu, lung; duo, duodenum; me, metanephros; j, lower jaw; br, branchial arch; lo, lower limb; na, nasal process. O-U are higher magnification of livers from H-N. Scale bars in A and H represent 350 μm; in O represents 87 μm.

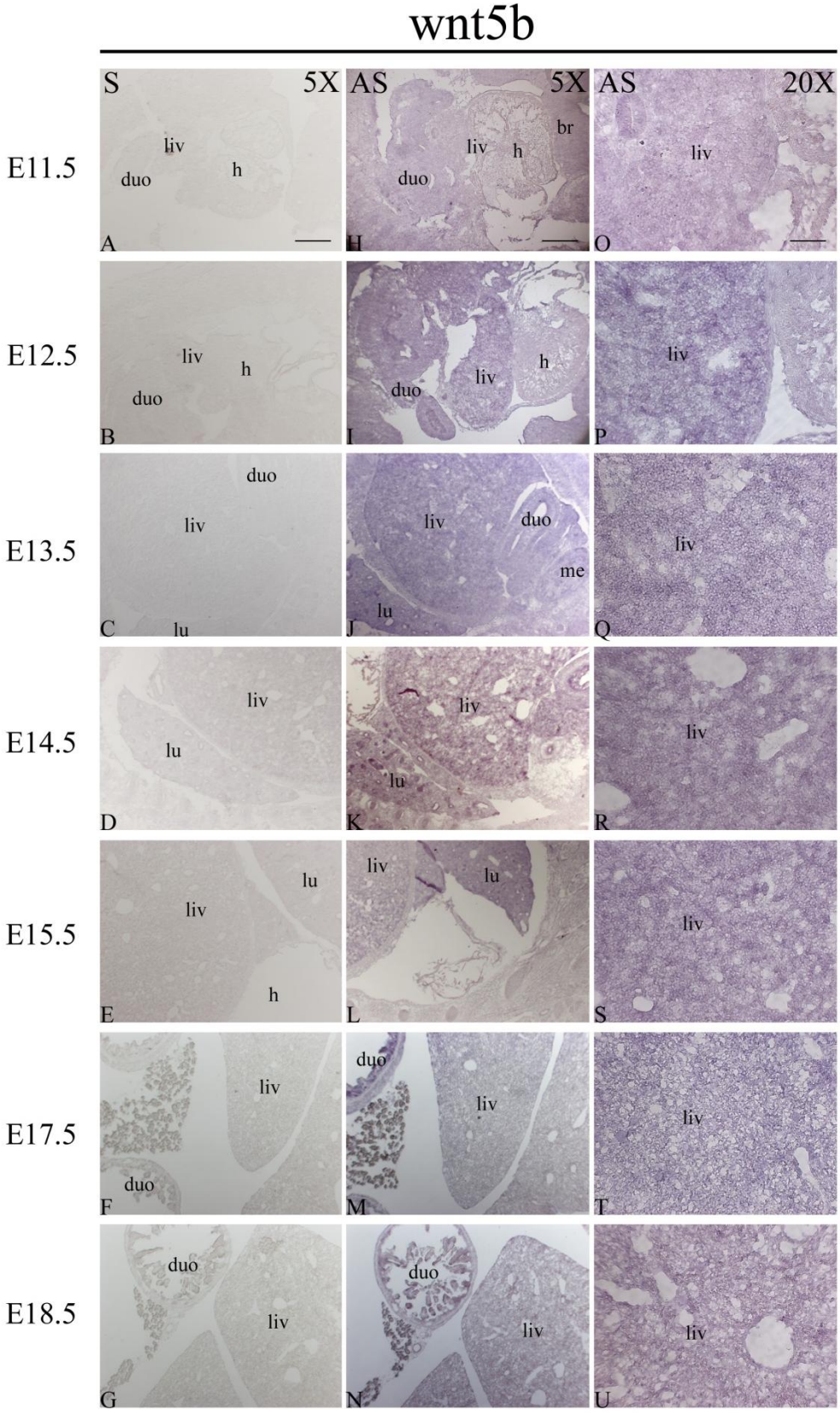
wnt5b
S
5X
AS
5X
AS
20X
E11.5
liv
duo
h
br
A
H
O
E12.5
B
I
P
E13.5
C
J
Q
me
lu
E14.5
D
K
R
E15.5
E
L
S
E17.5
F
M
T
E18.5
G
N
U

Figure 3.9 *Wnt5b* is expressed throughout E11.5 to E18.5 in developing mouse liver

Sections were hybridized with sense (A-G) and anti-sense probes (H-N). *Wnt5b* was expressed in mouse embryonic liver from E11.5 to E18.5. Annotations as follows: h, heart; liv, liver; lu, lung; duo, duodenum; me, metanephros. O-U are higher magnification of livers from H-N. Scale bars in A and H represent 350 μm; in O represents 87 μm.

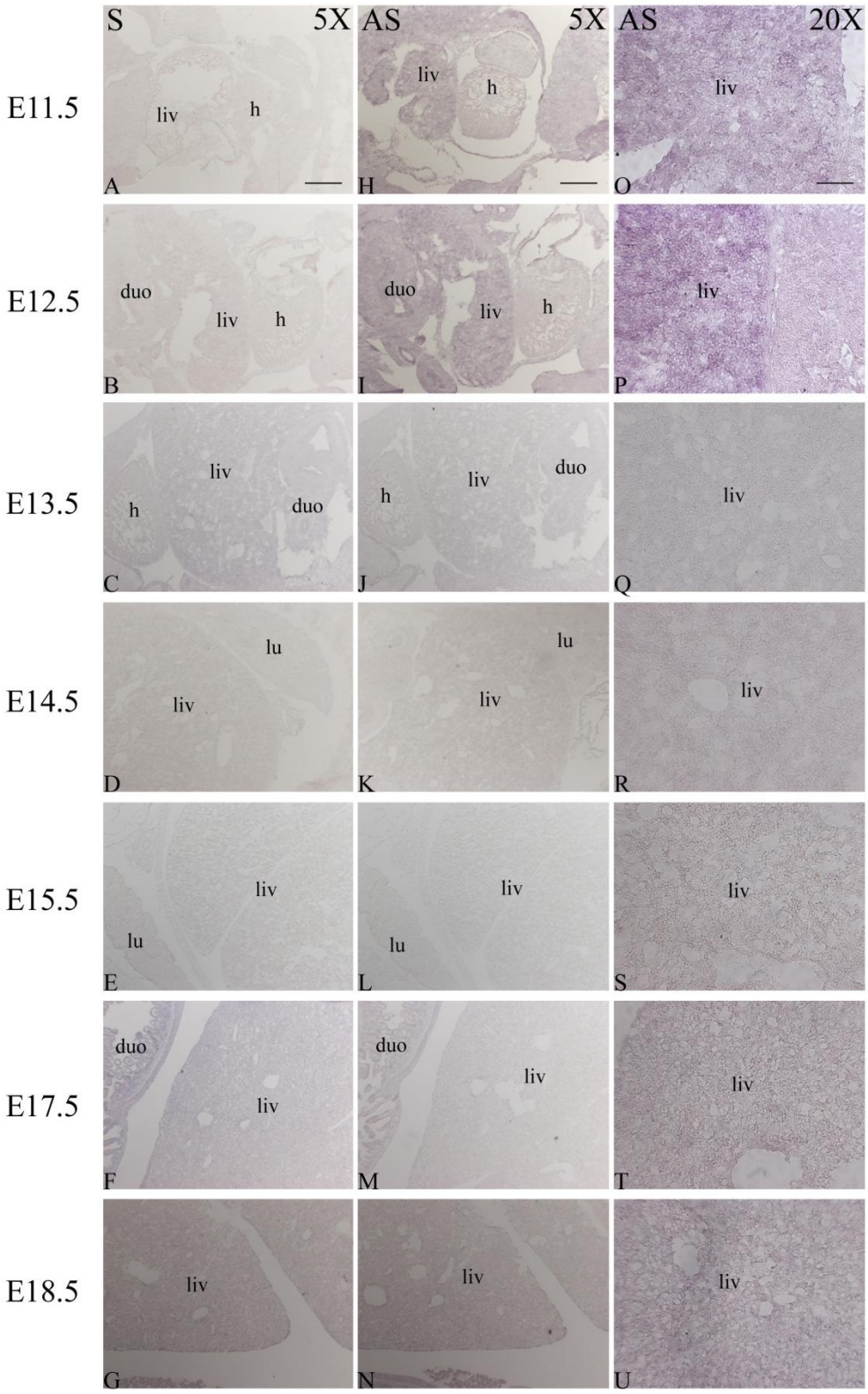
wnt9b
S
5X
AS
5X
AS
20X
E11.5
liv
h
liv
h
liv
A
H
O
E12.5
duo
liv
h
duo
liv
h
liv
B
I
P
E13.5
liv
h
duo
h
liv
duo
liv
C
J
Q
E14.5
lu
liv
lu
liv
liv
D
K
R
E15.5
liv
lu
liv
lu
liv
E
L
S
E17.5
duo
liv
duo
liv
liv
F
M
T
E18.5
liv
liv
liv
G
N
U

Figure 3.10 Expression of *Wnt9b* was restricted in E11.5 and E12.5 during mouse liver development

Sections were hybridized with sense probes (A-G) and anti-sense probes (H-N) to *Wnt9b* . Magnified areas were shown in the framed upper right corner corresponding to the pointed region. *Wnt9b* expression in the embryon was restricted to between E11.5 and E12.5. Annotations as follows: h, heart; liv, liver; lu, lung; duo, duodenum; me, metanephros. O-U are higher magnification of livers from H-N. Scale bars in A and H represent 350 μm; in O represents 87 μm.

Frizzled 1

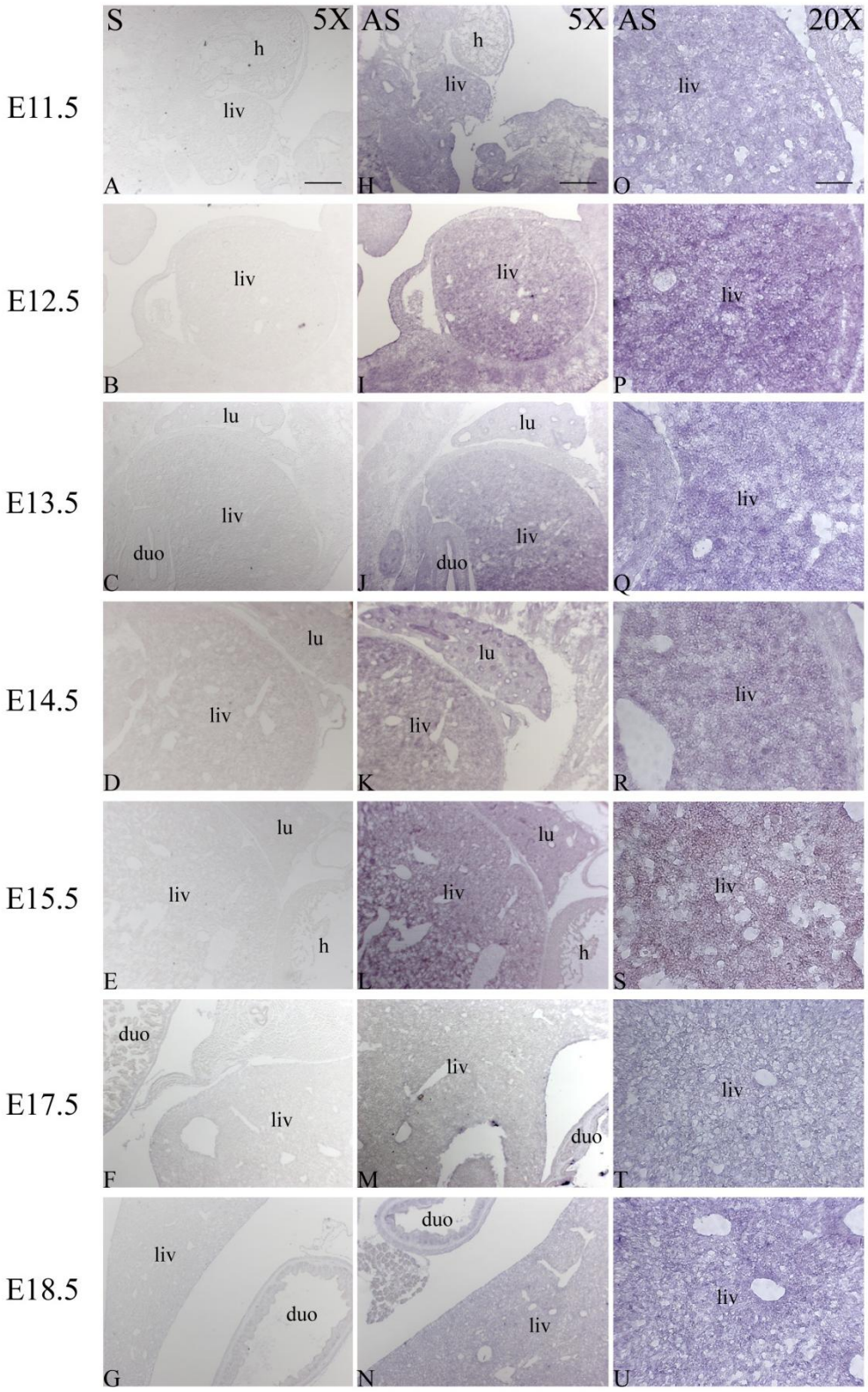
E11.5
E12.5
E13.5
E14.5
E15.5
E17.5
E18.5
S
5X
AS
5X
AS
20X
h
liv
lu
duo
A
H
O
B
I
P
C
J
Q
D
K
R
E
L
S
F
M
T
G
N
U

Figure 3.11 *Fzd1* is expressed from E11.5 to E18.5 during mouse liver development

Sections were hybridized with sense (A-G) and anti-sense probes (H-N) to *Fzd1*. Magnified areas were shown in the framed upper right corner corresponding to the arrow pointed region. *Fzd1* was expressed in the mouse embryonic livers throughout the stages of development examined from E11.5 to E18.5. Annotations are as follows: h, heart; liv, liver; lu, lung; duo, duodenum; me, metanephros. O-U are higher magnification of livers from H-N. Scale bars in A and H represent 350 μm; in O represents 87 μm.

Frizzled 2

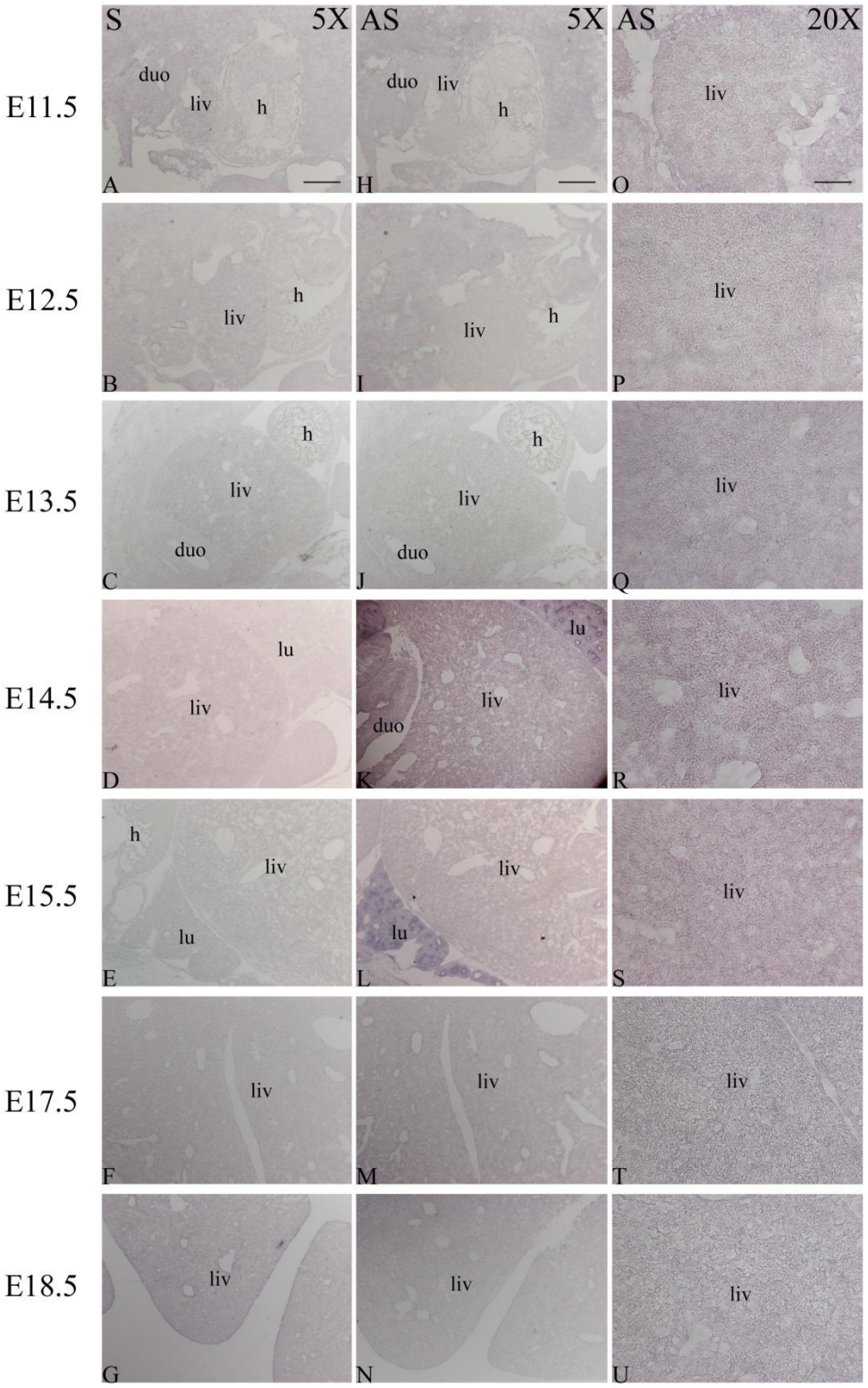
S
5X
AS
5X
AS
20X
E11.5
E12.5
E13.5
E14.5
E15.5
E17.5
E18.5
duo
liv
h
lu
A
H
O
B
I
P
C
J
Q
D
K
R
E
L
S
F
M
T
G
N
U

Figure 3.12 *Fzd2* is not expressed in developing mouse liver from E11.5 to E18.5

Sections were hybridized with sense (A-G) and anti-sense probes (H-N) to *Fzd2*. *Fzd2* expression was not expressed in the mouse embryonic liver at any of the stages examined (E11.5 to E18.5). Annotations are as follows: h, heart; liv, liver; lu, lung; duo, duodenum; me, metanephros. O-U are higher magnification of livers from H-N. Scale bars in A and H represent 350 μm; in O represents 87 μm.

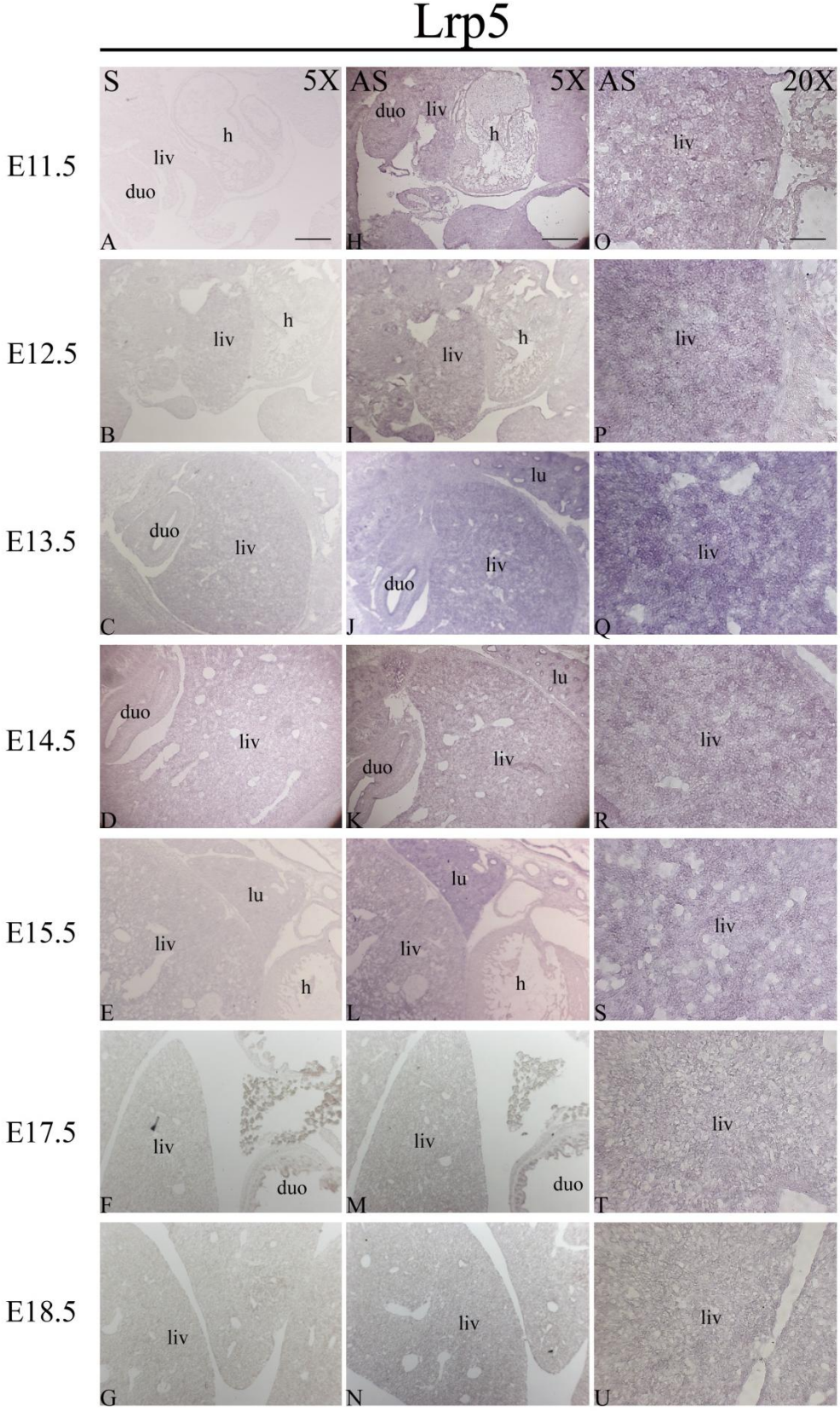
Lrp5
S
5X
AS
5X
AS
20X
E11.5
h
liv
duo
A
duo
liv
h
H
liv
O
E12.5
h
liv
B
h
liv
I
liv
P
E13.5
duo
liv
C
lu
liv
duo
J
liv
Q
E14.5
duo
liv
D
lu
duo
liv
K
liv
R
E15.5
lu
liv
h
E
lu
liv
h
L
liv
S
E17.5
liv
duo
F
liv
duo
M
liv
T
E18.5
liv
G
liv
N
liv
U

Figure 3.13 *Lrp5* is expressed in mouse liver during E11.5 to E13.5

Sections were hybridized with sense (A-G) and anti-sense probes (H-N) to *Lrp5*. *Lrp5* was expressed in the embryonic liver only at early stages of development from E11.5 to E13.5. Annotations are as follows: h, heart; liv, liver; lu, lung; duo, duodenum; me, metanephros. O-U are higher magnification of livers from H-N. Scale bars in A and H represent 350 μm; in O represents 87 μm.

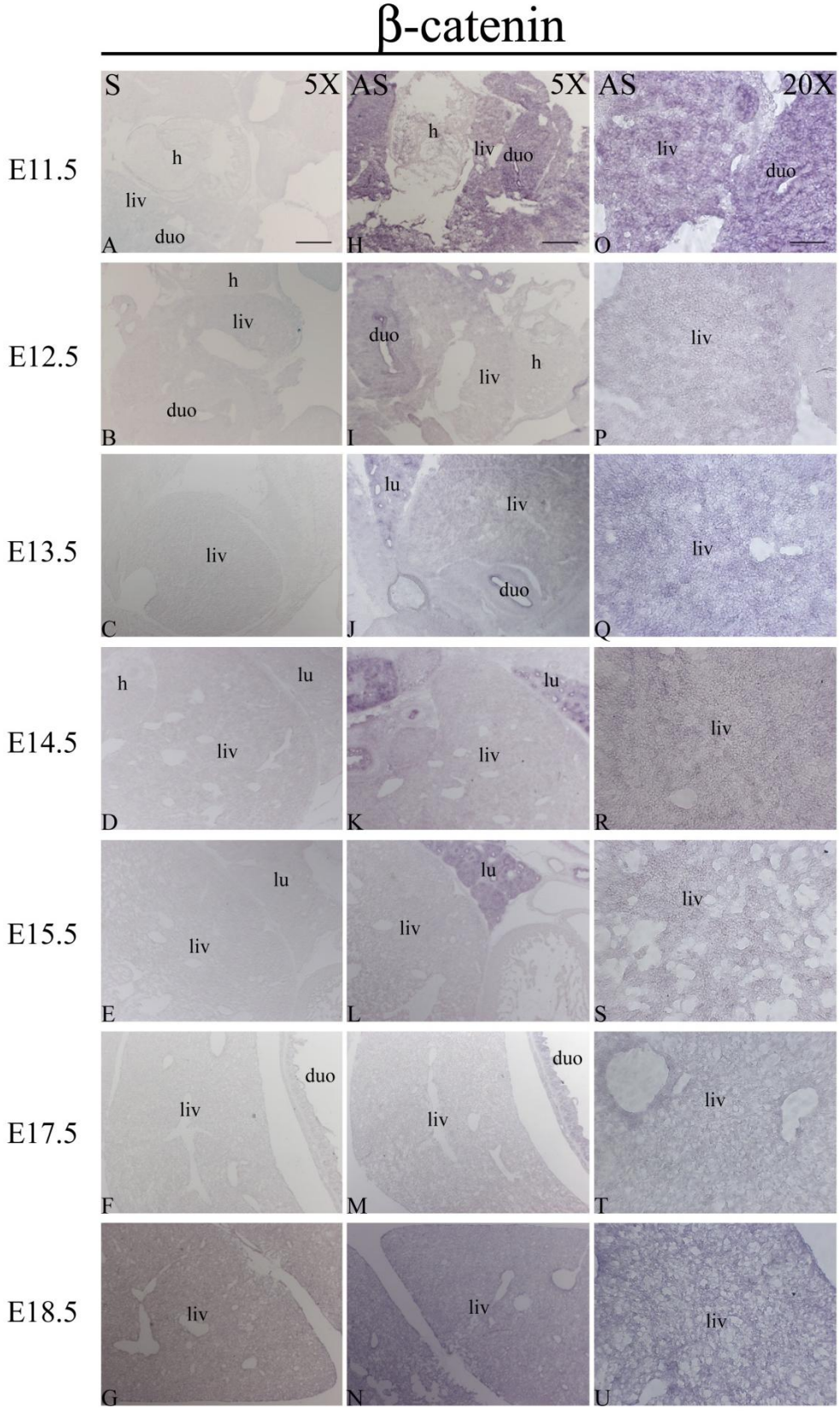
β-catenin
S
5X
AS
5X
AS
20X
E11.5
E12.5
E13.5
E14.5
E15.5
E17.5
E18.5
h
liv
duo
lu
A
H
O
B
I
P
C
J
Q
D
K
R
E
L
S
F
M
T
G
N
U

Figure 3.14 Robust *β-catenin* expression during E11.5 to E13.5 in mouse liver

Sections were hybridized with sense (A-G) and anti-sense probes (H-N) to *β-catenin*. *β-catenin* was found to be strongly expressed from E11.5 but then the expression was gradually reduced after E17.5. Annotations as follows: h, heart; liv, liver; lu, lung; duo, duodenum; me, metanephros. O-U are higher magnification of livers from H-N. Scale bars in A and H represent 350 μm; in O represents 87 μm.

3.3 Discussion

The overall aim of the research described in the present chapter was to determine the expression pattern in developing mouse liver for two enzymes involved in ammonia detoxification (CPS and GS) as well as members of the Wnt/β-catenin signalling pathway. We found that CPS protein became expressed between E13.5 and E14.5 and gradually increased thereafter while GS protein only became expressed between E17.5 and E18.5. This finding is in agreement with previous study conducted by Notenboom et al (1997).

The expression of urea cycle enzymes in hepatocytes, including CPS, varies between mammalian species. In rat and mouse hepatocytes, CPS expression is not observed until the beginning of the fetal period (Dingemanse et al., 1996; Gaasbeek Janzen et al., 1988; Moorman et al., 1990; Morris et al., 1989). However, in hepatocytes of human embryos, the expression of this enzyme begins shortly after the liver has differentiated from the embryonic foregut (Dingemanse and Lamers, 1994; van Roon et al., 1990). These interspecies differences in the developmental appearance of ornithine cycle enzymes in the liver are probably related to the intrauterine growth rate of the embryo (Dingemanse and Lamers, 1994; Meijer et al., 1990)

Previous *in situ* hybridization studies (Kuo and Darnell, 1991; Moorman et al., 1990) have revealed a strong and homogenous expression of GS mRNA in the liver of early mouse and rat (E13) embryos. However Janzen et al, 1987 could only demonstrate GS protein expression until E20 in rat hepatocytes, whereas Bennett et al, 1987 reported that mouse hepatocytes already contained immunohistochemically detectable amounts of GS at E15. The accumulation of GS protein in fetal hepatocytes following the onset of transcription appears to be delayed in both species. The reason for

this delay can be either a poor translational efficiency or instability of the protein in the early embryonic liver (Notenboom et al., 1997).

The discrepancy in the developmental appearance of GS protein in rat and mouse liver was also described by Notenboom et al, 1997. The authors suggested that GS starts to accumulate in mouse liver at E15 and Shiojiri et al, 1995 reported that GS immunoreactivity is not observed in mouse liver until 2-3 days after birth. These discrepancies could depend upon the effective antigen concentration of GS, antiserum generated from different laboratories and the fixation protocol. It has been reported that addition of glacial acetic acid to the fixation medium dramatically dimished immunohistochemiscal staining of GS in perinatal hepatocytes. Here we applied GS monoclonal antibody instead of pooled antiserum which was widely use in previous studies described above in immunohistochemistry analysis and western blotting to demonstrate more accurate GS expression. We show that GS protein expression only became apparently between E17.5 and E18.5 around central vein.

Micsenyi et al, (2004) showed peak expression of β-catenin during early liver development at E10-E12, followed by a decrease of β-catenin after E16 through the remaining prenatal period from microarray, northern and western blotting analysis. Here, *in situ* hybridization results shows abundant expression of β-catenin mRNA at E11.5 and E12.5 and western blotting showed more nuclear β-catenin protein expression at E12.5 that declined after E14.5. This data are in agreement with previous report (Micsenyi et al, 2004). However immunohistochemistry and fractionation followed by western blotting analysis revealed more detailed localization of β-catenin in which nuclear β-catenin, instead of membrane/cytosol β-catenin, was barely detectable at E14.5 and E15.5

and became robust between E17.5 and E18.5. This activated β-catenin is suggested to correlate with the induction of GS expression during perinatal stages described earlier in the discussion.

Although the Wnt/β-catenin pathway has been shown to be crucial in liver biology, the expression of Wnt and Frizzled genes during mouse development remains undetermined. Zeng et al, (2007) reported a total of 11 Wnts and 6 Frizzleds were expressed in normal adult mouse liver. Bi et al, (2009) determined the endogenous expression of the 19 Wnt genes identified so far in mice. Using semi-quantitative RT-PCR analysis, they demonstrated that the expression of 13 of the 19 *Wnt* genes was detectable. These include Wnt1, 2, 2B, 3, 3A, 4, 5A, 6, 8A, 9B, 10A, 10B, and 16. Among them, Wnt2B, 3A, 4, 8A, 9B, 10A, and 10B were highly expressed at all of the tested stages of liver development. Wnt2 and 5A were expressed at the later stages (e.g., 1 week after birth), while Wnt6 and 16 were expressed at the early stages (e.g., before E14.5) of liver development. These results suggest that Wnt family members may exert a diverse effect on hepatic differentiation. On the other hand, all ten Fzd receptors and both LRP5 and 6were expressed in the isolated liver tissues. These results indicate that the expression of Wnt receptors and co-receptors is rather ubiquitous and abundant during liver development.

Bi et al examined the expression patterns of the components of Wnt signalling pathway in embryonic livers from freshly prepared mouse liver tissues. Embryonic liver buds were pooled together, minced and homogenized in TRIZol Reagents. It is highly possible to collect mixed cell populations through this protocol and the data described is limited by RT-PCR results which as well as the technique demonstrating relatively poor sensitivity. Here we demonstrated the expression of the Wnt signalling genes by in situ hybridization to reveal a more comprehensive and temporal expression pattern during mouse liver development.

The differences between our result and previous reports were summarized in Table 3-2. The expression of the members in Wnt/β-catenin pathway was also demonstrated in other organs such as lung, heart, intestine and kidney which will provide valuable information for further study.

Table 3-2 Summary of results of *in situ* hybridization

		E11.5	E12.5	E13.5	E14.5	E15.5	E17.5	E18.5
Fzd1	This thesis	+	+	+	+	+	+	+
	Bi et al,2009	+	+	+	+	+	+	+
Fzd2	This thesis	-	-	-	-	-	-	-
	Bi et al,2009	+	+	+	+	+	+	+
Lrp5	This thesis	+	+	+	+	-	-	-
	Bi et al,2009	+	+	+	+	+	+	+
Wnt4	This thesis	-	-	-	+	+	+	+
	Bi et al,2009		+	+	+	+	+	+
Wnt5a	This thesis	-	-	-	-	-	-	-
	Bi et al,2009	-	-	-	-	-	-	-
Wnt5b	This thesis	+	+	+	+	+	+	+
	Bi et al,2009	NA	NA	NA	NA	NA	NA	NA
Wnt9b	This thesis	+	+	-	-	-	-	-
	Bi et al,2009	+	+	+	+	+	+	+
β-catenin	This thesis	+	+	+	+	+	-	-
	Micsenyi et al, 2004	+	+	+	+	+	-	-

NA: not available

We were unable to detect liver expression of *Fzd2* in contrast to Bi et al (2009). The reason for the lack of liver expression could be due to inadequate penetration of the probe into the tissue, but since we detected *Fzd2* expression in the intestine this appears unlikely. RT-PCR is the most convenient method for the detection of low-abundance mRNA. However, it is a complex technique and there are substantial problems associated with its true sensitivity, reproducibility and specificity as a

quantitative method (Bustin, 2000).The data above suggests the Wnt pathway may exert different effects at different stages of liver development. In next chapter, we aimed to dissect the molecular basis of Wnt signalling in early liver development using conditional deletion of the Wnt effectors, *β-catenin* and regulator, *Apc*.

CHAPTER 4 CONDITIONAL DELETION OF *APC* DURING EMBRYONIC DEVELOPMENT PERTURBS THE ESTABLISHMENT OF LIVER ZONATION

4.1 Background

Wnt signalling pathways has been implicated in playing important role in hepatogenesis. Ober et al described the requirement in zebrafish for mesodermally-derived Wnt signals, acting through the canonical pathway, for specification of the hepatic endoderm (Ober et al, 2006). The temporal regulation of β-catenin in the developing mouse liver is implicated in biliary cell differentiation and in promoting liver growth and hepatocyte maturation (Monga et al, 2003). The most direct linkage between the Wnt/β-catenin pathway and zonation regulation, however, is the demonstration that liver tumours in mice carrying activating mutations in either β-*catenin* or *Ha-ras* exhibit altered zonal gene expression. That is, tumours carrying β-*catenin* mutations express GS throughout the lesion, whereas *Ha-ras* tumours are negative for GS but express E-cadherin (a periportal marker) (Hailfinger et al, 2006). It is observations such as this, from liver tumours, that first suggested that β-catenin may be required for mediating the expression of zone-specific genes. Recently, using conditional deletion technique Benhamouche et al and our lab have established a role for the Wnt/β-catenin pathway in regulating the zonation of ammonia detoxification along the portovenous axis in adult mice (Benhamouche et al 2006 and Burke et al, 2009). Therefore the aim of the research described in this chapter is to dissect the role of Wnt/β-catenin pathway during liver development especially hepatic zonation.

Previous studies on the knockout of *β-catenin* or *Apc* in hepatoblasts resulted in mid to late gestational lethality between E16.5 to E18.5 (Tan et al., 2008; Decaens et al., 2008). My data on the appearance of the zonal markers CPS and GS suggests that the periportal marker (CPS) is induced between E12.5-E13.5 days of mouse development (Figs 3.1-3.3) and the perivenous marker (GS) is

induced at a later stage (between E17.5 and E18.5, Figure 3.1). The fact that lethality occurred between E16.5 and E18.5 means that it is difficult to determine the direct effect of aberrant activation or loss of the Wnt/β-catenin pathway on development of metabolic zonation (and in particular appearance of glutamine synthetase-expressing perivenous cells). To address this problem, we used a conditional approach for deletion of *Apc* by AhCre-mediated recombination. In the AhCre transgenic line, Cre expression is under the control of the Cyp1A1 promoter element that is normally transcriptionally silent but can be up-regulated in response to lipophilic xenobiotics such as β-napthoflavone (β−NF) (Matsushita et al, 1993). The AhCre model provides an efficient approach for controlling Cre-mediated gene excision in the mouse liver and intestine (Ireland et al, 2004). AhCre mice were intercrossed with mice carrying the loxP flanked Apc allele:Apc580S ($Apc^{fl/fl}$) and have been used in studies of intestinal pathology (Sansom et al., 2004) and adult hepatic zonation (Burke et al, 2009). Pregnant mice were identified and injected intraperitoneally with 3 doses of β-NF over a 1-day period. The embryos were then removed from the pregnant females at the time points indicated and the embryonic livers isolated as described in the 2.2.7. The β-NF injection time points and incubation periods were designed as Table 4-1. The tissues were processed for changes in expression of markers of zonation (listed in Table 4-2) using RNA and protein analysis.

Table 4-1 Study design of β-NF injection induced *Apc* deletion in embryonic mouse liver

	E12.5	E13.5	E14.5	E15.5	E16.5	E17.5	E18.5
CPS expression			+	+	+	+	+
GS expression							+
Group 1		β-NF injection		Isolate embryos			
Group 2			β-NF injection		Isolate embryos		
Group 3			β-NF injection				Isolate embryos
Group 4					β-NF injection		Isolate embryos

Table 4-2 Markers of metabolic zonation

Zonated metabolism	
Periportal	**Perivenous**
Ammonia, Amino acid	
Urea formation: Carbamoylphosphate synthetase (Cps); Arginase (Arg); Argininosuccinate synthetase (Ass); Argininosuccinate lyase (Asl); Glutaminase2	**Nitrogen metabolism:** Glutamine synthetase (Gs), glutamate transporter 1 (Glt1) Rh family, Bglycoprotein (RhBG). RNase4
Glucose	
Gluconeogenesis: phosphoenolpyruvate carboxykinase (Pepck)	

4.2 Results

4.2.1 Effect of *Apc* deletion on zonation during development

β-NF was first injected to pregnant female mice at gestational day E13.5 and the embryos were isolated at E15.5. To confirm the loss of *Apc*, immunohistochemistry for β-catenin was performed (Figure 4.1). Nuclear accumulation of β-catenin was observed in $AhCre^{+}Apc^{fl/fl}$ livers (Figure 4.1, upper panel). As well as activation of β-catenin, the expression of known perivenous markers (*GS, RHBG, RNase4* and *Glt1*) were either induced or upregulated compared to RNA extracted from control ($AhCre^{-}$) mouse liver (Figure 4.2). These changes were accompanied by a down-regulation of gene expression profile typical of a periportal phenotype (*PEPCK, CPSI, ASL, ASS, Glutaminase2* and *Arginase*) (Figure 4.2).

To complement the changes in gene expression following *Apc* deletion, we also determined the expression of CPS and GS by immunohistochemistry (Figure 4.1) in pregnant female mice that were treated with β-NF at E13.5 and the livers were removed at E15.5. Under normal circumstances GS protein is not expressed until between E17.5 and E18.5. However, GS was detected in cells throughout the livers of $AhCre^{+}Apc^{fl/fl}$ embryos (Figure 4.1, middle panel). The change in GS expression was accompanied by a reduction in CPS expression (Figure 4.1, lower panel). In order to test the temporal dependence of *Apc* deletion, we injected β-NF into pregnant female mice at different stages of gestation. We injected β-NF at gestational day E14.5 and E16.5 and the embryos were removed at E16.5 and E18.5 respectively (Table 4-1). Consistent with the results for injection at E13.5, in all examined groups, perivenous genes were up regulated and periportal gene expression

was reduced (Figure 4.1 and 4.2). *Apc* deletion showed a dramatic effect on liver zonation regulation during development.

4.2.2 *Apc* deletion enhances cell proliferation

β-catenin activation is associated with an increase in cell proliferation and β-catenin activation is frequently observed during tumour formation (Reya and Clevers, 2005). A decrease in cyclinD1 (a member of the cyclin protein family that is involved in regulating cell cycle G1/S progression) was seen in the β-catenin-deficient livers, and this deficit became more pronounced during states requiring *de novo* cyclin D1 synthesis such as during liver regeneration after partial hepatectomy (Kato et al., 2005). These observations suggest a clear role of β-catenin in normal liver growth. Impaired proliferation has also been observed in the β-catenin knockout embryos by a decrease in number of Proliferating cell nuclear antigen (PCNA)-positive cells, especially after E14 (Tan et el, 2008). Therefore we also determined the proliferative activity of cells using phospho-histone 3 (PH3) as a marker of mitotic cells. We observed a significant increase in the number of PH3-positive cells in $AhCre^{+}Apc^{fl/fl}$ livers compared to control ($P<0.05$) and an up-regulation of CyclinD1 RNA expression in the E18.5 $AhCre^{+}Apc^{fl/fl}$ livers injected with β-NF at E14.5 and taken at E18.5 (Figure 4.3). The up-regulation of PH3 in other groups with different injection time point and incubation period was not statistically significant (results not shown).

4.2.3 Enhancement of the ductal phenotype following deletion of *Apc*

Previously, it was suggested that β-catenin may have a critical role in the biliary differentiation from hepatoblasts. In the absence of β-catenin, there is a reduction in CK-19-positive primitive intrahepatic bile ducts (Hussain et al., 2004). In order to test whether biliary differentiation was altered following deletion of *Apc* we investigated whether the activation of β-catenin was accompanied by any changes in expression of ductalmarkers. We initially performed haematoxylin-eosin staining of sections taken from embryos that were treated with ・-NF at different stages of development (E13.5, E14.5, E14.5 and E16.5 and removed the tissues for processing at E15.5, E16.5, E18.5 and E18.5 respectively). In one group of embryos (treated at E16.5 and taken at E18.5) we observed ductal-like structures in the livers of $AhCre^{+}Apc^{fl/fl}$ mice (Figure 4.4). To further elucidate the phenotype, we examined ductal morphogenesis by investigating the expression of the progenitor ductal marker, Sox9 (Figure 4.5). Sox9 is detected in the developing bile duct of the mouse liver (Furuyama et al., 2011). Surprisingly, Sox9 expression was up-regulated in the $AhCre^{+}Apc^{fl/fl}$ livers from all the time points examined. The Sox9 staining pattern in the $AhCre^{+}Apc^{fl/fl}$ livers was also different to control livers. In the $AhCre^{+}Apc^{fl/fl}$ livers Sox9 was found scattered throughout the sections where the staining pattern in control sections formed a ring around the ductal-like structures. We also investigated the expression of other ductal markers including connexin43, cytokeratin7 and cytokeratin19. We detected, by RT-PCR, an increase of expression of these ductal genes. Thus β-catenin may therefore play an important role in regulating biliary differentiation during the E16.5 – E18.5 stage of development.

In order to address the mechanisms underlying the ductal phenotype seen following *Apc* loss, we turned our attention to the Notch signalling pathway. The role of the Notch pathway in hepatoblast differentiation was demonstrated by immunohistochemical analysis of mid gestational embryos

(Tanimizu et al., 2004). Jagged1 was shown to be expressed in the cells adjacent to ductal plates surrounding the portal veins suggesting that the Notch signalling is activated in hepatoblasts that undergo differentiation into cholangiocytes. Activating Notch signalling pathway by expression of the Notch intracellular domain in hepatoblasts inhibited hepatic differentiation and significantly reduced the expression of albumin, a marker of both hepatoblasts and hepatocytes. By contrast, downregulation of the Notch signalling by siRNA specific for Notch2 mRNA as well as by the gamma-secretase inhibitor promoted hepatic differentiation (Tanimizu et al., 2004).

The canonical Wnt pathway has been shown to regulate the Notch pathway genes (at least in the HT29 colorectal cancer cell line and in murine intestinal adenomas) (Ungerback et al., 2011). We hypothesized that the ductal phenotype may arise from the Wnt/β-catenin pathway regulating ductal morphogenesis through the Notch signalling pathway. To investigate this possibility, we determined the expression of Notch downstream target genes including Hairy and enhancer of split 1 (Hes1), Hairy/enhancer-of-split related with YRPW motif protein 1 (Hey1) and Manic Fringe (Artavanis-Tsakonas et al., 1999). Only at the stage E16.5 to E18.5 (under the conditions where the ductal markers cytokeratin7, cytokeratin19 and connexin43 were upregulated), did we observe an up-regulation of Hes1, Hey1 and Manic Fringe (Figure 4.6).

4.2.4 Characterization of the liver phenotype in β–catenin-deleted embryos

In order to determine the embryonic liver phenotype in $AhCre^{+}$β-$catenin^{fl/fl}$ embryos we injected β–NF at E14.5 and collected the embryos at E18.5. We found a decreased level of β-catenin

expression (at both the RNA and protein levels) (Figure 4.7). We also determined the effect of deleting β–catenin on the expression of periportal and perivenous markers by both PCR and also by immunhistochemistry. The perivenous markers (GS, Rhbg and Rnase4) were either absent or reduced in comparison with control livers. In contrast, there was no obvious difference observed between control and $AhCre^{+}\beta\text{-catenin}^{fl/fl}$ embryos for the periportal markers (Cps, Asl, Ass, Glutaminase2 and Arg) (Figure 4.7). These data suggest that either deletion of β-catenin is not sufficient to induce a change in the periportal phenotype or, that as well as β-catenin, some other mechanism(s) might be involved in regulating hepatic zonation in the periportal region.

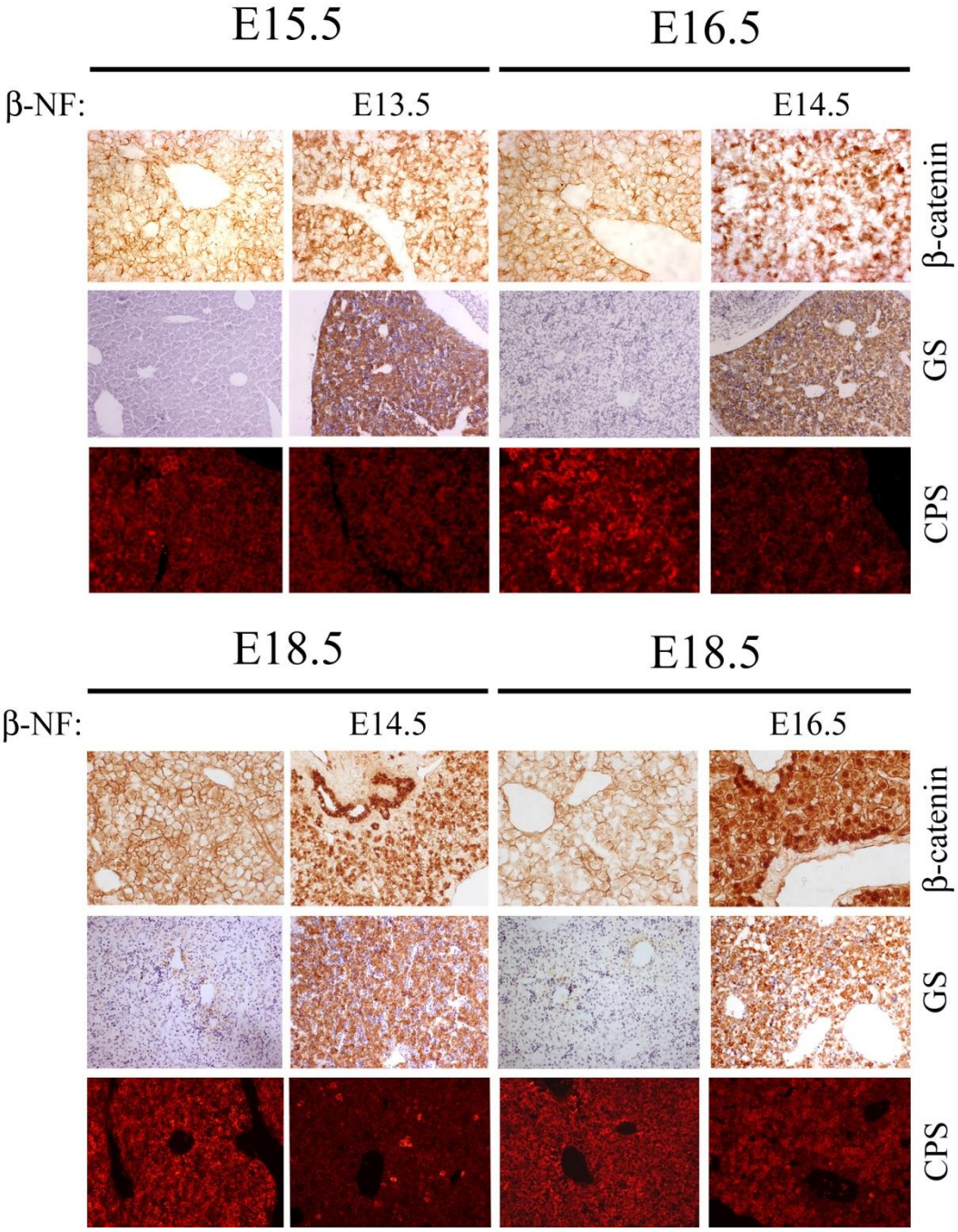

Figure 4.1 Changes in the expression of CPS and GS in in embryonic liver following conditional deletion of *Apc*. β-NF was injected into pregnant female mice and embryos were isolated at different stages of gestation indicated on the top of the figure. Immunostaining for β-catenin, CPS and GS in control (*AhCre*$^{-}$) and *AhCre*$^{+}$*Apc*$^{fl/fl}$ liver. *Apc* deletion induced nuclear accumulation of β-catenin and complementary changes in GS and CPS protein expression during mouse development. (Magnification X 400)

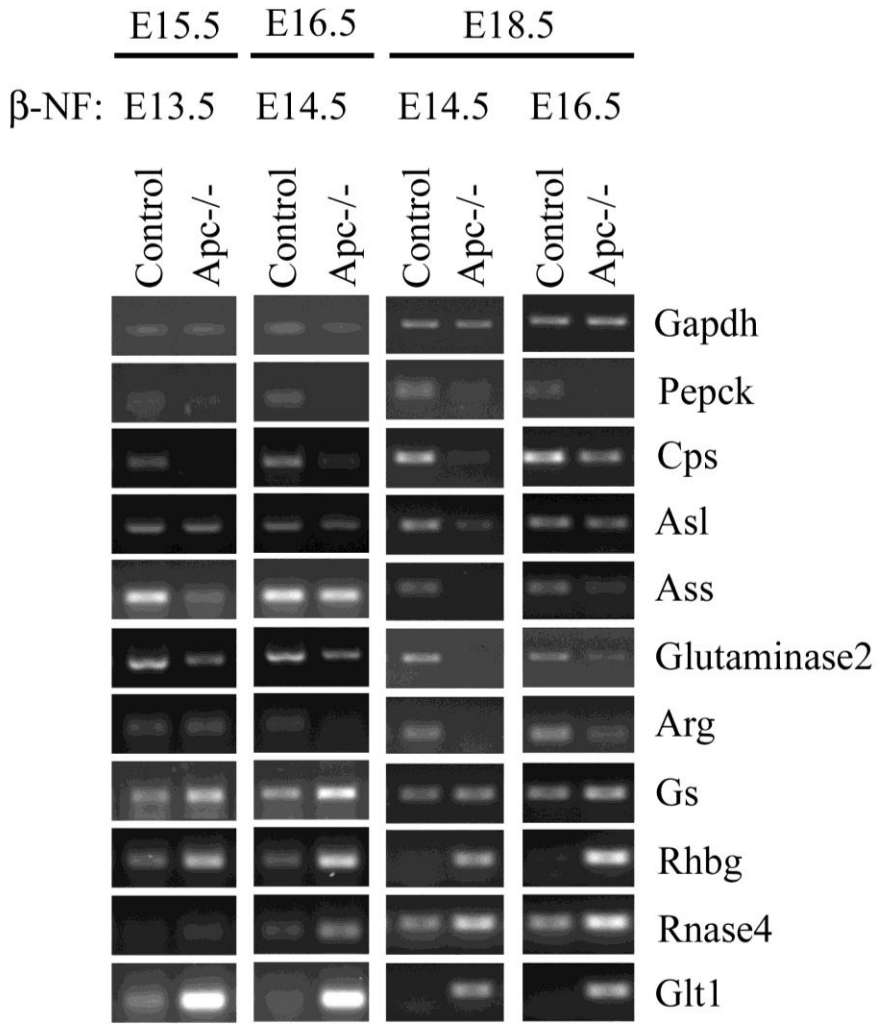

Figure 4.2 Deletion of *Apc* at different stages of development results in a change in the expression of periportal and perivenous hepatic markers.

β-NF was injected into pregnant female mice and embryos were isolated at different stages of gestation indicated on the top of the figure. RT-PCR analysis of cDNA from control (*AhCre*$^{-}$) and *AhCre*$^{+}$*Apc*$^{fl/fl}$ (Apc-/-) mice for the periportal markers *PEPCK, CPS, ASL, ASS, glutaminase2, Arginase* and perivenous markers *GS, RHBG, RNase4* and *Glt1*. *Apc* deletion induced complementary changes in expression of perivenous and periportal genes during mouse development.

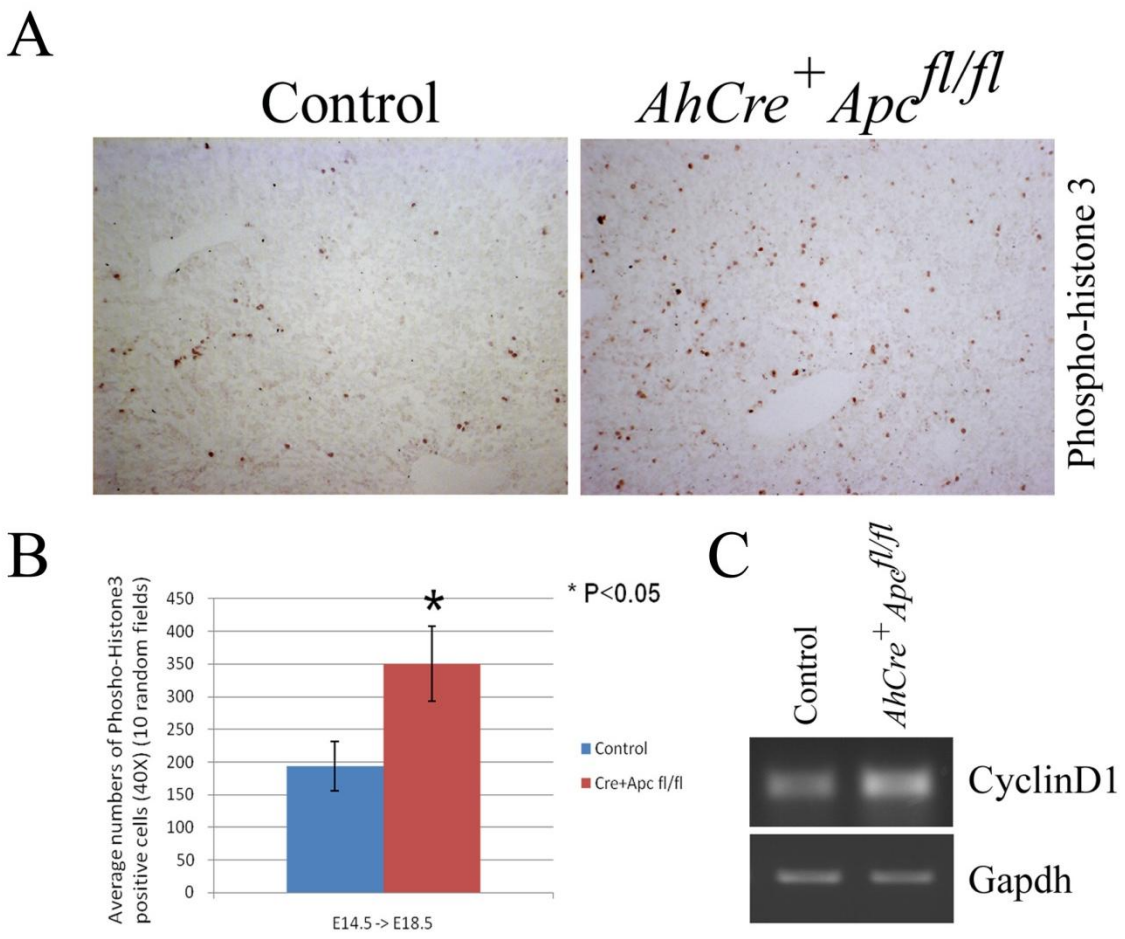

Figure 4.3 Proliferative markers are increased in *Apc*-deficient liver.

β-NF was injected into pregnant female mice at E14.5 and embryos were isolated at E18.5. (A) Immunostaining for phosphohistone 3 in liver sections from control (*AhCre*$^{-}$) and *AhCre*$^{+}$*Apc*$^{fl/fl}$ mice. (Magnification X 400) (B) Quantitative analysis of the numbers of phosphohistone H3-positive (PH3) cells in liver sections from control and *AhCre*$^{+}$*Apc*$^{fl/fl}$ mice. PH3-positive cells were counted in the 10 fields under 400X magnification. Significant differences are shown by * (T-Test, $p<0.05$). Bar values are means ± standard deviation of three experiments. (C) CyclinD1 expression is increased in livers from *AhCre*$^{+}$*Apc*$^{fl/fl}$ mice compared to controls.

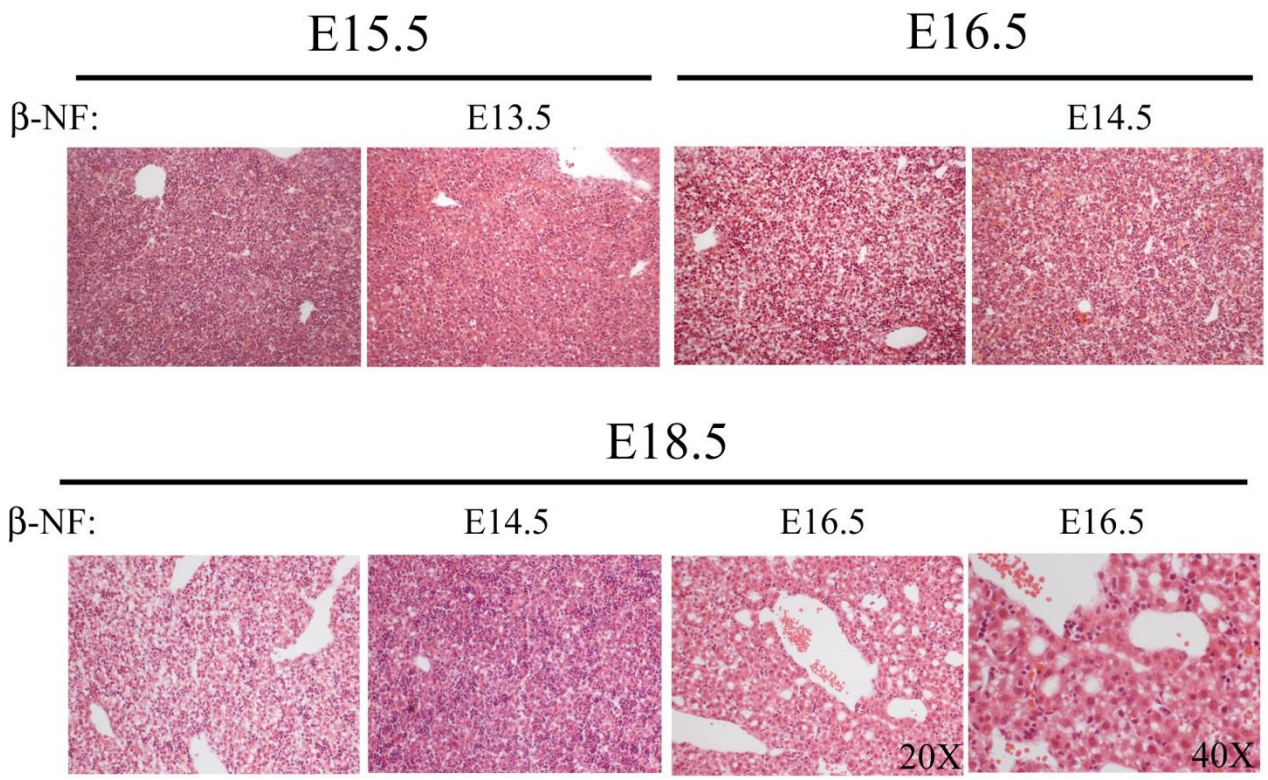

Figure 4.4 Haematoxylin and eosin analysis in embryonic livers following β-NF induction of *AhCre*$^{+}$*Apc*$^{fl/fl}$.

β-NF was injected into pregnant female mice and embryos were isolated at different stages of gestation indicated on the top of the figure. Isolated embryonic livers were fixed, processed and embedded in the paraffin wax. Control (*AhCre*$^{-}$) and *AhCre*$^{+}$*Apc*$^{fl/fl}$ liver sections were stained with hematoxylin and eosin.

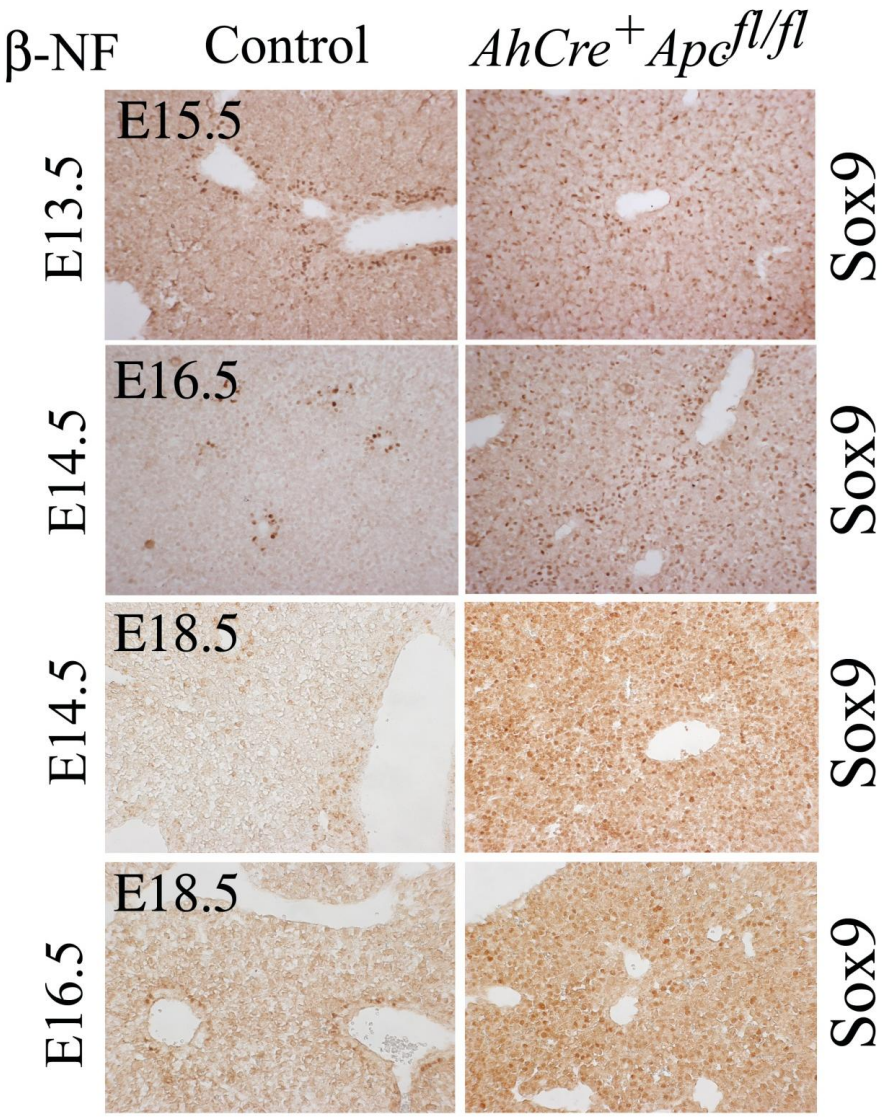

Figure 4.5 Deletion of *Apc* induces changes in hepatic ductal morphogenesis.

β-NF was injected into pregnant female mice and embryos were isolated at the stages indicated on the left of the picture. Liver sections from control (*AhCre*$^{-}$) and *AhCre*$^{+}$*Apc*$^{fl/fl}$ mice were immunostained for Sox9. (Magnification X 200)

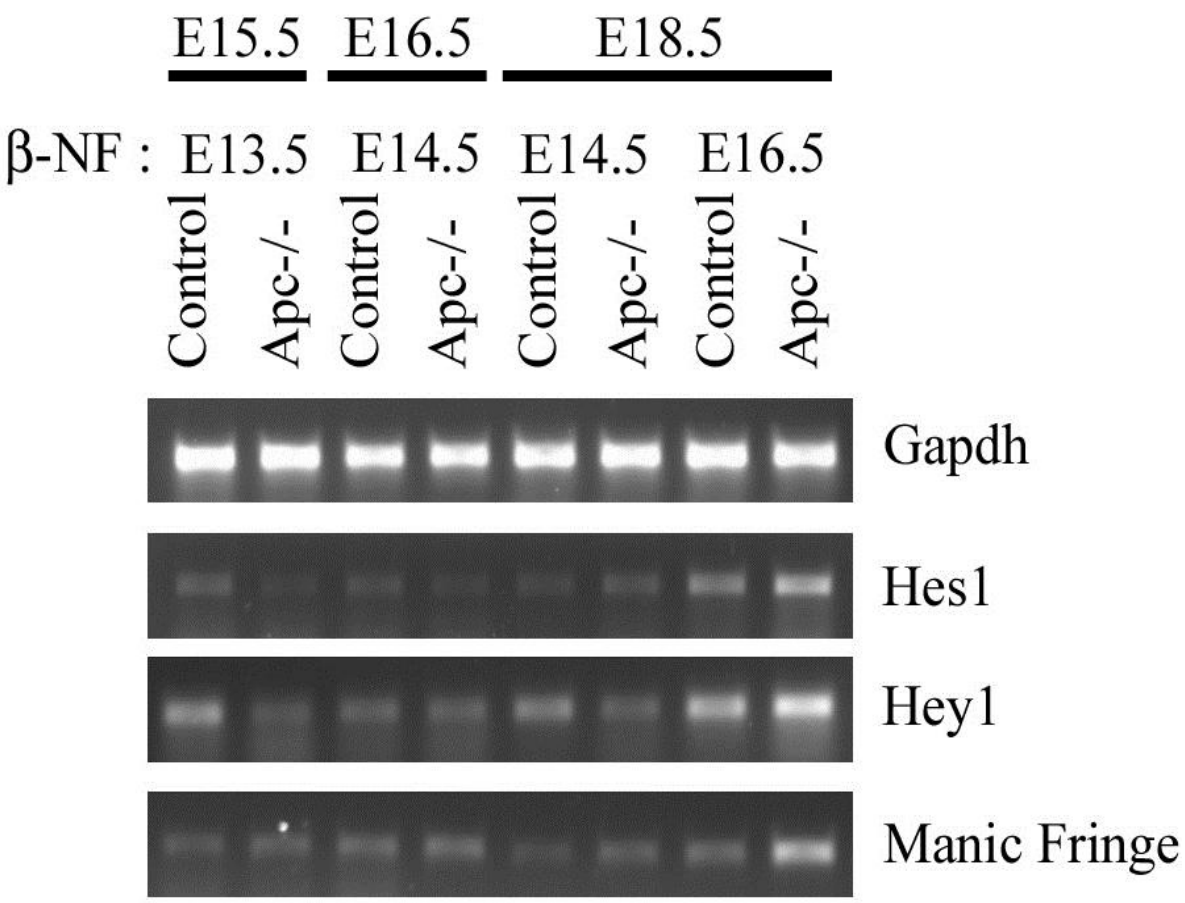

Figure 4.6 Activation of Notch pathway downstream target genes in *Apc* deleted embryonic livers

β-NF was injected into pregnant female mice and embryos were isolated at the stages indicated on the top of the picture. RT-PCR analysis of cDNA from control (*AhCre*$^{-}$) and *AhCre*$^{+}$*Apc*$^{fl/fl}$ (Apc-/-) mice for *Hes1*, *Hey1* and *Manic fringe.*

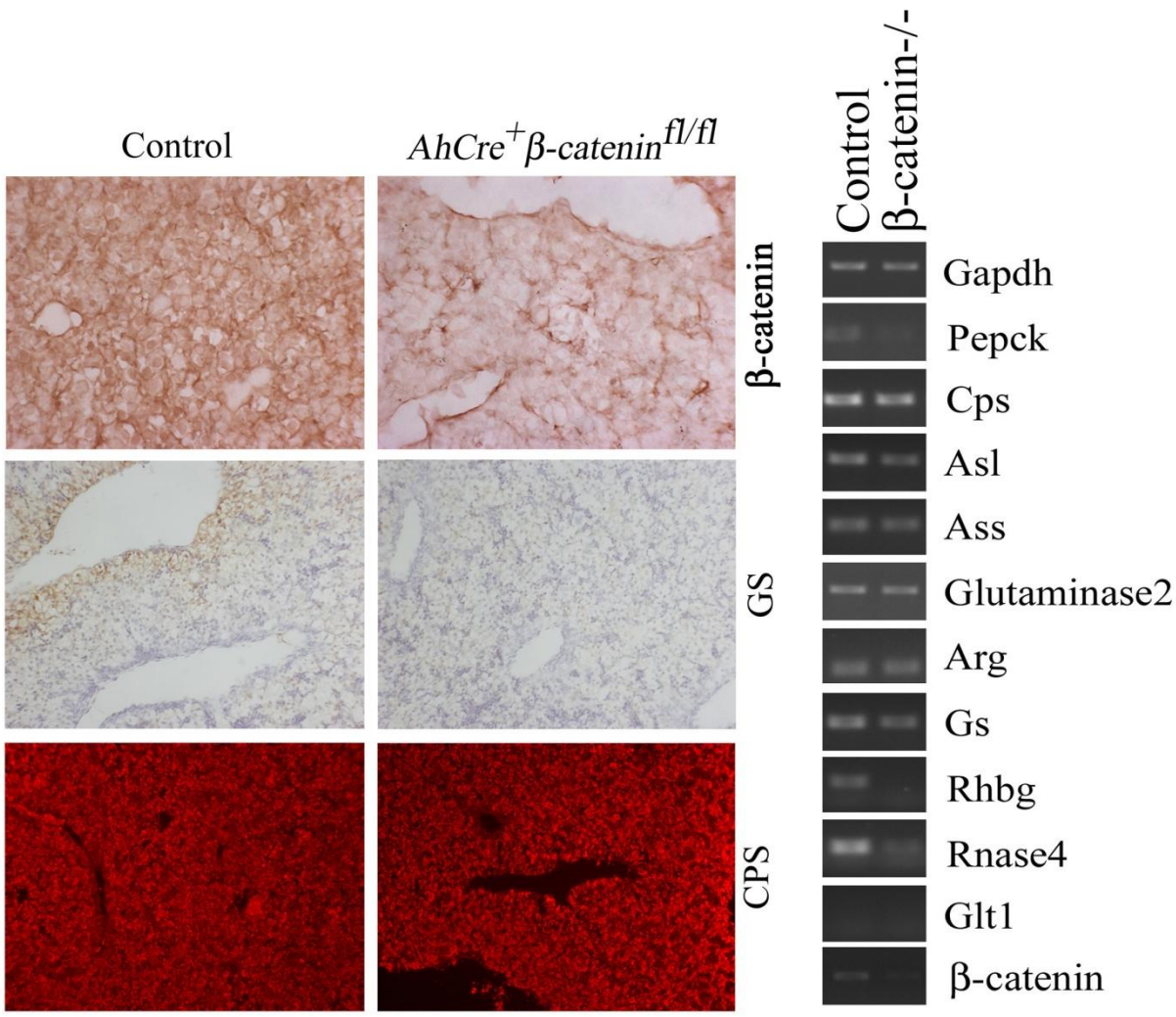

Figure 4.7 Deletion of β-catenin results in a down-regulation in perivenous gene expression.

β-NF was injected into pregnant female mice at E14.5 and embryos were isolated at E18.5 of gestation. RT-PCR analysis for perivenous and periportal markers and immunostaining for β-catenin, GS and CPS were performed on control (*AhCre*$^{-}$) and *AhCre*$^{+}$*β-catenin*$^{fl/fl}$ liver. *β-catenin* deletion resulted in faint stained of β-catenin and decrease in perivenous transcripts and GS protein expression. (Magnification X 400)

4.3 Discussion

The overall aim of the research described in this chapter was to dissect the role of the Wnt/β-catenin pathway in the development of the embryonic liver and in particular the development of metabolic zonation or hepatocyte heterogeneity. Previous studies had suggested a role for Wnt signalling in liver development. However, the issue with these studies was that the loss of β-catenin was lethal before the embryonic liver started to express the enzyme GS. Based on our data we saw that CPS expression was induced between E13.5 and E14.5 whereas GS became expressed between E17.5 and E18.5 (Figures 3.3 and 3.4). We therefore sought to capitalize on a conditional deletion model we previously used to investigate the role of the Wnt/β-catenin pathway in the induction of hepatic zonation in the adult mouse liver (Burke et al, 2009). We used *AhCre* mice to conditionally delete *Apc* or β-*catenin* at different stages of liver development. The *AhCre* mice were generated by using the promoter of the rat *Cyp1A1* gene to drive *Cre* recombinase expression. The *Cyp1A1* gene is not transcriptionally active but can be induced by lipophilic xenobiotics acting through the aryl hydrocarbon receptor (Ah) (Nebert et al., 2000). The mechanism of *Cyp1A1* gene expression involves the binding of the xenobiotic to the cytoplasmic Ah receptor which is normally bound to Hsp-90. Once the xenobiotic binds, the Ah receptor dissociates from the Hsp-90. The dissociation then permits the Ah receptor to translocate to the nucleus where it probably interacts with other factors (including Ah receptor nuclear translocator (ARNT)) to activate the promoters of responsive genes including the *Cyp1A1* gene. In the adult, recombination occurs in the liver and intestine following administration of β-NF (Ireland et al., 2004). We and others had previously shown that the Cre was active in the adult mouse liver (Burke et al, 2009; Ireland et al 2004). We confirmed that the *Ah-Cre* transgene was responsive in the embryonic liver since following treatment

of the pregnant female mice with β-NF at the times indicated, β-catenin accumulates in the liver (Figure 4.2). The data suggest that the β-NF can be used for inducing transplacental Cyp1A1 activity in the embryos and that these mice could be used for studying conditional deletion of genes in the developing mouse liver.

While we know something about the role of the Wnt/β-catenin pathway in the maintenance of zonation in the adult liver, there is a lack of information on whether the pathway is also critical for the induction of zonation in the developing mouse liver. To address this shortfall we initially deleted *Apc* at different stages of liver development. We found for the first time that the Wnt/β-catenin pathway may also be responsible for inducing zonation (at least for the ammonia detoxification pathway). The most remarkable result came from the group while we deleted *Apc* in embryonic mice at E14.5, incubated for 4 days and analysed at E18.5. With disruption of the *Apc* gene, nuclear β-catenin was observed in the majority of cells, indicating activation of Wnt signalling in liver. Gene expression analysis revealed an alteration in a number of genes, including an increase in GS, the glutamate transporter Glt1, and the ammonia transporter RhBG. GS and Glt 1 have previously been reported as β-catenin target genes (Cadoret et al., 2002); hence, changes in expression after deletion of *Apc* are consistent with previous observations. We also examined the periportal genes and found a complementary loss of genes, suggesting a switch in phenotype from periportal to perivenous-like hepatocytes.

We observed a significant increase in the number of PH3-positive cells and an up-regulation of CyclinD1 RNA expression in $AhCre^{+}Apc^{fl/fl}$ livers comparing to control in the E18.5 $AhCre^{+}Apc^{fl/fl}$ livers injected with β-NF at E14.5. This correlation between Wnt/β-catenin and embryonic liver proliferation was also seen in β-catenin deleted in the developing hepatoblasts utilizing Foxa3-Cre

and *floxed*-β-catenin transgenic mice from E8 to E8.5 (Tan et al, 2008). Deletion of β-catenin in developing livers resulted in significantly underdeveloped livers after E12. Histological analysis of the mice revealed a decreased cyclin-D1 and impaired proliferation (Tan et al, 2008).

From haematoxylin-eosin staining of sections taken from in the β-NF induced $AhCre^{+}Apc^{fl/fl}$ embryos (Figure 4.4), we saw an accumulation of ductal-like structures. Staining for progenitor ductal marker, Sox9 staining revealed up-regulation of the primitive ductal plate in the β-NF induced $AhCre^{+}Apc^{fl/fl}$. This was accompanied with an up-regulation of expression of other ductal markers transcripts including connexin43, cytokeratin7 and cytokeratin19 suggested Wnt/β-catenin may play an important role in regulating biliary differentiation during the E16.5 – E18.5 stage of development. This is consistent with previous studies showed that β-catenin may play important role in biliary specification during liver development. Monga et al, showed that β-catenin antisense ablation in E10 liver cultures led to an absence of cytokeratin-positive biliary cells (Monga et al, 2003). Growth in Wnt3a-conditioned media showed survival and proliferation of predominantly Cytokeratin 19-positive cells as compared with the control media (Hussain et al., 2004). Tan et al, suggested β-catenin deletion in embryonic livers resulted in a markedly decreased of cytokeratin19 positive cells in the primitive ductal plates E16 or E18 stages (Tan et al, 2008). Decaens et al further described a partial commitment of *Apc* deleted hepatoblasts to biliary lineage while the activation of β-catenin signalling in hepatoblasts induced premature, mislocalized, and incomplete differentiation of these cells toward the biliary lineage. We have tried to further analyse the ductal phenotype induced by *Apc* deletion using immunostaining for ductal markers such as Cytokeratin7, Cytokeratin19, Connexin43 and Sox9. However we could only successfully detected Sox9 expression in either paraffin sections or cryosections. This could be due to the problems of staining

conditions or might indicate these are premature ductal-like structures as suggested by Decaens et al. The detail mechanism of β-catenin activation induced premature biliary differentiation reeds further investigation.

We have also characterized liver phenotypes of AhCre^{+}β-catenin$^{fl/fl}$ embryos. β-catenin deletion resulted in reduced of the perivenous markers, however there was no obvious difference observed for the periportal markers. In previous study for zonation maintenance in adult mice, deletion of β-catenin induced a loss of GS and a complementary increase of CPS (Burke et al, 2009). The discrepancy from results of adults and embryos suggested that the regulation of periportal genes expression might be different during development. Deletion of β-catenin is either not sufficient to induce a change in the periportal phenotype or, that as well as β-catenin, some other mechanisms might be involved in regulating hepatic zonation in the periportal region during embryonic development which needs further investigation in the future.

CHAPTER 5 DIRECTED DIFFERENTIATION OF EMBRYONIC LIVER TOWARDS A PERIPORTAL OR PERIVENOUS-LIKE PHENOTYPE BY MANIPULATING THE WNT/β-CATENIN PATHWAY

5.1 Background

Culturing embryonic tissue in an *in vitro* setting offers the unique ability to manipulate the external medium and therefore to investigate the pathways involved in regulating normal organogenesis as well as providing models for developmental disorders. *In vitro* organ culture also provides a useful tool for studying the mechanisms involved in regulating normal organogenesis. Embryonic tissues including pancreas (Burke et al, 2010), liver (Burke et al, 2010), lung (Carraro et al., 2010), kidney (Zhang et al., 2012) and salivary glands (Spooner et al., 1989) have all been successfully cultured with the developing organs exhibiting many of the morphological features specific to their tissue type**.** One advantage provided by using an *in vitro* model is that the affect of exogenous factors on development can be monitored directly, thereby eliminating the need for lengthy procedures in which transgenic animal models have to be generated and maintained.

Herein we use *in vitro* culture of embryonic mouse liver to investigate the role of the Wnt/β-catenin pathway in the developing liver. The liver tissue was dissected from E11.5 mouse embryos (see section 2.2.8). The buds were then placed on fibronectin-coated coverslips in Basal Medium Essential (BME) medium supplemented with 10% FBS, penicillin (100U/ml), streptomycin (100μg/ml) and 2mM L-glutamine and allowed to attach. Over the next few days, the buds grow as flattened structures which are thin enough to allow the use of wholemount immunostaining methods.

5.2 Results

5.2.1 Characterisation of the in vitro liver culture model

5.2.1.1 Characterization of the in vitro culture model

The protocol here we used is based on a modification of the technique described by Percival and Slack **(**Percival and Slack, 1999**).** We have applied this technique to studying pancreas development and transdifferentiation in an *in vitro* setting (Kurash et al., 2004; Shen et al., 2003; Shen et al., 2000; Thowfeequ et al., 2007). More recently we have established a protocol for the maintenance of embryonic liver in culture (Burke et al, 2010). The culture system allows the embryonic liver tissue to grow as a flattened structure. This approach facilitates analysis of the tissue by enabling efficient wholemount immunostaining without the requirement for sectioning small and delicate samples.

Within hours of culture, the liver buds adhered to the fibronectin-coated coverslips. Gradually over the next few days, the explants flatten out and mesenchymal cells migrate out from the original buds to form a monolayer surrounding and covering the epithelium (Figure 5.1).

To address the role of the Wnt/β-catenin pathway in regulating metabolic zonation in developing liver, we initially monitored the expression of the perivenous marker, Glutamine synthetase (GS) in the *in vitro* liver bud culture model (Figure 5.2). Liver buds dissected from E11.5 mouse embryos were cultured in serum-containing BME medium in the presence of 1μM Dex. By day 7, differentiated hepatocyte-like cells started to express the GS protein. The expression peaked on day 9 and then declined at day 11 (Figure 5.2).

5.2.1.2 Optimization of adenoviral infection in cultured liver buds

While one key advantage of the embryonic liver culture model is the easy manipulating we also felt that the ability to ectopically express genes of interest may also be an important goal. Previous attempts by members of the lab showed that the cultured liver tissue was refractory to ectopic gene expression by transfection (Kuang-Ming Liu and David Tosh, personal communication). We therefore considered alternative approaches to gene transfection to achieve ectopic gene expression. One possibility was test the utility of adenoviral infection. We therefore chose a replication-defective, first generation adenoviral approach for gene delivery as actively dividing cells are not required for infection and the virus exhibits a broad range of infectivity in mammalian tissues and up to 8kb of genetic material can be transferred. Moreover the adenovirus does not integrate into the host genome and remains epichromasomally.

We first tried to optimize the conditions for adenoviral infection. To address this we used an Ad-RSV-GFP vector to infect cultured liver buds. The Ad-RSV-GFP uses the Rous sarcoma virus (RSV) promoter to drive GFP expression. Liver buds were dissected from E11.5 mouse embryos and cultured in serum containing BME medium in the presence of 1μM Dex. Once the buds attached to the fibronectin-coated coverslips after approximately 24hrs, Ad-RSV-eGFP was added to the medium at an M.O.I. of 100. This M.O.I was chosen based on our previous experience with using adenovirus infection of embryonic tissues (Quinlan et al., 2006). The media containing the virus was removed after 24 hours of incubation and replaced with fresh medium. Live images were collected after two days of infection (72hrs of culture). Robust GFP protein was expressed in the buds (Figure 5.3) suggesting good infection was achieved. I have also tried to infect cultured buds

with M.O.I. of 10 and 200. The result of infection with M.O.I. of 10 showed poor infection rate and M.O.I. of 200 lead to the buds detaching.

We wished to know whether GFP was expressed in the epithelium and/or mesenchymal component of the liver buds. To demonstrate protein expression in the cultured buds, liver explants were isolated and allowed to attach on fibronectin-coated coverslips for 24hrs. The virus was then applied for 24hr and then the medium was removed and the explants were then cultured for a further 48hr after which they were fixed and subjected to immunostaining for anti-GFP and anti-E-cadherin (an epithelial marker) antibodies. GFP was shown in both E-cadherin positive and E-cadherin-negative epithelial cells (Figure 5.4). This result indicates that the adenoviral vectors can successfully infect and carry the targeted genes to the epithelium layer of the liver cells in the cultured buds.

5.2.1.3 Effect of modulators of the Wnt/β-catenin pathway on expression of periportal and perivenous markers in cultured embryonic liver

In section 5.1.1, we showed that GS began to be expressed in the liver buds around Day 7 in the presence of 1μM Dex. To provide sufficient time to see an affect we decided to infect adenoviral genes (which could alter the activity of Wnt/β-catenin pathway) on Day 5 of culture and collect the samples on Day 10 for analyses.

E11.5 buds were isolated and cultured in the presence of 1μM Dex for 5 days. To activate the Wnt/β-catenin pathway, we infected the liver buds with adenoviral vectors carrying the Wnt ligands, Wnt1 and Wnt5a. Virus were incubated for 24hrs and replaced with fresh medium containing 1μM

Dex. Medium with freshly added Dex was then replaced every other day, After 5 days of incubation, the buds were collected and then subjected to immunostaining and RNA extraction. Compared to control, (which was infected with Ad-null to control for the adenoviral infection), the number of cells expressing GS was dramatically increased in the Ad-Wnt1 infected groups (Figure 5.5 and 5.8). In contrast, following infection with Ad-Wnt5a the number of GS-expressing cells was only modestly increased compared with infection of Ad-Wnt1 (Figure 5.5 and 5.8). Similarly, GS was also slightly up-regulated following ectopic expression of β-catenin, in the cultured liver buds (Figure 5.6 and 5.8).

We tested the use of a novel and selective small molecule inhibitor of glycogen synthase kinase 3 (GSK-3) termed TD114-2 (Bone et al, 2009). TD114-2 can robustly inhibit GSK-3 in mouse embryonic stem cells (ESCs) and enhance ESC self-renewal (Bone et al, 2009). In contrast, addition of TD114-2 to human ESCs has quite distinct effects and promotes differentiation towards the hepatoblast stage of liver differentiation (Bone et al., 2011). *In vitro* assays suggested that TD114-2 has an IC_{50} value for GSK-3-β inhibition of 3nM, and in mouse ESCs TD114-2 treatment leads to activation of the canonical Wnt pathway, exemplified by decreased β-catenin phosphorylation and activation of TCF/LEF transcriptional activity (Bone et al, 2009). E11.5 buds were isolated and cultured in the presence of 1μM Dex for 5 days. TD114-2 was then added to the culture medium to the final concentration of 1μM. Medium with freshly added Dex and TD114-2 was then replaced every other day, After 5 days of incubation, the buds were collected and then subjected to immunostaining and RNA extraction. After treated with TD114-2, GS expression was increased in the culture livers based on both immunostaining and RT-PCR results (Figure 5.6 and 5.8).

Other than activating the Wnt/β-catenin pathway, we also tried to block the Wnt pathway by infecting the buds with an adenoviral vector carrying the Dickkopf (DKK1) gene. DKK1 is a secreted protein with two cysteine rich regions and is involved in embryonic development through its inhibition of the Wnt pathway (Semenov et al., 2001). DKK1 blocks the Wnt pathway as a high affinity antagonistic ligand to LRP6, which is a Wnt co-receptor (Mao et al., 2001). By the same procedures described above, with the Ad-DKK1 infection for 5 days (Figure 5.7), GS expression was decreased in the cultured liver buds.

To complement the immunostaining data we carried out RT-PCR analysis of the liver buds following infection with Ad-Wnt1 and Ad-Wnt5a and Ad-DKK1 (Figure 5.8). We also performed RT-PCR analysis on RNA isolated from liver cultures treated with and without the GSK3 inhibitor TD114-2. We found that in agreement with the immunostainng data, Wnt1, Wnt5a and TD114-2 all increased expression of *GS* whereas DKK inhibited *GS* expression.

Surprisingly, infection with Ad-β-catenin did not enhance *GS* gene expression based on the RT-PCR analysis (Figure 5.8). We suspected it is much easier for adenovirus to infect mesenchymal than epithelial cells in the *in vitro* culture setting. Wnt1, Wnt5a and DKK are all secreted proteins which might still exert their effect on epithelial cells via both paracrine (when they infect mesenchyme) and autocrine mechanisms (when they infect the epithelial cells). β-catenin is a downstream effector in the Wnt/β-catenin pathway therefore can only alter the pathway in the infected cells. The lack of changing in GS expression following Ad-β-catenin infectionmay reflects this limitation. The other point is that the transgene expression was only confirmed by hemagglutinin (HA) immunostaining for Ad-HA-tagged Wnt1 and RT-PCR for DKK1 transcripts expression (data not shown). Further techniques need to be established to confirm Ad-β-catenin and Ad-Wnt-5a expression.

From the results above, we clearly showed that manipulating Wnt/β-catenin pathway leads to a marked effect on the expression of the perivenous marker, GS, in an *in vitro* model of liver development.

5.2.1.4 Challenges of monitoring CPS expression with Dex treated liver buds culture model

To address the role of Wnt/β-catenin pathway in regulating metabolic zonation in developing liver, we needed to provide evidence that not only the perivenous expression profile (e.g. GS) but also periportal gene expression (e.g. CPS) was also affected. We therefore dissected liver buds from E11.5 mouse embryos and cultured them in serum-containing BME with addition of Dex to final concentration of 1μM. We have shown that CPS starts to be expressed in embryonic liver between E13.5 and E14.5 (Figure 3.1). Based on our previous experience we predicted that in the *in vitro* culture system, CPS should become detectable from about Day3 or even later due to lack of the natural liver microenvironment. Surprisingly, CPS showed robust expression at both the RNA and protein levels in the liver buds after only 24 hours of Dex treatment suggesting that the glucocorticoid is able to induce the premature expression of CPS (Figures 5.9 and 5.10). From the literature we realized that the glucocorticoid receptor binds directly to the distal promoter of CPS (Schoneveld et al., 2005). The premature expression of CPS in the Dex-treated cultures makes it more difficult to use this culture system as a model for looking at how members of the Wnt/β-catenin pathway regulate CPS expression. Therefore we moved on to test other supplements other than Dex which could also induce embryonic liver bud maturation.

5.2.2 Enhanced maturation of embryonic liver in culture following treatment with ITS

To find an alternative to Dex we searched the primary literature. Previous reports of Insulin-Transferrin-Selenium (ITS) suggested it could be a potential candidate. ITS was first designed to be used as a supplementation to FBS thereby allowing for a reduction in the FBS culture requirements. Later, studies showed that ITS, Dex and the addition of growth factors (such as HGF and EGF) are important factors in the maintenance of the liver phenotype in hepatocyte cultures (Oyadomari et al., 2000; Sato et al., 1999). ITS has been shown to be effective in enhancing the proliferation and survival of primary hepatocytes while Dex has been reported to promote the expression of a hepatocyte phenotype through the suppression of cell division (Chivu et al., 2009; Michalopoulos et al., 2003).

Insulin is a hormone that promotes glucose and amino acid uptake by the cell. It is thought that mitogenic effects of insulin are due to the insulin-like growth factor receptor, IGF-1 receptor (Brameld et al., 1995). Transferrin is an iron transport protein that functions to transport iron to the cell. The protein also serves to detoxify the medium from oxygen radicals and peroxidase. Selenium is a cofactor that activates glutathione peroxidase, a player in the detoxification of oxygen radicals (Meredith, 1988).

To determine the effect of ITS on the hepatic phenotype, we dissected E11.5 liver buds and cultured the explants in BME with addition of 1x ITS (ITS Liquid Media Supplement 100x, Sigma, UK). *Gs* and *Cps* RNA expression were determined by RT-PCR (Figure 5.11). *Gs* expression peaked around

day 7 of culture while *Cps* started to be expressed by day 3 after ITS treatment on the liver buds dissected from E11.5 mouse embryos. The result suggested culture with ITS could lead to liver buds maturation in a more reasonable timeframe in terms of *Gs* and *Cps* expression according to *in vivo* data (Figure 3.1). Therefore we decided to infect ITS cocultured liver buds with Ad-Wnt1 and Ad-DKK1 and monitor both CPS and GS expression.

5.2.2.1 Effect of ectopic Wnt1 and DKK1 on expression of CPS and GS in cultured embryonic mouse liver

We cultured embryonic for 5 days in BME and supplemented with ITS. Thereafter we infected liver buds with Ad-null, Ad-Wnt1 or Ad-DKK1 viruses on Day5 of culture (at an M.O.I. of 100) and collected samples for analysis on Day10. Immunostaining results showed that the perivenous marker, GS, was induced in the buds infected with Ad-Wnt1 and suppressed in the buds infected with Ad-DKK1. Conversely, the expression of the periportal marker CPS was suppressed in the buds infected with Ad-Wnt1 and increased in the buds infected with Ad-DKK1 (Figure 5.12). This effect has also been confirmed at the RNA level (Figure 5.12).

5.2.2.2 Effect of TD114-2 and Quercetin on developing liver

While the application of the Wnt1 and DKK1 adenoviruses to the cultured embryonic livers demonstrated a role for the Wnt/β-catenin pathway in establishing the zonation of ammonia metabolizing enzymes, we also decided to strengthen this data using pharmacological application of two compounds, (TD114-2 and Quercetin) since these modulate the activity of the Wnt/β-catenin pathway.

TD114-2, is a chemically synthesized novel small-molecule which can activate the Wnt/β-catenin pathway through inhibition of GSK-3 (Bone et al., 2009). Quercetin is a plant-derived flavonoid widely distributed in the nature. Studies showed that Quercetin is also a potent inhibitor against Wnt/β-catenin pathway (Park et al, 2005). Nuclear β-catenin conveys signals though interaction with the Tcf/Lef family of transcription factors. In the absence of a Wnt signal, TCF/LEF factors bind DNA at Wnt-responsive genes and interact with other factors (e.g. Groucho, histone deacetylase) to repress transcription. β-catenin binding to TCF/LEF proteins provides a transcription activation domain so target gene expression is activated. The binding of Tcf complexes to its specific binding sites are strongly suppressed by Quercetin treatment of colon cancer cells (Park et al., 2005).

We initially tested the concentration dependence of TD114-2 and Quercetin on the morphology of the embryonic mouse livers maintained in BME with ITS for up to 7 days. TD114-2 was added to the culture medium up to final concentrations of 0, 0.2, 1and 2μM (Figure 5.13). Liver buds spread out and grew normally in the control and 0.2 and 1 μM concentrations of TD114-2. However, the buds treated with 2μM TD114-2 appeared to lose their epithelial cells. Therefore based on these observations we chose to treat the liver buds with 1μM TD114-2 for subsequent experiments.

Quercetin was added to the culture medium to final concentrations of 0, 10, 50 and 100 μM (Figure 5.14). Liver buds spread out and grew normally in the control even in media supplemented with the highest concentration of 100μM Quercetin. Therefore we chose to treat buds with 100μM Quercetin in later experiments.

5.2.2.3 Treatment of embryonic liver cultures with TD114 and Quercetin alters the expression of ammonia detoxifying enzymes

E11.5 liver buds were dissected and cultured in serum containing medium with addition of TD114-2 or Quercetin on Day5 to the concentration of 1μM and 100 μM, respectively. RNA was extracted from samples on Day10 of culture and subjected to RT-PCR analysis. Results indicated that perivenous genes (e.g. *Gs* and *Glt1*) were down-regulated and periportal genes (e.g. *Cps* and *Pepck*) were up-regulated in Quercetin-treated buds (Wnt pathway suppression) (Figure 5.15). In TD114-2-treated buds (Wnt pathway activation), perivenous genes were up-regulated and periportal genes were down-regulated (Figure 5.15). The result fit with our hypothesis that the Wnt/β-catenin pathway could be an important regulator in the development of zonation in the developing liver.

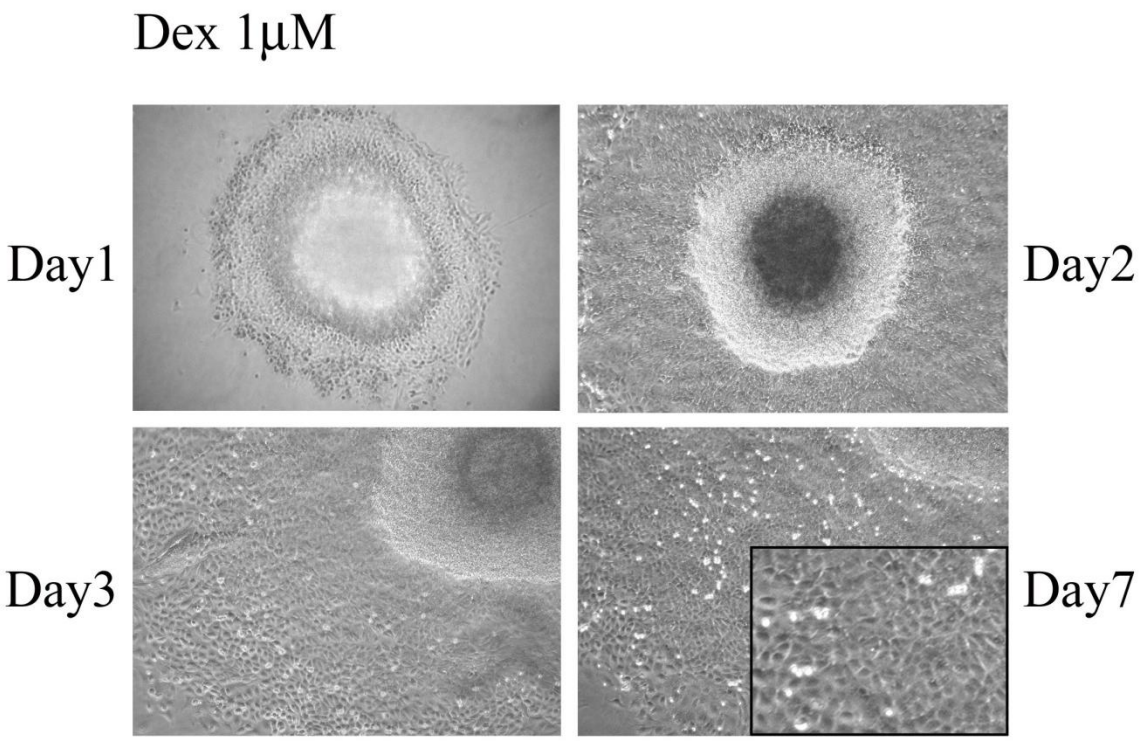

Figure 5.1 Morphological changes in mouse embryonic liver buds cultured in the presence of Dexamethasone.

Liver buds were dissected from E11.5 mouse embryos and maintained in complete BME supplemented with 1μM Dex for 1, 2, 3 and 7 days (Magnification X 200). Magnified image of Day7 X400 is indicated at right lower corner.

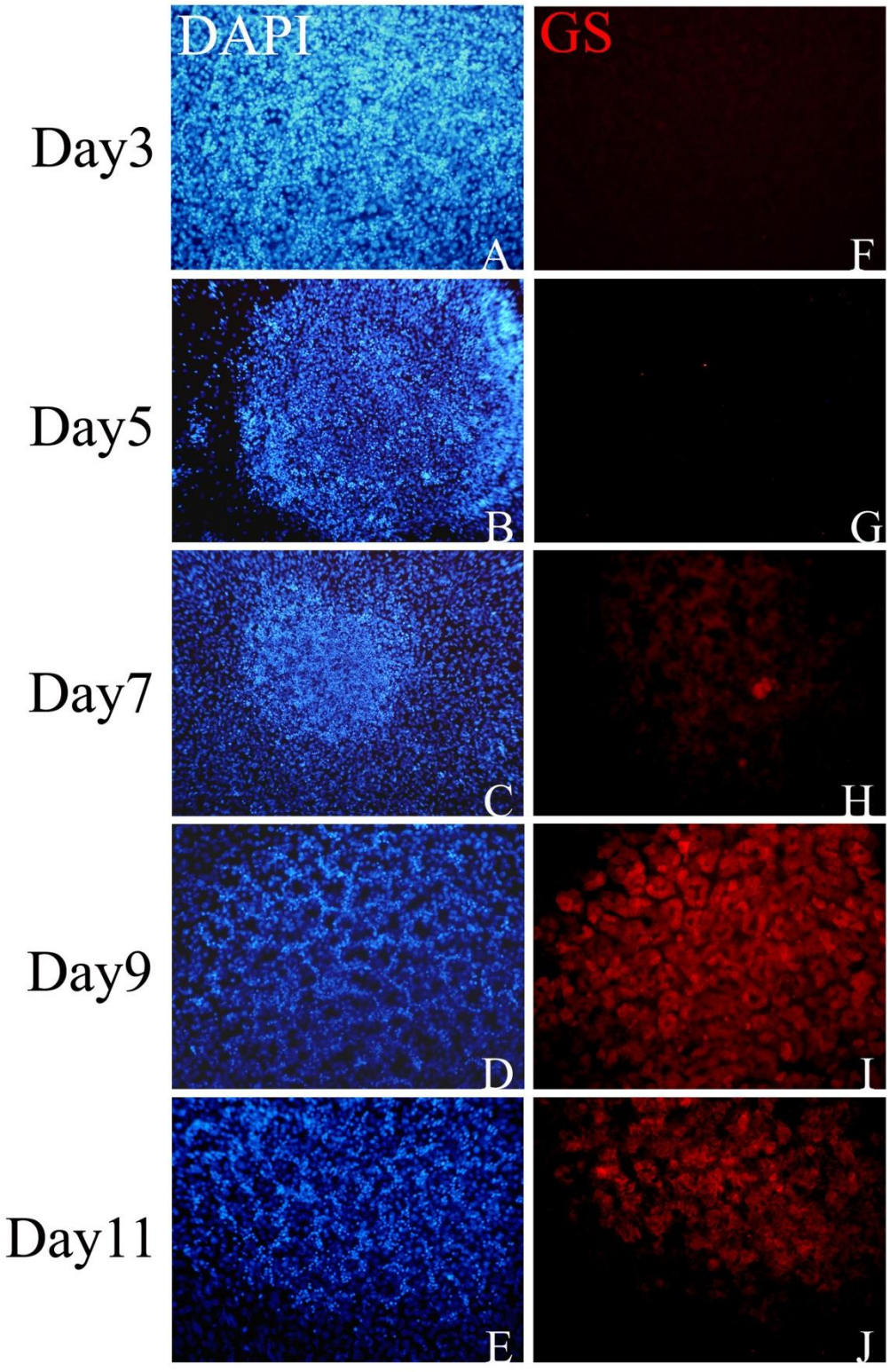
DAPI
GS
Day3
A
F
Day5
B
G
Day7
C
H
Day9
D
I
Day11
E
J

Figure 5.2 Time course of GS expression in embryonic liver buds maintained in culture

Liver buds were dissected from E11.5 day old embryos as described in the Materials and Methods sections. The buds were then cultured with 1μM Dex for up to 11 days. The embryonic tissue was fixed and immunostained for GS (red) and counterstained with the nuclear stain DAPI (blue). The results show that GS starts to be expressed between day 5 and 7 of culture. (Magnification X 400)

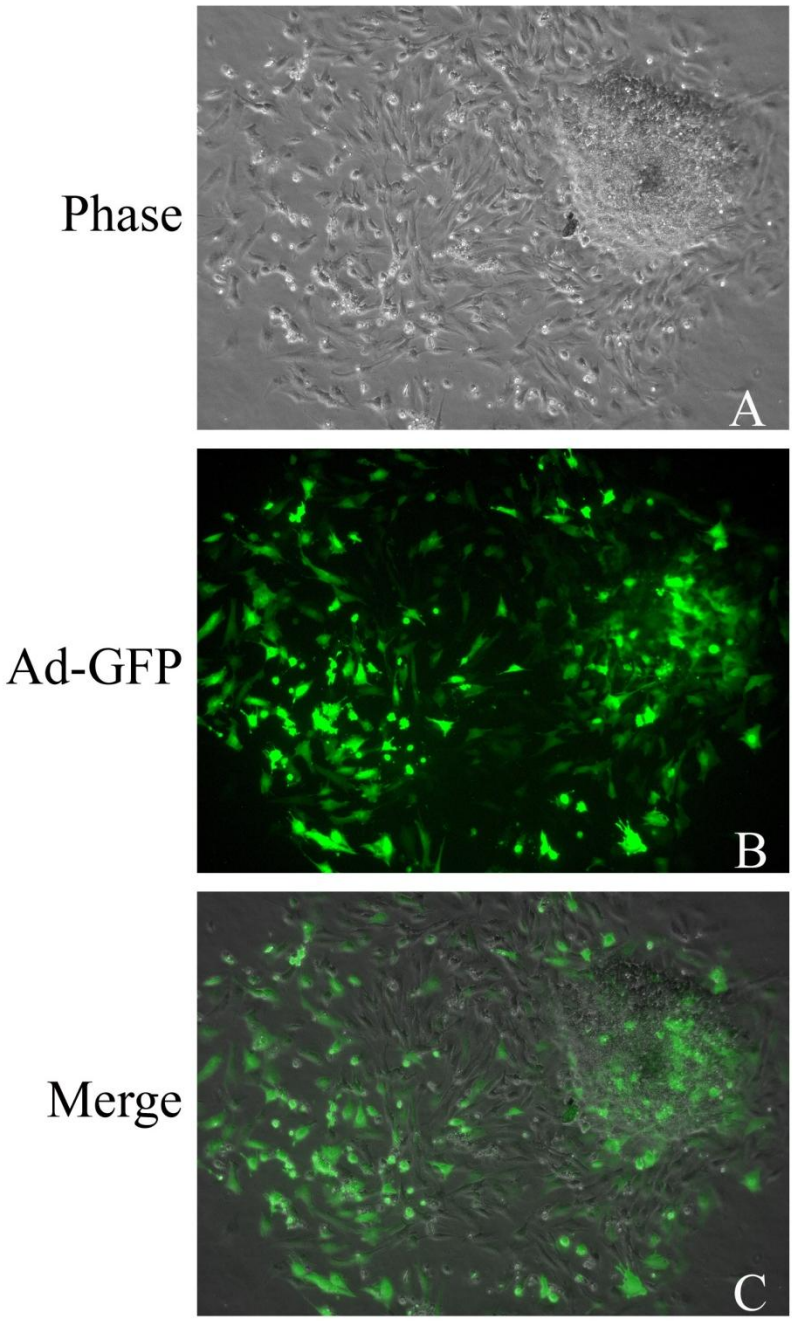

Figure 5.3 Cultured liver buds are amenable to adenoviral infection

Liver buds were cultured with 1μM Dex for 24 hours and then infected with Ad-eGFP (M.O.I. 100) for 24 hours. Live imaging of the embryonic buds shows that GFP was expressed in the buds after a further 48hr. (Magnification X 200)

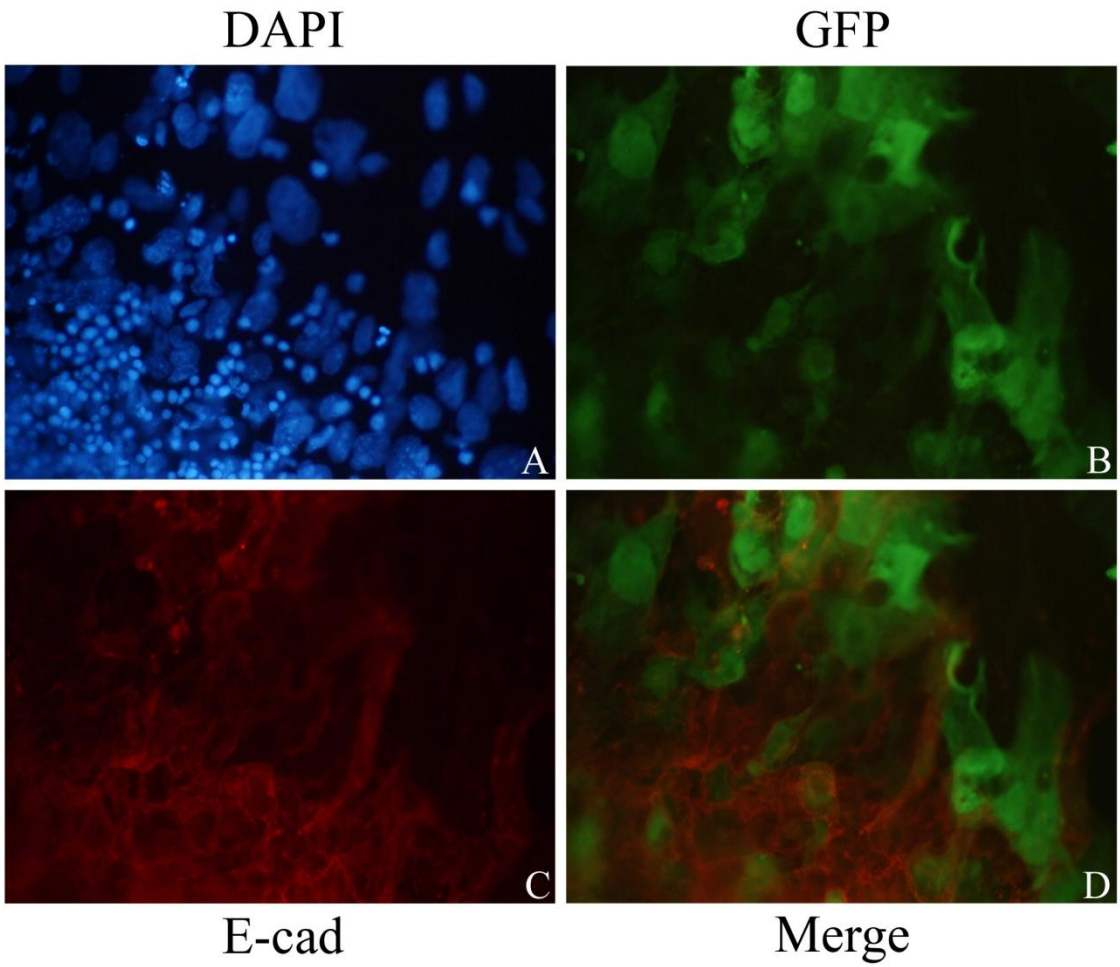

Figure 5.4 Adenovirus infects both E-cadherin-positive and negative embryonic liver cells

Liver buds were cultured with 1μM Dex for 24 hours and then infected with Ad-eGFP (M.O.I. 100) for 24 hours. After 48 hours, the buds were immunostained for the epithelial marker, E-cadherin (red) and counterstained with DAPI. GFP was expressed (B). E-cadherin marked the epithelial region of the buds (C). A merged image of GFP and E-cadherin is shown in (D) and demonstrates that GFP was expressed both in the E-cadherin positive (epithelial) and E-cadherin (presumptive mesenchymal cells) cells. (Magnification X 400)

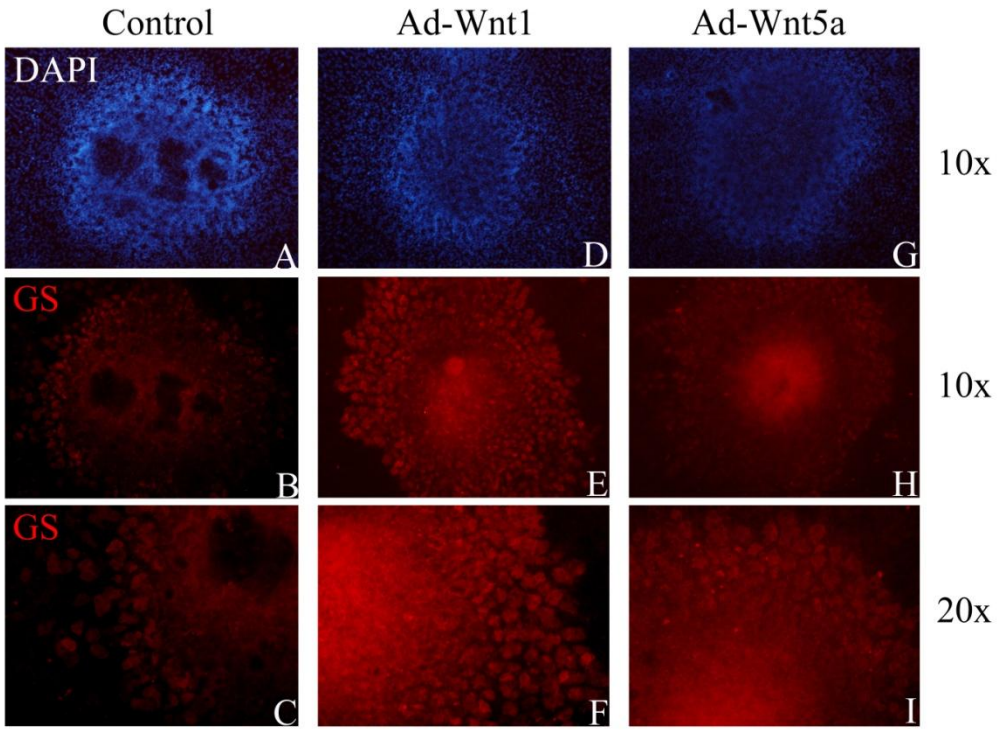

Figure 5.5 Adenoviral infection of Wnt1 and Wnt5a induces GS expression in cultured liver buds

Liver buds were cultured with 1μM Dex for 5 days and then infected with Ad-null (M.O.I. 100) (A-C) as control, Ad-Wnt1 (M.O.I. 100) (D-F) or Ad-Wnt5a (M.O.I. 100) (G-I) for 24 hours at 37℃. The virus was then removed and the buds were supplied with fresh medium. After 5 days, buds were fixed and immunostained for the perivenous marker, GS (red) and counterstained with DAPI. Both Ad-Wnt1 and Ad-Wnt5a appeared to enhance the number (and intensity) of cells expressing GS protein. C, F and I (Magnification X 200) are the higher magnification from B, E and H (Magnification X 100), respectively.

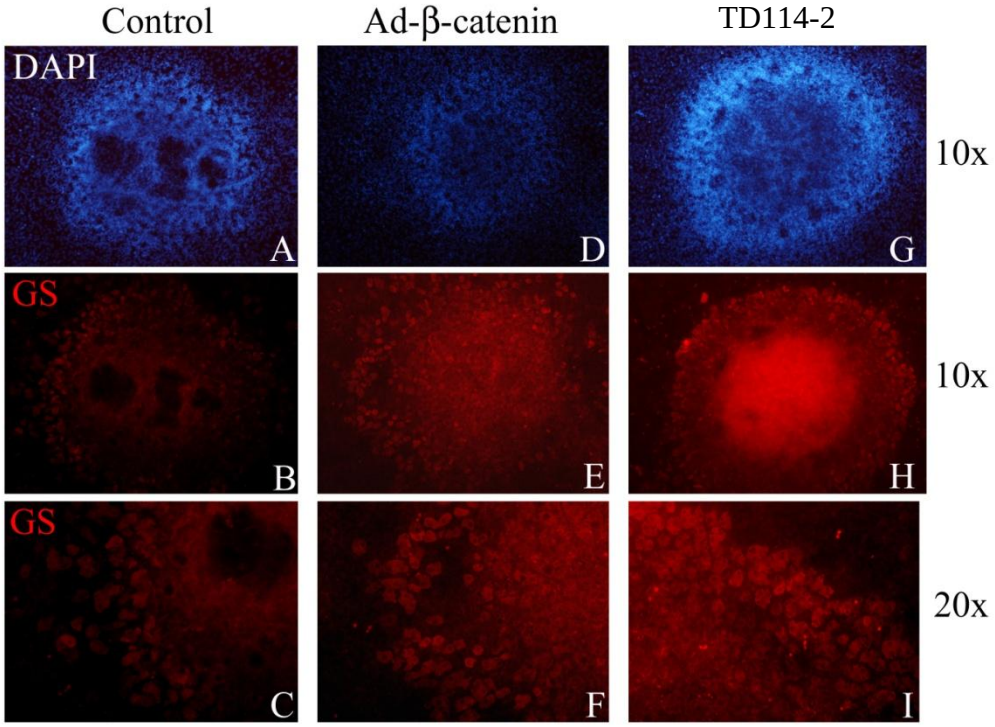

Figure 5.6 Adenoviral infection of β-catenin or treatment with TD114-2induces GS expression in cultured embryonic liver buds

Liver buds were cultured with 1μM Dex for 5 days and infected with Ad-null (M.O.I. 100) (A-C) as control or Ad-β-catenin (M.O.I. 100) (D-F) for 24 hours at 37℃. The virus was then removed and the medium was replaced with fresh medium. After 5 days, the buds were fixed and subject to immunostaining. TD114-2 (1μM) (G-I) was added in the medium on day 6 with Dex and cultured until 10 days prior to fixation. Fixed buds were then immunostained for the perivenous marker, GS (shown in red) and counterstained with DAPI. Both Ad-β-catenin and TD114-2 treatment induced expression of GS protein. C, F and I (Magnification X 200) are the higher magnification images from B, E and H (Magnification X 100), respectively.

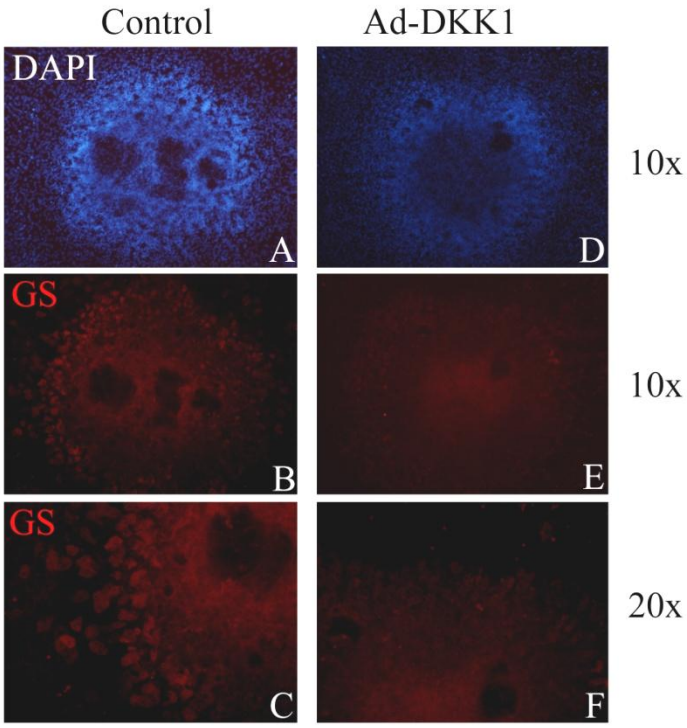

Figure 5.7 Ectopic DKK1 expression suppressed GS in cultured embryonic liver buds

Liver buds were cultured with 1μM Dex for 5 days and then infected with Ad-null (M.O.I. 100) (A-C) as control or Ad-DKK1 (M.O.I. 100) (D-F) for 24 hours at 37℃. After 5 days of culture, buds were fixed and immunostained for GS (red) and also counterstained with DAPI. Ad-DKK1 suppressed expression of GS protein.B and E (Magnification X 200) are higher magnification images from C and F (Magnification X 100), respectively.

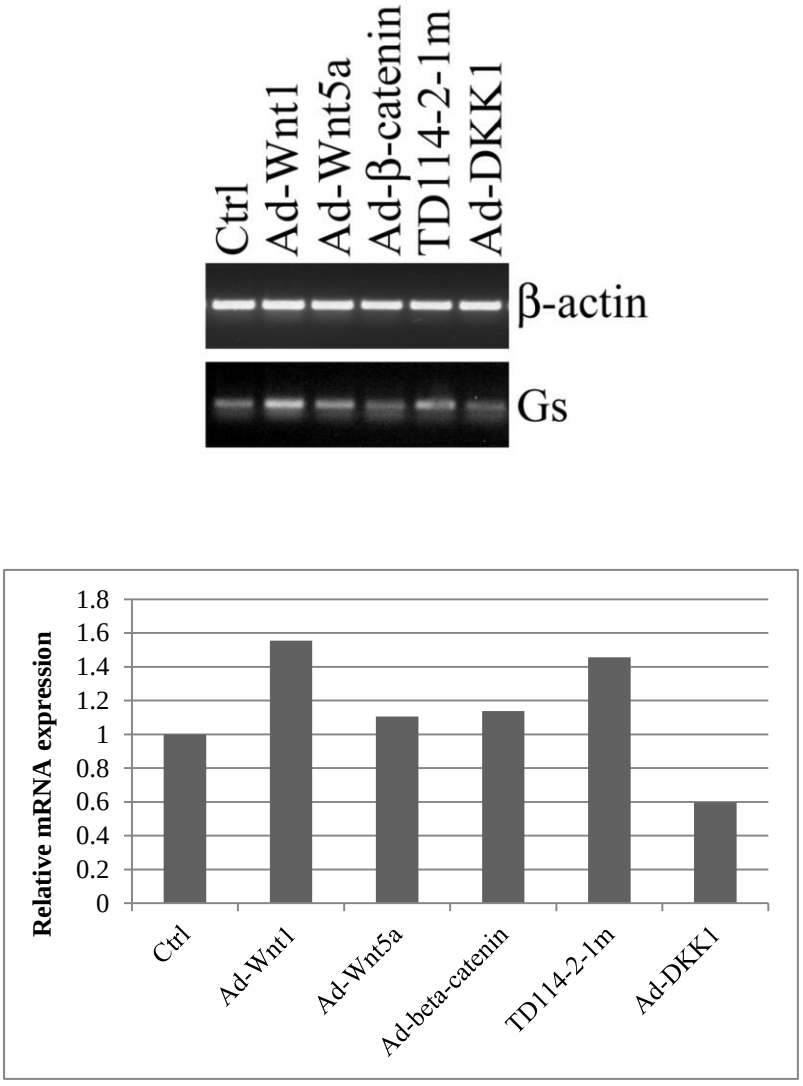

Figure 5.8 *GS* gene expression is associated with Wnt/β-catenin pathway manipulation

Liver buds were cultured for 5 days in the presence of 1μM of Dex were then infected with adenovirus or treated with TD114-2. Total RNA was extracted from liver buds infected with Ad-Wnt1, Ad-Wnt5a, Ad-β-catenin, and Ad-DKK1 or treated with TD114-2 on day 10. 2μg of RNA was reverse transcribed. 100ng of the cDNA was amplified by PCR using specific primers to the *GS* gene (Upper panel). Ad-Wnt1, Ad-Wnt5a and TD114-2 induced *GS* expression; Ad-DKK1 repressed *GS* gene expression; Ad-β-catenin in contrast did not really alter *GS* expression. The relative mRNA expression of selected genes was shown in each culture conditions. Data are fold change normalised to β-actin and are presented relative to control (lower panel).

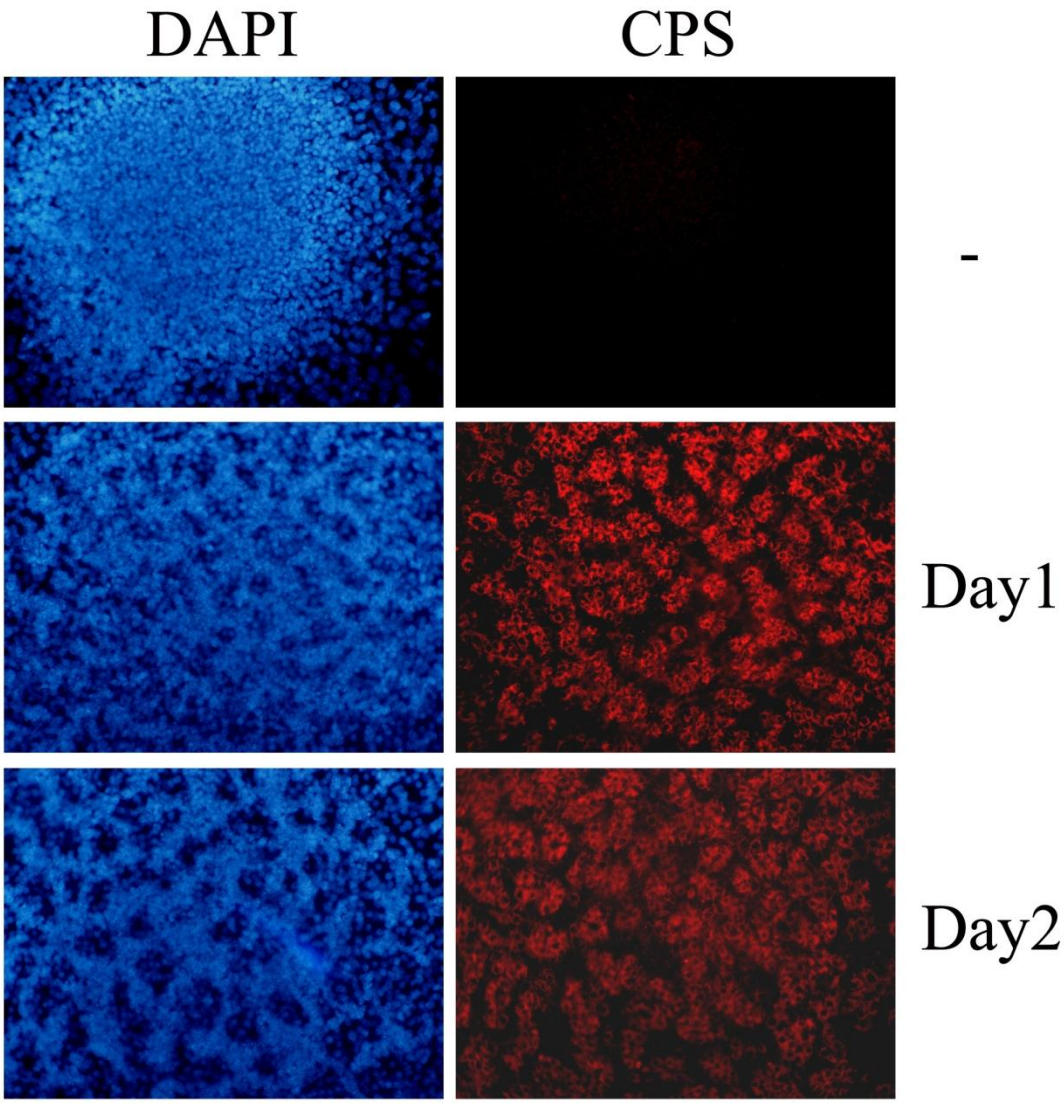

Figure 5.9 CPS expression is induced in embryonic liver cultures following Dex treatment

Liver buds were cultured in the absence (-) and presence of 1μM Dex for 1 and 2 days and then fixed. We then immunostained fixed tissue for CPS (shown in red) and counterstained with DAPI (shown in blue). The results demonstrate that CPS starts to be expressed on Day 1 following Dex treatment. (Magnification X 400)

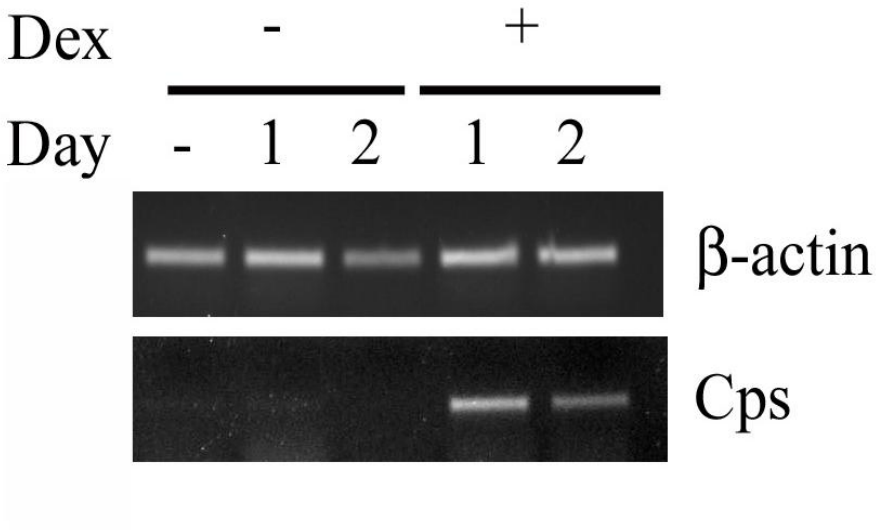

Figure 5.10 Dex treatment induces *Cps* expression in liver bud explants

RT-PCR analysis of RNA extracted from liver buds cultured with absence and presence 1μM Dex for 1 and 2 days. The results show that the *Cps* gene starts to be expressed on Day 1 of 1μDex treatment.

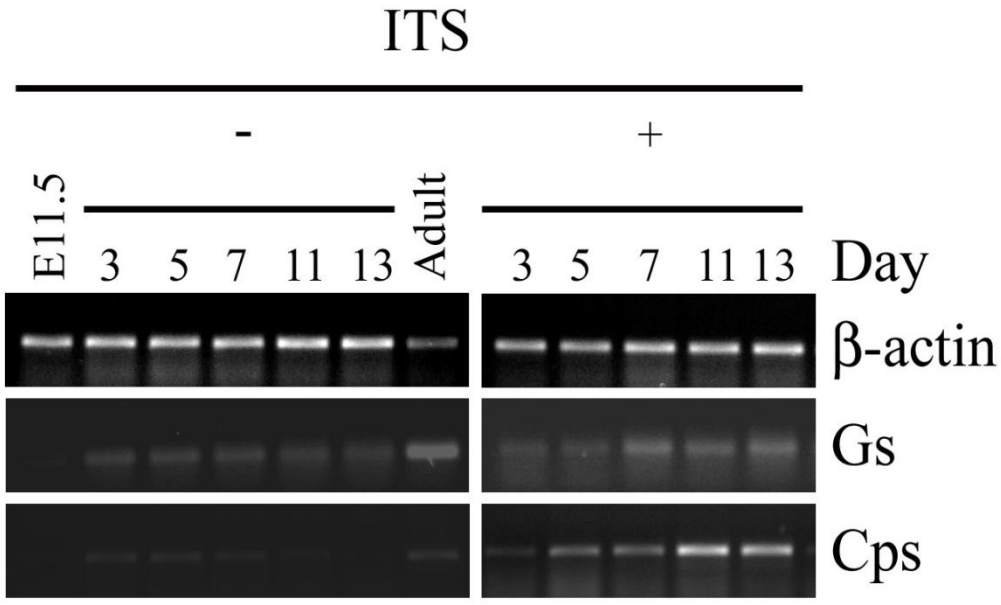

Figure 5.11 Time course of *Gs* and *Cps* gene expression in ITS-treated liver cultures

RNA was extracted from liver buds cultured with 1xITS for 3, 5, 7, 11 and 13 days. The results show that *Gs* starts to be expressed on Day 5 while the *Cps* gene begins to be expressed between Day3 and Day5 with ITS treatment.

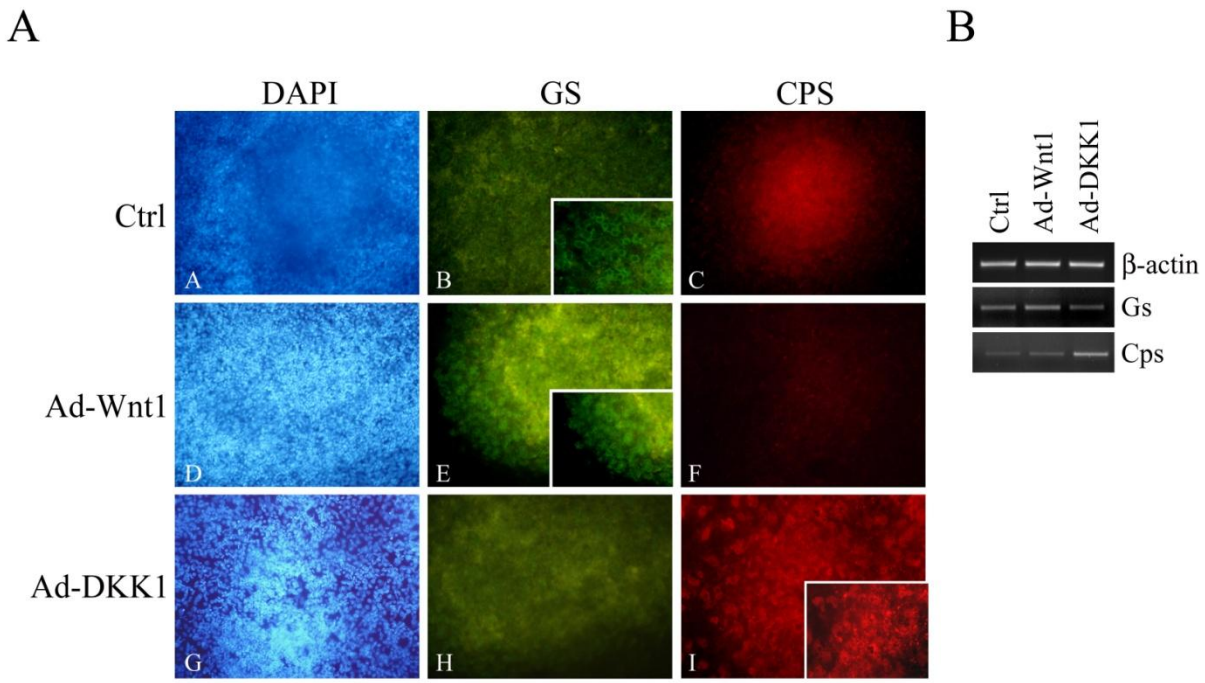

Figure 5.12 Adenoviral expression of Wnt1 and DKK1 induces complementary changes in Cps and Gs in ITS-treated liver buds

Liver buds were cultured with ITS for 5 days and then infected with Ad-null (M.O.I. 100) (A-C) as control, Ad-Wnt1 (M.O.I. 100) (D-F) or Ad-DKK1 (M.O.I. 100) (G-I) for 24 hours at 37℃. The virus was then removed and fresh medium added to the liver buds. After 5 days, the buds were subjected to RT-PCR analysis (B) or alternatively fixed and immunostained for Gs (green), Cps (red) and counterstained with DAPI (A). Ad-Wnt1 induces Gs expression and suppresses Cps expression while Ad-DKK1 induces the converse changes in the phenotype. (A-I: magnification X 200; magnification X 400 at right lower corner)

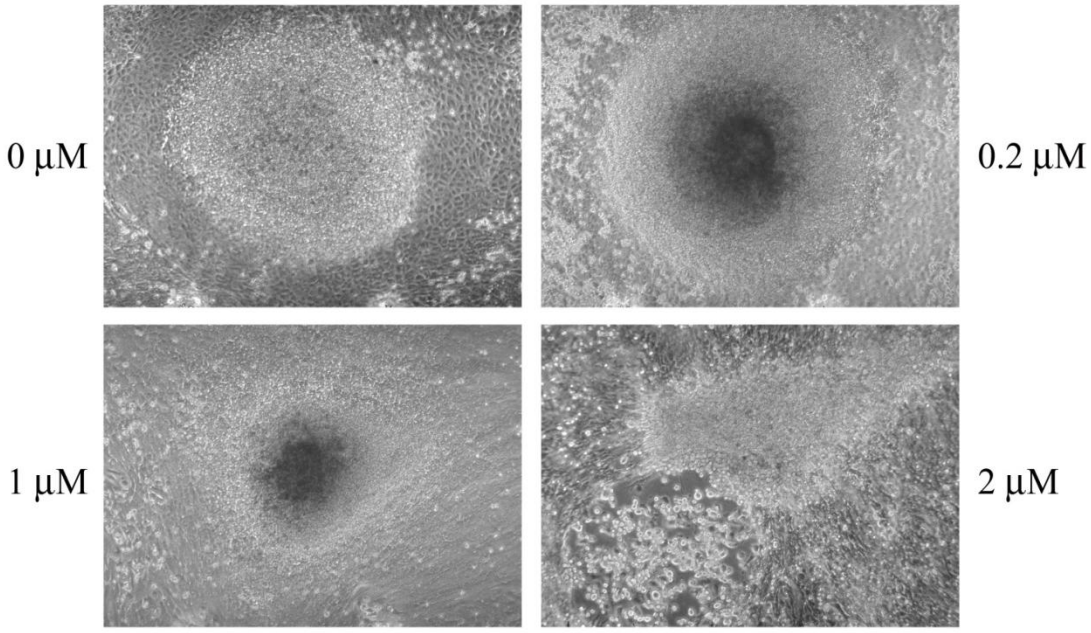

Figure 5.13 Morphological changes in mouse embryonic liver buds culture with TD114-2.

Liver buds were dissected from E11.5 mouse embryos, cultured on fibronectin-coated coverlips and incubated without (0) or with TD114-2 (0.2, 1 and 3µM) for 7 days (Magnification X 200)

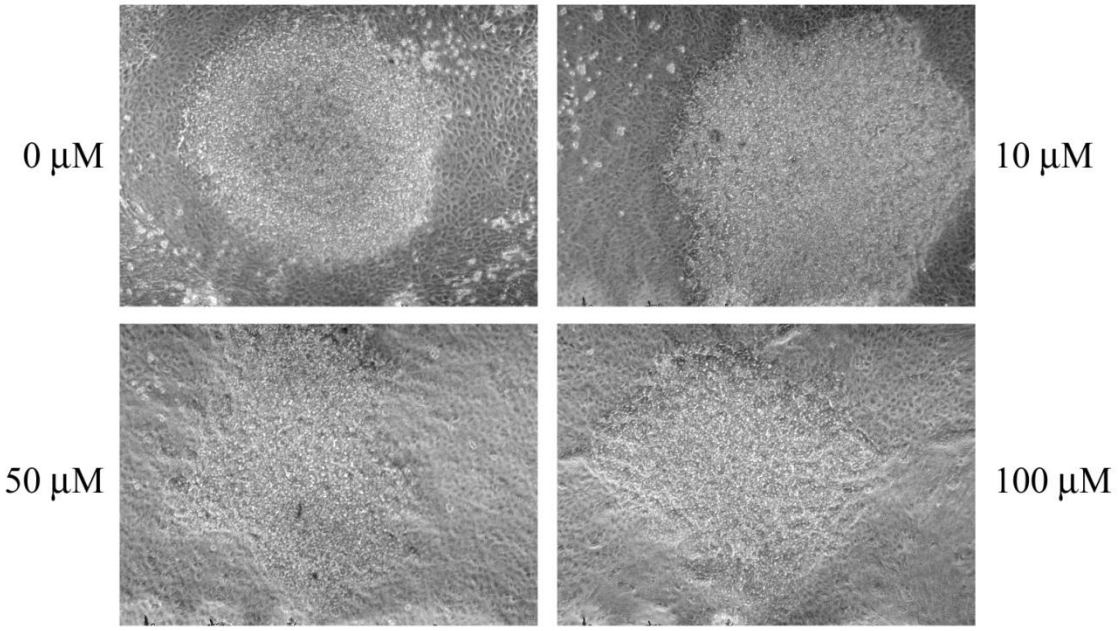

Figure 5.14 Morphological changes in liver buds following culture with Quercetin.

Liver buds were dissected from E11.5 mouse embryos, cultured on firbonectin and incubated without (0) or with Quercetin (10, 50 and 100μM) for 7 days (Magnification X 200)

A

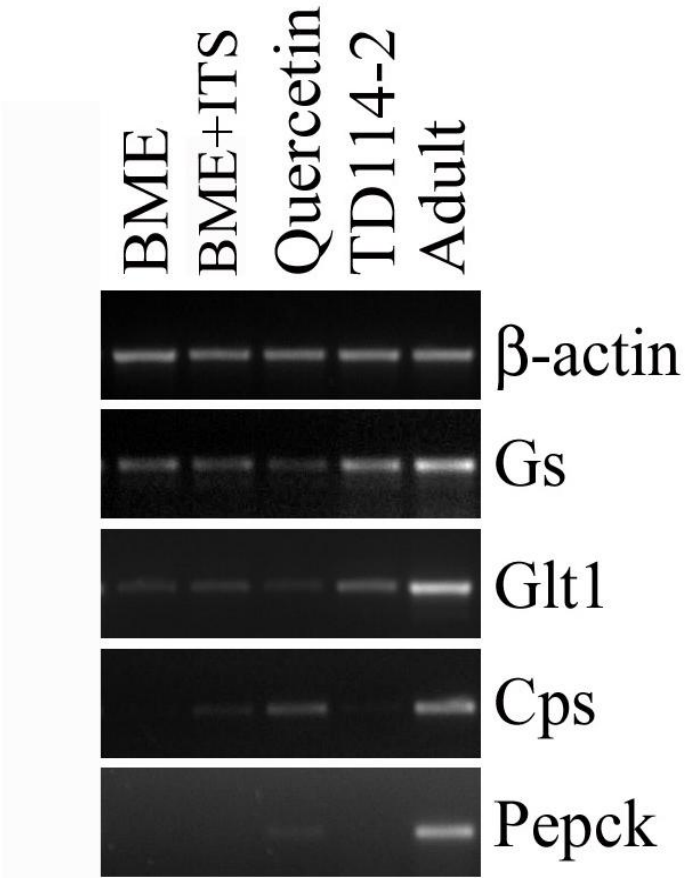

B

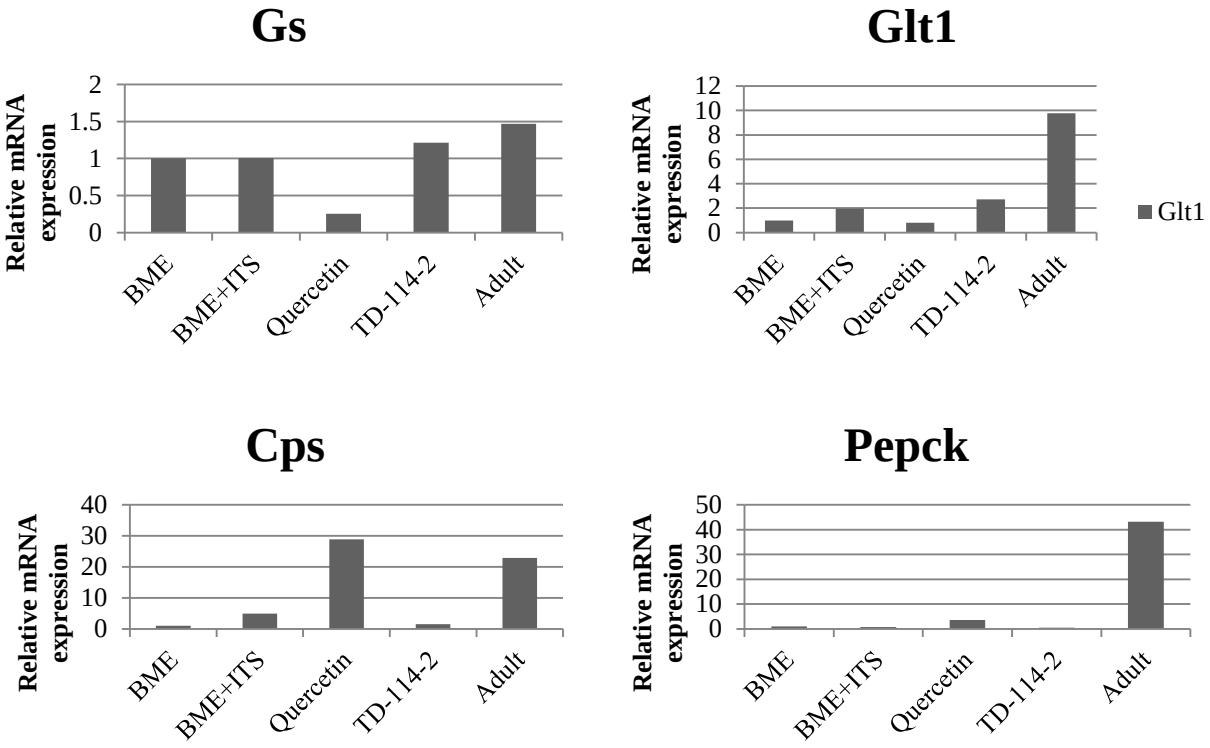

Figure 5.15 Quercetin and TD114-2 induce complementary changes in periportal and perivenous genes in cultured embryonic liver buds

Liver buds were cultured in the presence of ITS and Quercetin (100μM) or TD114-2 (1μM) was added for 10 days. Following RNA isolation, RT-PCR analysis was performed. (A) The results showed that TD114-2 induces perivenous gene expression (*Gs* and *Glt1*) and suppresses periportal gene expression (*Cps* and *Pepck*) while Quercetin induces complementary changes in the phenotype. (B) The relative mRNA expression of selected genes in each culture conditions was shown as bar chart. Data are fold change normalised to β-actin and are presented relative to BME.

5.3 Discussion

The aim of the research described in this chapter was to translate the results obtained from the *in vivo* transgenic mice to an *in vitro* setting. We specifically wished to examine the direct effect of modulating the Wnt/β-catenin pathway on the development of the zonation of ammonia detoxifying enzymes CPS and GS. To address this aim we used an *in vitro* model of embryonic mouse liver development previously developed in the lab (Burke et al, 2010). Liver tissue was dissected from E11.5 mouse embryos and chopped into small sized buds. The buds were placed into cloning rings on fibronectin-coated coverslips in BME medium supplemented with 10% FBS, penicillin (100U/ml), streptomycin (100μg/ml) and 2mM L-glutamine and allowed to attach. Over the next few days, the buds grow as flattened structures and can be subjected of wholemount immunostaining methods, protein and RNA analysis.

Buds dissected from E11.5 embryos and cultured for 7 days may be equivalent to E18.5 *in vivo* although *in vitro* culture might result in a slight delay in maturation compared to *in vivo* due to lack of soluble factors secreted from endothelial cells such as Vascular endothelial growth factor, (VEGF), hepatic mitogen, hepatic growth factor (HGF), and interleukin-6 (IL-6) which have been reported to support hepatocyte survival and proliferate (Coultas et al., 2005). In Chapter 3, we demonstrated that GS first became detectable between E17.5 and E18.5 *in vivo* (Figure 3.1). Our *in vitro* data (Figure 5.2 and Figure 5.11) showed only 1-2 days delay compared to in *vivo* data therefore shows some correlation with the *in vivo* data suggesting that the liver buds were maintained under conditions that promoted hepatic growth and differentiation.

This in vitro culture system also provided us with a feasible tool to manipulate the culture environment. By changing the component in the medium, we can easily activate or block the signalling pathway during the buds growth and monitor its effect for example morphology and viability. Previous attempts by members of the lab showed that the cultured liver tissue was refractory to ectopic gene expression by transfection (Kuang-Ming Liu and David Tosh, personal communication). Herein, we took advantage of previous established standard protocol in the lab to generate and amplify adenovirus carrying interested gene fragments and showed high infection efficiency to the culturing liver buds. 24 hrs incubation of culturing liver buds with adenovirus carrying GFP genes showed robust GFP protein expression in buds including epithelial component. The liver buds culture described here also provided a potential platform for drug screen especially for evaluating for reproductive and developmental toxicity.

CHAPTER 6 MOLECULAR BASIS OF THE CONVERSION OF PANCREATIC AR42J-B13 CELLS TO THE HEPATOCYTE PHENOTYPE

6.1 Background

Transdifferentiation is the conversion of one differentiated cell type to another and may occur either with or without cell division (Beresford, 1990; Tosh and Slack, 2002). A number of *in vitro* models have been developed by our lab for converting pancreatic cells to hepatocytes, including the rat pancreatic amphicrine call line AR42J-B13 (B13) (Shen et al. 2000) and cultured mouse embryonic pancreas (Percival and Slack 1999). The B13 cell line is a subclone derived from the parent AR42J cell line (Mashima et al, 1996). The B13 line is more amenable to differentiation to the pancreatic β-cell phenotype (Mashima et al, 1996). Shen et al. (2000) have shown after culturing B13 cells with synthetic glucocorticoid dexamethasone (Dex) for 2 weeks that the cells can transdifferentiate into hepatocytes (Transdifferentiated hepatocytes or TD hepatocytes) and start expressing hepatocyte markers such as glucose-6-phosphatase, transferrin (TFN) and albumin. The induction of C/EBP-β has also been identified as part of the molecular basis of the switch. Transfection of *C/EBP*β into B13 cells mimics Dex-induced transdifferentiation. In contrast, introduction of the dominant-negative form of C/EBPβ (termed liver-inhibitory protein or LIP) prevents Dex-induced transdifferentiation of pancreatic B13 cells to hepatocytes.

The time course of the Dex induced transdifferentiation of B13 cells was studied by Shen et al (2000). Some cells became flattened by 5 days, and some of these cells began to express glucose-6-phophatase. Albumin started to appear from 9 days, but only in those cells already expressing glucose-6-phophatase. These results indicate that transdifferentiation is a progressive process. It is presumed that initially the cells lose the pancreatic phenotype; then they start to express hepatic genes that typical of fetal liver (e.g. α-fetoprotein and transferrin); and later they

express larger amounts of albumin and other gene products characteristic of adult liver (e.g. Cyp3A1, UGT) (Tosh et al, 2002).

The CCAAT-enhancer binding proteins (C/EBP) are basic region/leucine zipper (bZIP) transcription factors expressed during differentiation of adipose tissue and liver (Manchado et al., 1994) (Birkenmeier et al., 1989; Descombes et al., 1990). C/EBPβ was found induced after just three days of treatment with Dex and cells with activated C/EBPβ also showed reduction of amylase and induction of expression of glucose-6-phosphatase (Shen et al, 2000).

Although transfection of C/EBPβ caused a similar hepatic transdifferentiation programme to treatment of Dex, it did not cause the same degree of morphological flattening suggesting that additional factors may be required to produce a more differentiated hepatic phenotype from pancreatic cells.

HNF4α is a protein that is abundant in both adult and fetal liver as well as the intestine (reviewed by Shen et al. 2003). Several studies have shown the importance of HNF4α in regulation of liver differentiation and regeneration (Li et al. 2000; Nagy et al. 1994). A knockout study in the fetal livers of mice revealed that as a consequence of HNF4α removal, some genes essential for liver function are absent e.g. HNF1α and the pregnane X receptor (PXR) (Li et al, 2000). The retinoid X receptor α (RXRα) is involved in regulation of hepatic metabolism. RXRα regulates cholesterol, fatty acid, bile acid, steroid and xenobiotic metabolism (Wan et al., 2000).

Transdifferentiated cells induced by treatment with Dex also showed nuclear expression of HNF4α (Shen et al.2000). Expression of HNF4α is first observed when oval cells differentiate

morphologically and functionally into hepatocytes and form basophilic foci (Nagy et al, 1994). HNF4α may be responsible for the final commitment of a small portion of oval cells to differentiate into hepatocytes (Nagy et al., 1994). The oval cells are thought to be the progeny of a liver stem cell compartment and evidence now exits indicating that these cells can participate in liver regeneration by differentiating into different hepatic lineage (Evarts et al., 1987; Tatematsu et al., 1985).

To test the role of the liver-enriched transcription factor HNF4α we co-expressed C/EBPβ and HNF4α in B13 cells by using adenoviral infection. Results showed that ectopic expressed HNF4α and C/EBPβ could induce the expression of hepatic genes and morphological changes of B13 cells reminiscent of hepatocytes.

6.2 Results

6.2.1 C/EBPβ and HNF4α □are key components of the transdifferentiationof pancreatic cells to hepatocytes

6.2.1.1 Optimizing the infection efficiency of adenoviral vectors in pancreatic B13 cells

B13 cells grow rapidly while being cultured in normal serum containing DMEM medium. Previous experience in the lab suggested that seeding the B13 cells at a lower density to start with might help with adenoviral infection (Al-Adsani et al., 2010). We initially determined the utility of infecting pancreatic B13 cells (seeded at a density of 30%) and infected at an M.O.I. of 100 for both Ad-HNF4α and Ad-GFP-C/EBPβ (Figure 6.1). Infected cells were subjected to immunoflourescence staining for HNF4α and C/EBPβ four days after infection. The results showed that close to 100% of cells expressed HNF4α and 50% positive of cells expressed C/EBPβ. Based on the morphology, cell viability did not appear to be affected (Figure 6.1).

6.2.1.2 Ectopically expressed HNF4α and C/EBPβ induce morphological changes in pancreatic B13 cells

B13 cells infected with adenoviral vectors expressing *C/EBPβ* and *HNF4α* showed changes in morphology under the transmitted light microscope (Figure 6.1). Cells infected with Ad-C/EBPβ alone showed a morphology similar to B13 cells infected with an Ad-null virus. The cells infected with Ad-C/EBPβ were round in shape and small in size. In contrast, B13 cells infected with Ad-HNF4α adenovirus showed a more dramatic morphology change in which the cells become

larger and flatter and were more hepatocyte-like. We also tested combining *C/EBPβ* and *HNF4α* transgenic expression on cellular morphology. Similar changes were observed in Ad-HNF4α and Ad-GFP-C/EBPβ infected cells as for cells infect with Ad-HNF4α alone.

6.2.1.3 Ectopically expressed HNF4α and C/EBPβ induce a programme of hepatic gene expression

To further characterize the Ad-HNF4α and Ad-C/EBPβ infected B13 cells, we determined the phenotype of the cells by investigating hepatocyte-specificgene expression including transferrin, albumin, α-fetoprotein and Carbamoylphosphate synthetase (CPS). As well as Ad-C/EBPβ we also tested whether the addition of another member of the C/EBP family of transcription factors (Ad-C/EBPα) enhanced hepatic gene expression.

After 4 days of infection, cDNA was reverse transcribed from mRNA isolated from cells either uninfected, or infected with HNF4α, C/EBPβ, C/EBPα alone or in combination (HNF4α + C/EBPβ, HNF4α + C/EBPα, C/EBPα + C/EBPβ and HNF4α + C/EBPβ + C/EBPα) (Figure 6.3). We looked at the expression of a panel of hepatic markers including *Albumin (Alb)*, α-fetoprotein (Afp), *Pepck, Cps* and *Glt1*. Compared to control (uninfected or Ad-null virus infected cells), the combination of Ad-HNF4α and Ad-CEBPβ alone appeared to be sufficient to induce the hepatic genes including *Alb, Afp, Pepck, Cps* and *Glt1*.

6.2.1.4 Ectopic expression of HNF4α and C/EBPβ induce hepatic protein expression

In order to test whether ectopic expression of *HNF4α* and *C/EBPβ* can induce proteins typical of hepatocytes we infected B13 cells with the two adenoviral vectors and four days later fixed the cells prior to immunostaining. Expression of hepatic proteins (including Albumin, α-fetoprotein, CPS and

Transferrin) was observed in the B13 cells infected with the combination of Ad-HNF4α and C/EBPβ (Figures 6.4-8).

6.2.1.5 Analysis of time course effect of HNF4α and C/EBPβ on hepatic gene expression

To monitor the hepatic gene expression following Ad-HNF4α and Ad-C/EBPβ infection of pancreatic B13 cells, we collected cell extracts from day 2, day 4 and day 7 post infection and generated RNA for RT-PCR analysis. The expression of *Alb* and *Afp* mRNA peaked on day 4 after infection and decreased dramatically thereafter (Figure 6.9).

6.2.1.6 OSM does not enhance CEBPβ and HNF4α derived transdifferentiation

A number of growth factors have been implicated in the early development of liver (Zaret, 2002). Oncostatin M (OSM), a member of the interleukin 6 cytokine family promotes differentiation of rodent hepatocytes in culture (Miyajima et al., 2000). Treatment of human fetal hepatocyte cultures with OSM increased cell size and enhanced cell differentiation and formation of bile canaliculi, probably through an effect on HNF4α (Lazaro et al., 2003). We wished to know whether OSM could also improve CEBPβ and HNF4α-induced transdifferentiation. To address this point we added OSM to the culture medium 1 day after the pancreatic B13 cells were infected with CEBPβ and HNF4α. Fresh medium containing OSM (10ng/ml) was replaced every other day during the 4-day incubation. RT-PCR analysis showed that OSM treatment did not enhance the hepatic phenotype (Figure 6.10).

6.2.1.7 The role of histone deacetylase inhibitors in transdifferentiation

Recently, new insights into the underlying molecular mechanisms have unveiled key regulatory roles of epigenetic marks driving cellular pluripotency, differentiation and proliferation (Atkinson and Armstrong, 2008; Yamashita et al., 2003). The transcription of genes, governing cell-fate decisions during development and maintenance of the differentiated status of a cell adult life, critically depends on the chromatin accessibility of transcription factors to genomic regulatory and coding chromatin modulation.

A previous study demonstrated that trichostatin (TSA), a histone deacetylase inhibitor, is a potent inhibitor of cell proliferation and induces hepatocyte differentiation in human hepatoma cell lines (Yamashita et al., 2003). Valproic acid (VPA) and Sodium butyrate (NaB) are also histone deacetylase inhibitors and are under investigation for treatment of HIV and various cancers (Hrebackova et al., 2010; Routy et al., 2012).

We examined the effect of addition of the histone deacetylase inhibitors TSA, VPA and NaB on CEBPβ and HNF4α induced hepatic transdifferentiation of pancreatic B13 cells. B13 cells with 30% confluence were infected with Ad-null or Ad- CEBPβ and Ad- HNF4αTSA. After 24hrs of infection, TSA, VPA and NaB were added to the medium to final concentration of 15nM, 0.5mM and 0.5mM, respectively. RNA were collected 4 days after adenovirus infection and subjected to RT-PCR analysis. Figure 6.11 showed that there was no dramatic difference between B13 cells infected with Ad-CEBPβ and Ad-HNF4α and B13 cells infected with Ad-CEBPβ and Ad-HNF4α treated with the histone deacetylase inhibitors TSA, VPA and NaB.

6.2.2 Role of the Wnt/β-catenin signalling pathway on transdifferentiation of pancreatic cells to hepatocytes

It has previously been reported that AR42J-B13 cells express Wnt signalling components [e.g. glycogen synthase kinase 3 (GSK3)], β-catenin and several T-cell factor/lymphoid enhancer factor (Tcf/Lef) (Wallace et al., 2009). The expression of many of these genes is modulated by glucocorticoid in such a way as to suggest that the Wnt signalling activity is probably suppressed in AR42J-B13-derived hepatocyte-like cells (Wallace et al, 2009). Wright and colleagues in 2010 reported that glucocorticoid-dependent transdifferentiation of B13 cells into hepatocytes is dependent on transient suppression of WNT signalling (Wallace et al., 2010). The authors showed that glucocorticoid treatment resulted in a transient loss of constitutive WNT3a expression, phosphorylation and depletion of β-catenin, loss of β-catenin nuclear localisation, and significant reduction in T-cell factor/lymphoid enhancer factor (Tcf/Lef) transcriptional activity before overt changes in the phenotype into hepatocyte-like cells. The authors refer to the hepatocyte-like cells as B-13/H cells. A return to higher Tcf/Lef transcriptional activity correlated with the re-expression of WNT3a in B-13/H cells. Quercetin - a Tcf/Lef inhibitor - did not promote transdifferentiation into B-13/H cells, but did potentiate glucocorticoid-mediated transdifferentiation. These data demonstrate that the transdifferentiation of B13 cells into hepatocyte-like cells in response to glucocorticoid was dependent on the repression of constitutively active WNT signalling. A serine/threonine kinase termed SGK1 has also been suggested to play a crucial role in B13 transdifferentiation to hepatocytes through direct phosphorylation of β-catenin (Wallace et al., 2011).

To further examine the role of Wnt/β-catenin pathway in transdifferentiation, Quercetin, TD114-2 or DKK1was added to our Dex induced B13 transdifferentiation model.

6.2.2.1 Quercetin and TD114-2

Quercetin is a Tcf/Lef inhibitor (Park et al, 2005). We attempted to repeat the experiment described by Wallace et al (2010), Quercetin was added to the culture medium to a final concentration of 50μM (Wallace et al 2010) (Figure 6.12). Cells were treated for 14 days and then subjected to RT-PCR analysis. Quercetin alone resulted in the induction of mRNA encoding *CEBP/β* but not *Albumin* or *Cyp2e1*.In contrast to the data provided by Wright et al (Wallace et al., 2010).

To determine whether activating the Wnt/β-catenin pathway through inhibition of GSK3 is important for transdifferentiation, we utilized our novel GSK3 inhibitor TD114-2. We used the inhibitor at a concentration of 0.2μM. Cells were cultured for 7 or 14 days and RT-PCR analysis of *Albumin* and α-*fetoprotein* were performed (Figure 6.13). Figure 6.13 demonstrated that treatment with TD114-2 resulted in a reduction of Albumin mRNA, producing a lower level of expression than Dex treatment, however Quercetin treatment did not result in the elevation of albumin and apha-fetoprotein mRNA expression. The over-exposure of the bands shown in the last three lanes of the albumin mRNA in Figure 6.13 indicate that the conditions of the experiment were not optimized and reduced amount of template or cycle numbers may be worth testing in the future.

6.2.2.2 DKK1

DKK1 is a secreted protein and blocks the Wnt pathway as a high affinity antagonistic ligand for LRP6, which is a Wnt co-receptor (Tamai et al., 2000). To examine whether DKK1 activity is crucial

for transdifferentiation, B13 cells were either treated with DKK1 recombinant protein or infected with Ad-DKK1 adenovirus. Figure 6.14 demonstrated that neither DKK1 protein nor DKK1 adenovirus alone could induce Albumin mRNA expression.

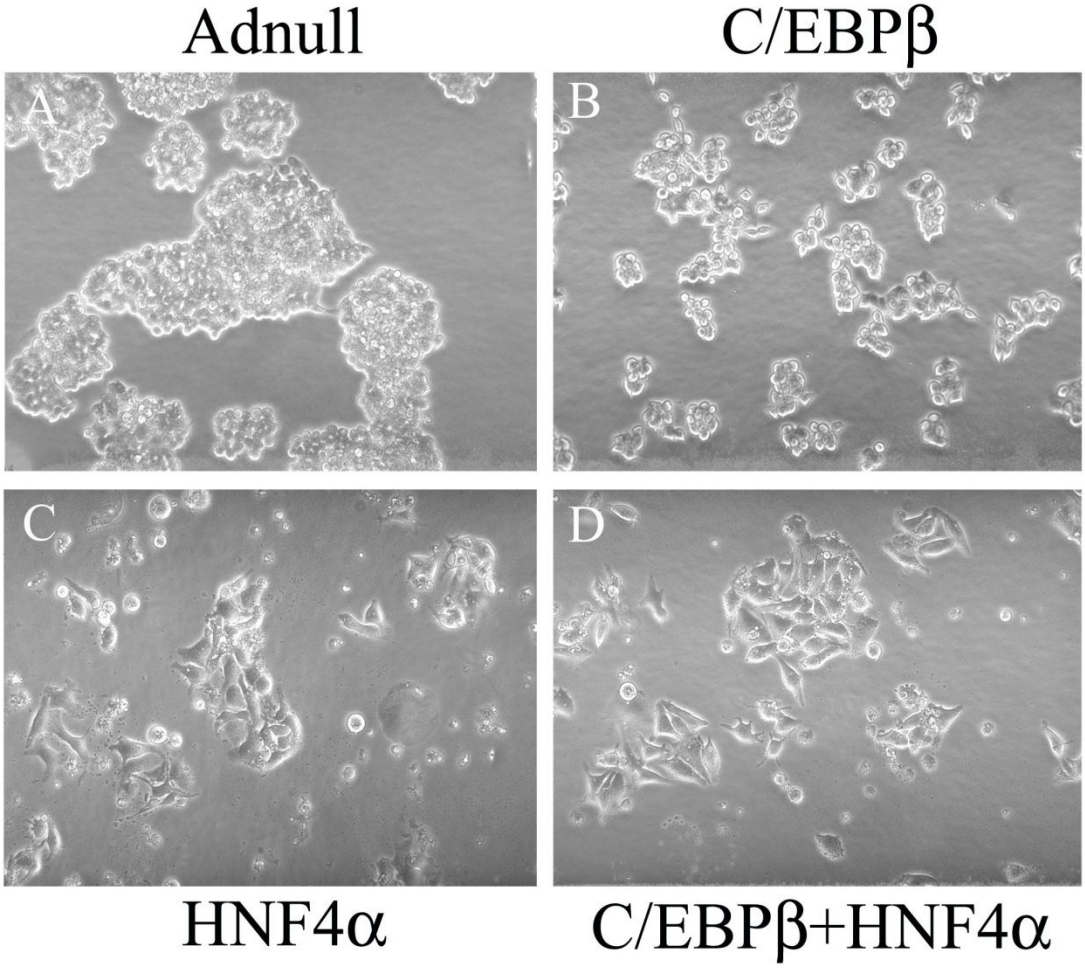

Figure 6.1 Morphological changes in pancreatic cells B13 cells following infection with Ad-C/EBPβ and/or Ad-HNF4α.

B13 cells were infected with Ad-null (M.O.I. 200), Ad-C/EBPβ (M.O.I. 100), Ad-HNF4α (M.O.I. 100) or both for 24 hours at 37℃. The virus was then removed and the cells were supplied with fresh medium. Live images were taken 4 days after infection. Ad-HNF4α induces a dramatic morphology changes in B13 cells. The cells become larger and flatter. In contrast, the B13 cells infected with Ad-C/EBPβ remain morphologically similar to the control cells.

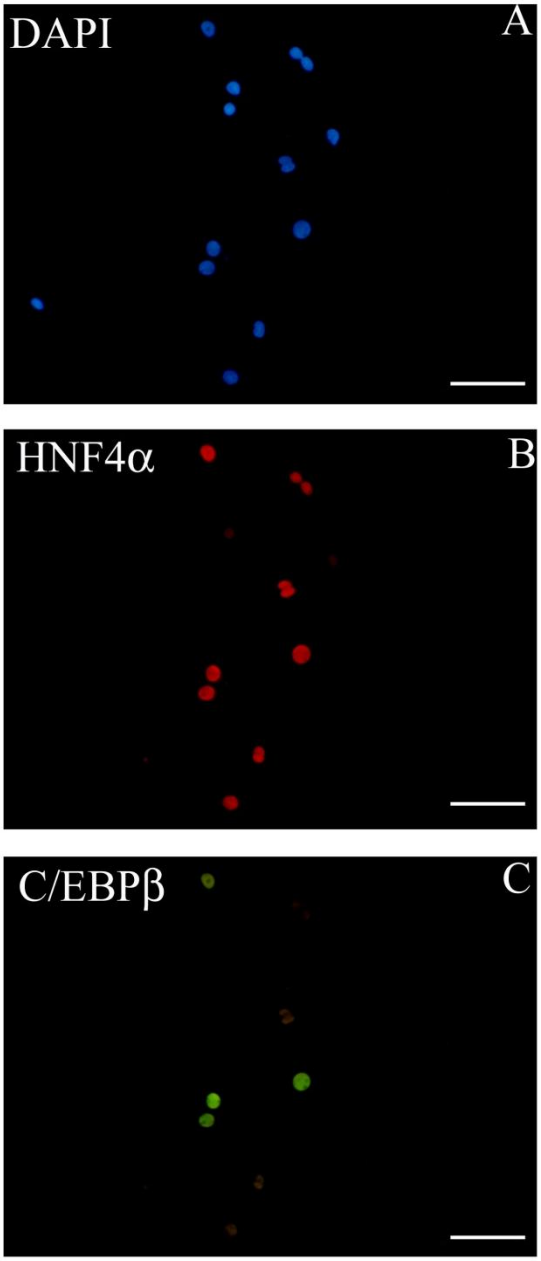

Figure 6.2 Expression of C/EBPβ and HNF4α in B13 cells following adenoviral infection

B13 cells were infected with Ad-C/EBPβ (M.O.I. 100) and Ad-HNF4α (M.O.I. 100) for 24 hours at 37℃. The virus was then removed and the cells were supplied with fresh medium. Infected cells were immunostained for HNF4α (red), C/EBPβ (green) and counterstained with DAPI. Scale bars represent 87μm.

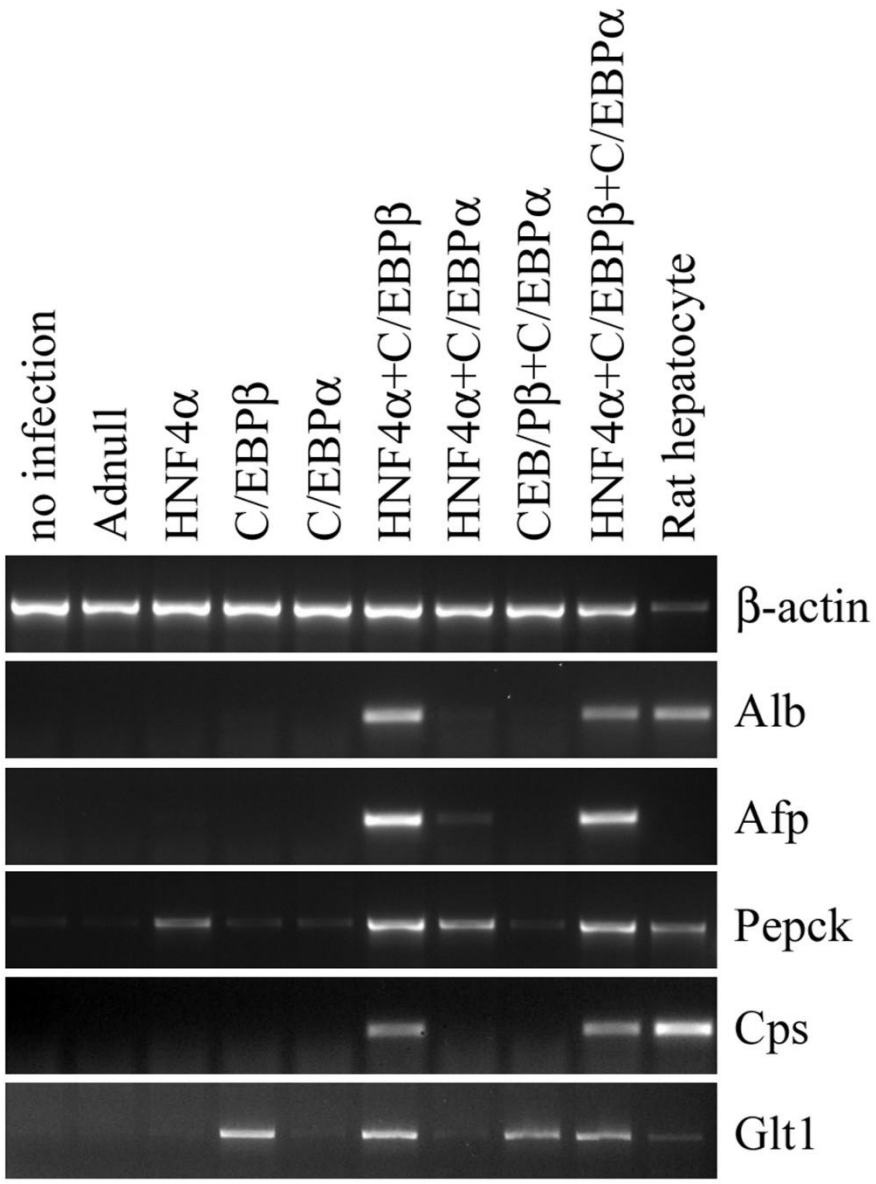

Figure 6.3 Ectopic expression of C/EBPβ and HNF4α induces hepatic transdifferentiation of pancreatic B13 cells

Total RNA was isolated from B13 cells on Day 4 following adenoviral infection. RT-PCR analysis using specific primers for hepatic genes including *Alb, Albumin; Afp, α-fetoprotein; Pepck, phosphoenolpyruvatecarboxykinas; Cps, Carbamoylphosphate synthetas; Glt1, Glutamate transporter 1*. Ad-C/EBPβ and Ad-HNF4α alone is sufficient to induce hepatic gene expression.

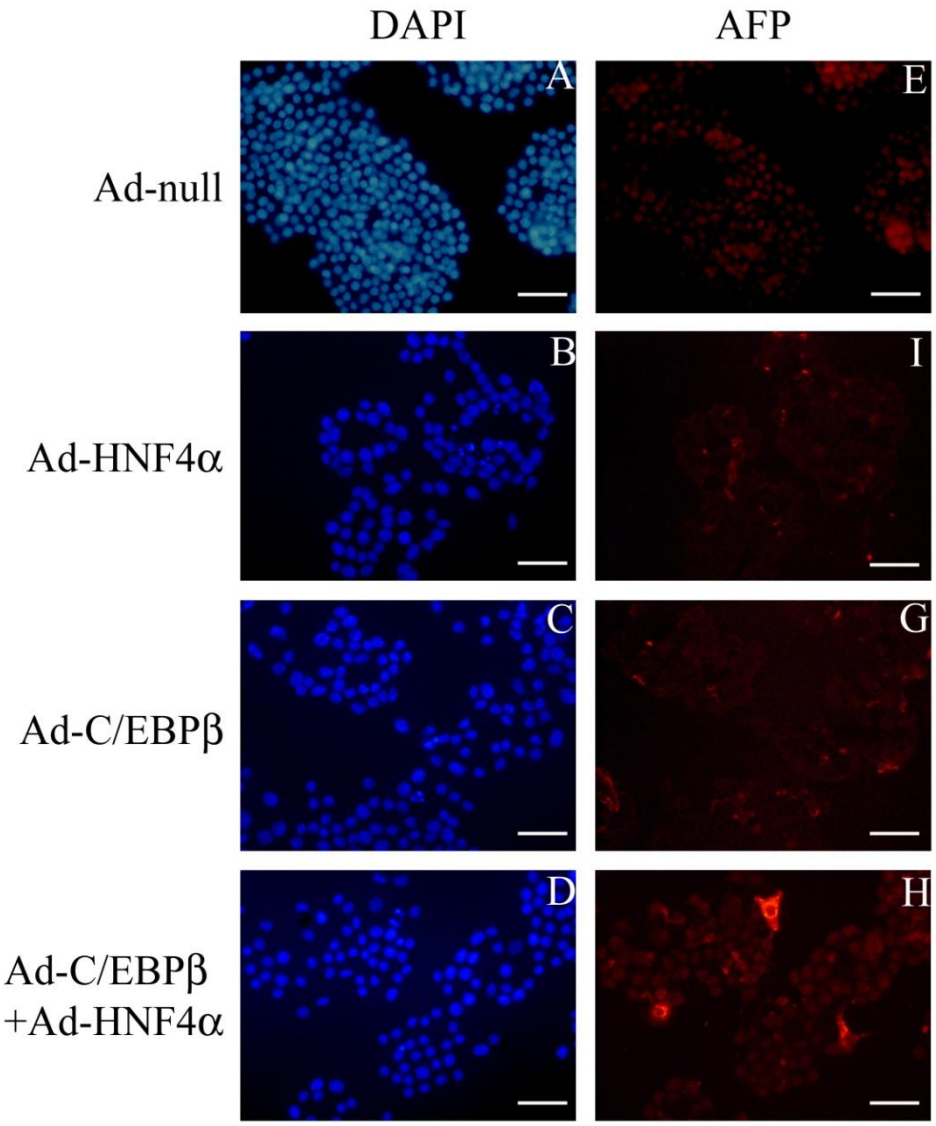

Figure 6.4 C/EBPβ and HNF4α induces AFP protein expression in B13 cells

B13 cells were infected with Ad-C/EBPβ (M.O.I. 100) and Ad-HNF4α (M.O.I. 100) for 24 hours at 37℃. The virus was then removed and cells were supplied with fresh medium. Infected cells were immunostained for AFP (red) and counterstained with DAPI. Result shows that Ad-C/EBPβ and Ad-HNF4α alone is sufficient to induce AFP protein expression. Scale bars represent 87μm.

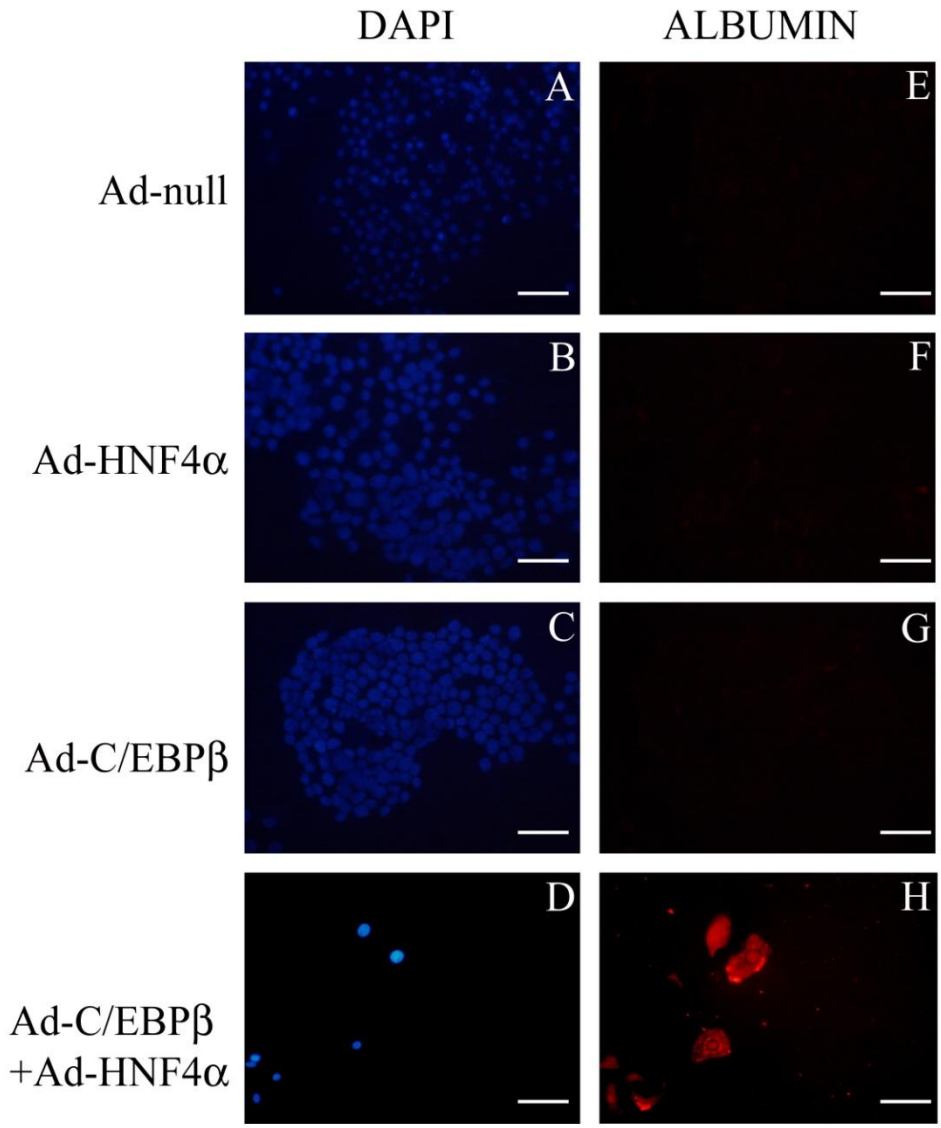

Figure 6.5 Albumin protein was induce in B13 cells after ectopic C/EBPβ and HNF4α

B13 cells were infected with Ad-C/EBPβ (M.O.I. 100) and Ad-HNF4α (M.O.I. 100) for 24 hours at 37 ℃. Virus was then removed and cells were supplied with fresh medium. Infected cells were immunostained for Albumin (red) and counterstained with DAPI. Result shows that Ad-C/EBPβ and Ad-HNF4α alone is sufficient to induce Albumin protein expression. Scale bars represent 87μm.

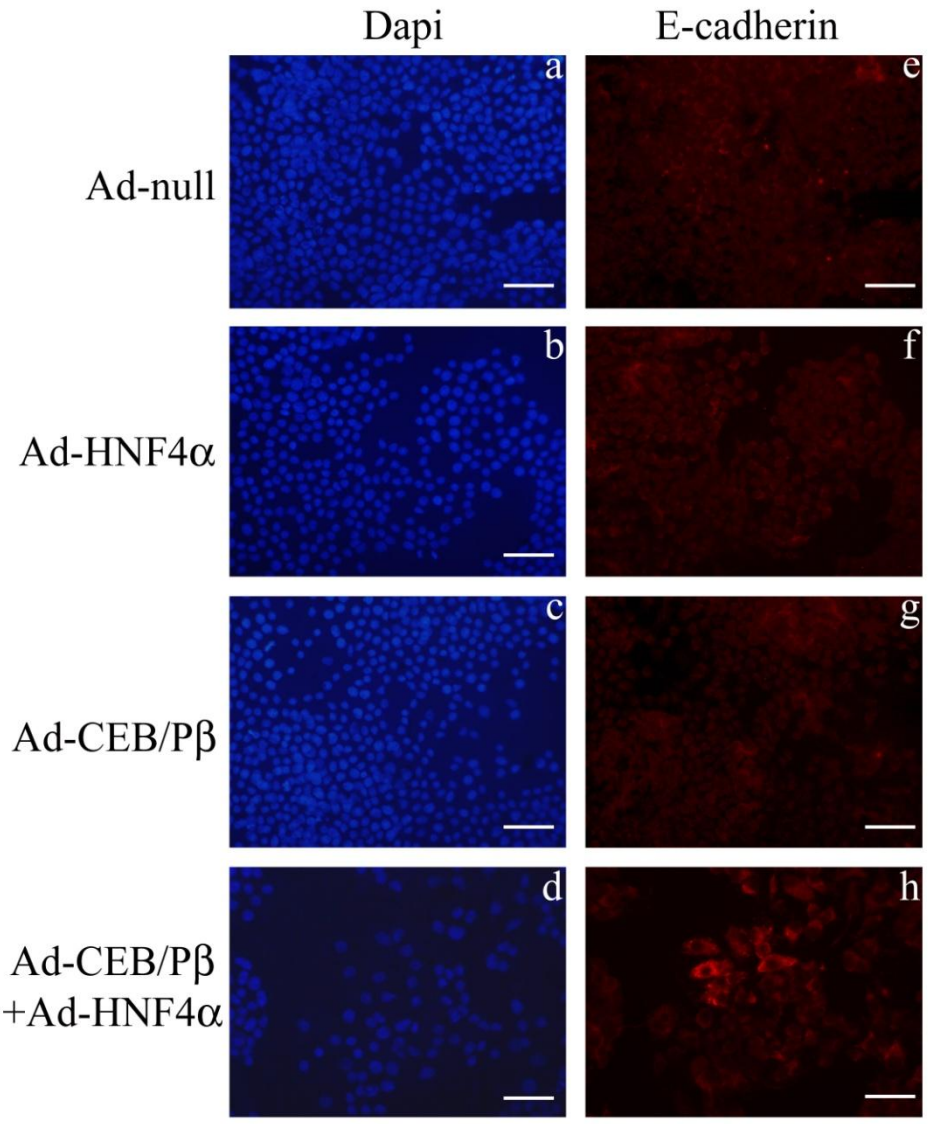

Figure 6.6 C/EBPβ and HNF4α induce E-cadherin protein expression in B13 cells

B13 cells were infected with Ad-C/EBPβ (M.O.I. 100) and Ad-HNF4α (M.O.I. 100) for 24 hours at 37 ℃. Virus was then removed and cells were supplied with fresh medium. Infected cells were immunostained for E-cadherin (red) and counterstained with DAPI. Result shows that Ad-C/EBPβ and Ad-HNF4α alone is sufficient to induce E-cadherin protein expression. Scale bars represent 87μm.

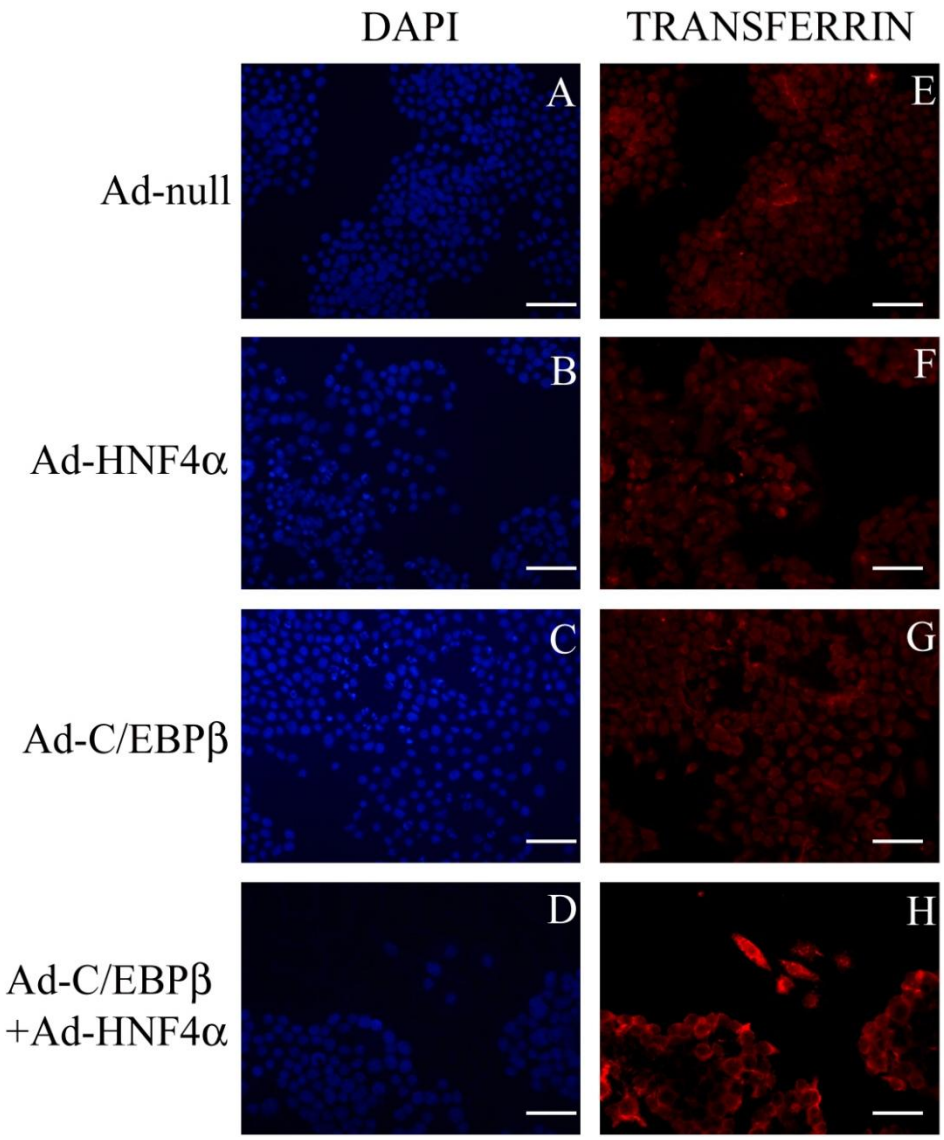

Figure 6.7 Ectopic C/EBPβ and HNF4α induce Transferrin protein expression in B13 cells

B13 cells were infected with Ad-C/EBPβ (M.O.I. 100) and Ad-HNF4α (M.O.I. 100) for 24 hours at 37 ℃. Virus was then removed and cells were supplied with fresh medium. Infected cells were immunostained for Transferrin (red) and counterstained with DAPI. Result shows that Ad-C/EBPβ and Ad-HNF4α alone is sufficient to induce Transferrin protein expression. Scale bars represent 87μm.

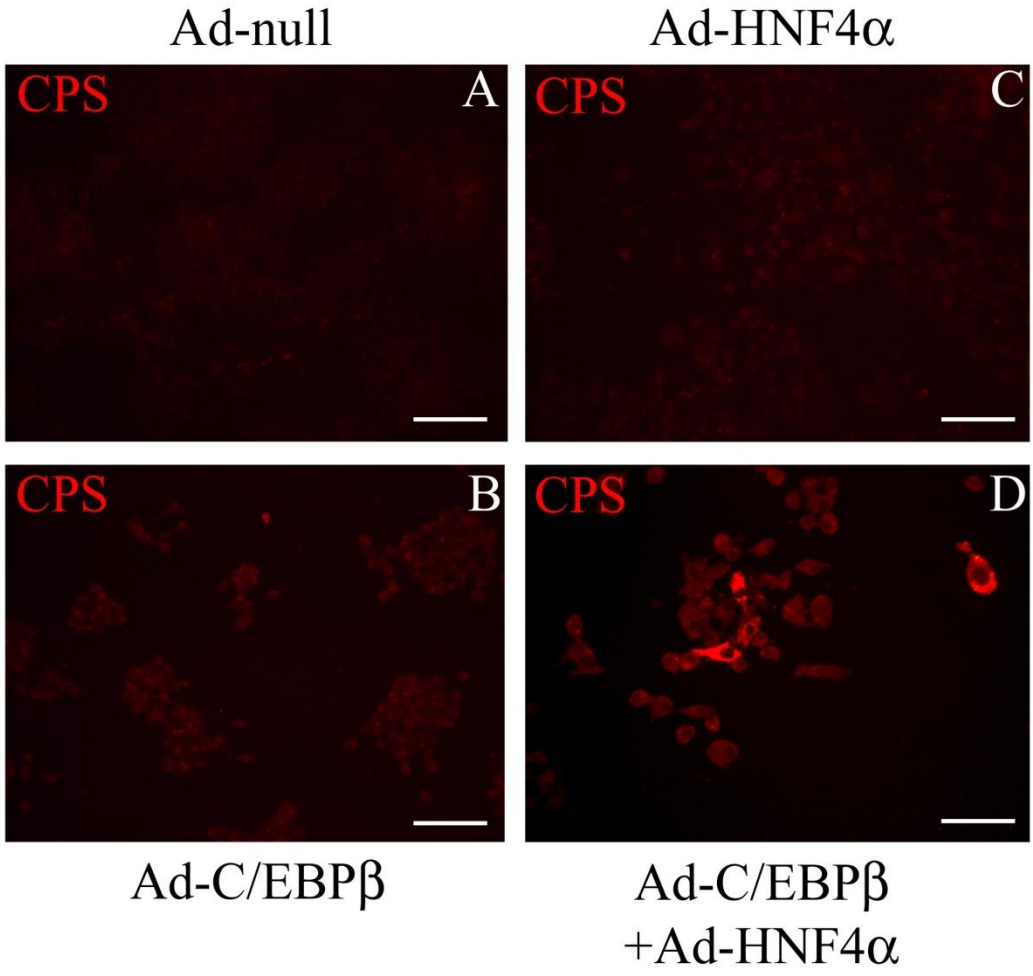

Figure 6.8 Ectopic C/EBPβ and HNF4α induce CPS protein expression in B13 cells

B13 cells were infected with Ad-C/EBPβ (M.O.I. 100) and Ad-HNF4α (M.O.I. 100) for 24 hours at 37 ℃. Virus was then removed and cells were supplied with fresh medium. Infected cells were immunostained for CPS (red) and counterstained with DAPI. Result shows that Ad-C/EBPβ and Ad-HNF4α alone is sufficient to induce CPS protein expression. Scale bars represent 87μm.

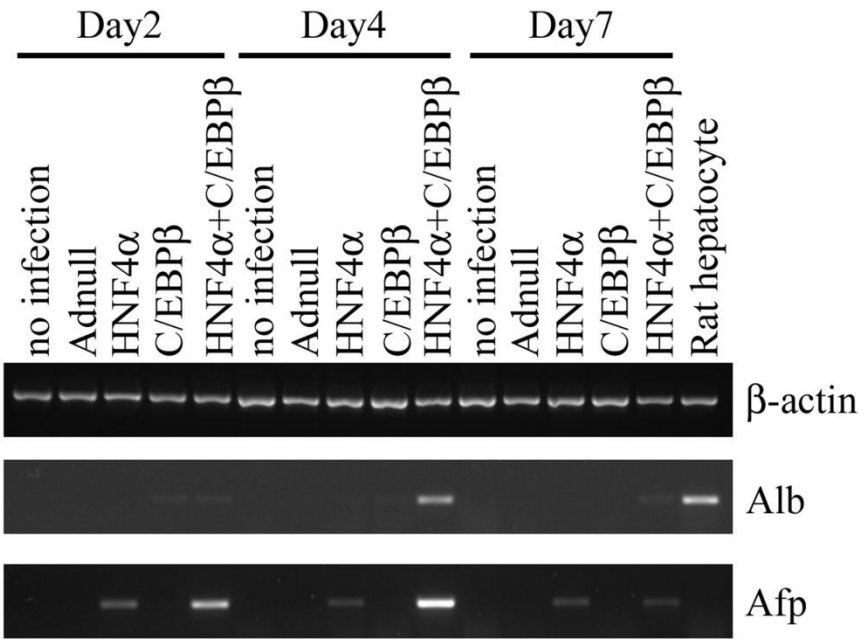

Figure 6.9 Time course of expression of hepatocyte markers following adenoviral infection of C/EBPβ and HNF4α

Total RNA was purified from B13 cells on Day 2, 4 and 7 after infection with the Adenoviral vectors indicated in the figures. RT-PCR analysis was performed using specific primers for the hepatic genes shown including *Alb, Albumin* and *Afp, α-fetoprotein.* Result suggested that C/EBPβ and HNF4α-derived transdifferentiation was maximal on Day4 of culture.

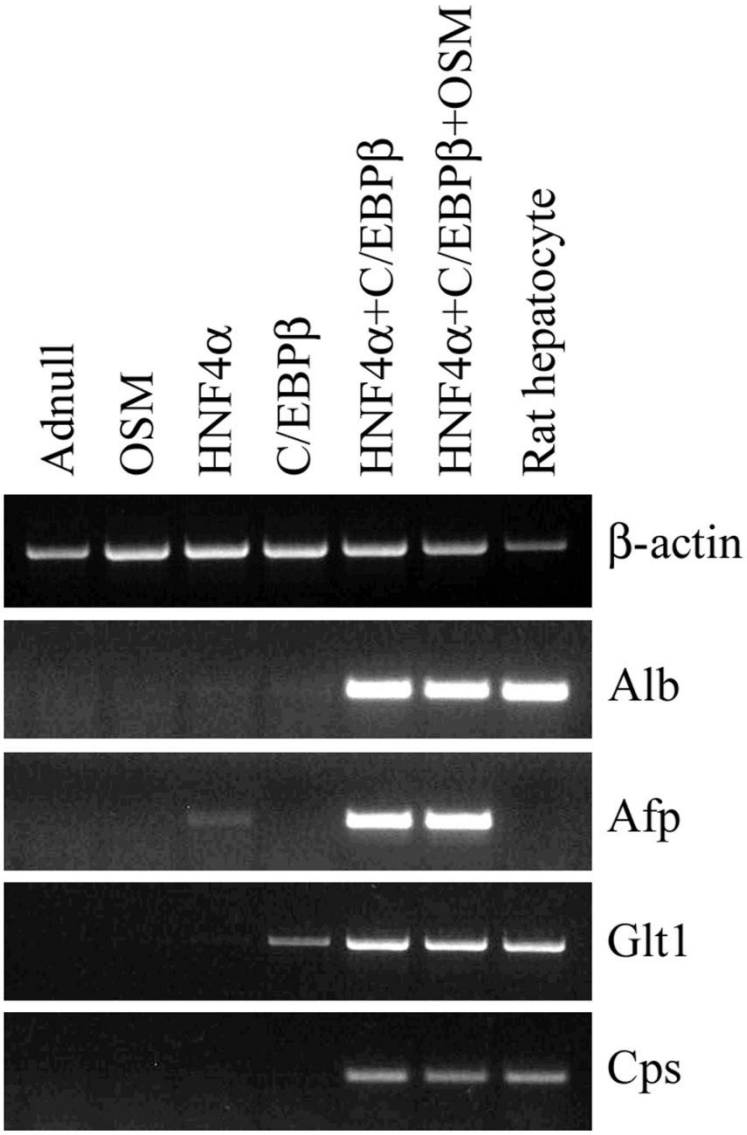

Figure 6.10 OSM did not enhance C/EBPβ and HNF4α –induced hepatic transdifferentiation of pancreatic B13 cells

Total RNA was isolated from B13 cells on day 4 after infection with the Adenoviral vectors indicated in the figures. Oncostatin M (OSM 10ng/ml) was added to B13 cells 24hrs after infected with Ad-C/EBPβ and Ad-HNF4α. RT-PCR analysis using specific primers for hepatic genes including *Alb, Albumin*; *Afp, α-fetoprotein; Cps, Carbamoylphosphate synthetase* and *Glt1, Glutamate transporter 1*. Results showed that OSM did not enhance hepatic gene expression.

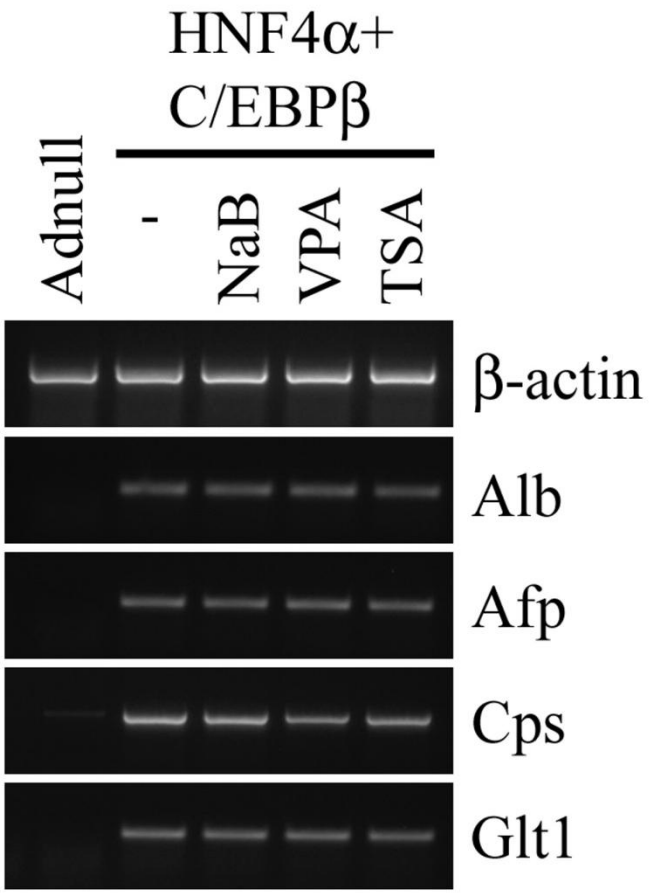

Figure 6.11 C/EBPβ and HNF4α directed transdifferentiation of pancreatic B13 cells to hepatocytes was not altered by the addition of inhibitors of histone deacetylase

Total RNA were purified from B13 cells on 4 after infected with Adenoviral vectors indicated in the figures with or without addition histone deacetylase inhibitors (NaB, VPA and TSA). RT-PCR analysis using specific primers for hepatic genes including *Alb, Albumin*; *Afp α-fetoprotein; Cps, Carbamoylphosphate synthetase* and *Glt1, Glutamate transporter 1*. Results showed that there was no enhancement of hepatic gene expression following the addition of histone deacetylase inhibitors.

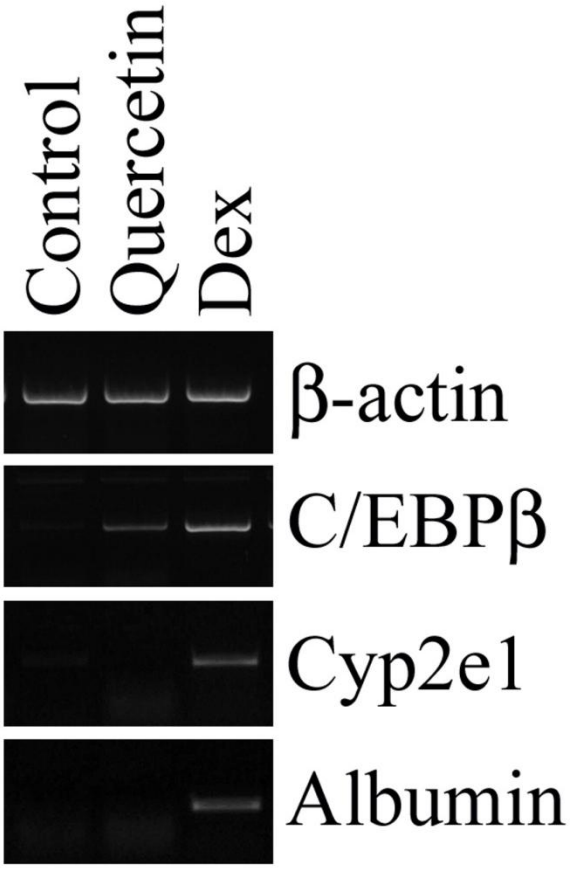

Figure 6.12 Inhibition of Tcf/Lef activity alone does not stimulate transdifferentiation

Dex and Quercetin were added to the medium 24hrs after cell seeded. Total RNA were purified from B13 cells on 14 after cultured in the medium with Quercetin (50μM) or Dex (1μM). RT-PCR analysis was performed using specific primers for hepatic genes including *C/EBPβ, Cyp2e1* and *Albumin.* Results showed Quercetin alone only induces *C/EBPβ* expression but not transdifferentiation.

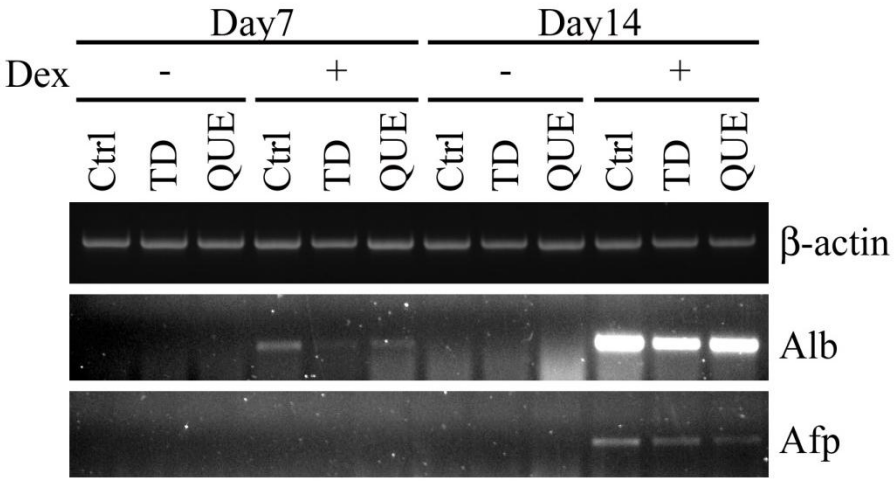

Figure 6.13 Quercetin and TD114-2 do not stimulate transdifferentiation of pancreatic B13 cells to hepatocyte-like cells

Total RNA was purified from B13 cells on Day14 after cultured in the medium with Quercetin (50μM), TD114-2 (0.2μM) with or without Dex (1μM). RT-PCR analysis was performed using specific primers for hepatic genes including *Alb*, *Albumin* and *Afp, α-fetoprotein.* Results showed that neither Quercetin nor TD114-2 alone was sufficient to induce transdifferentiation.

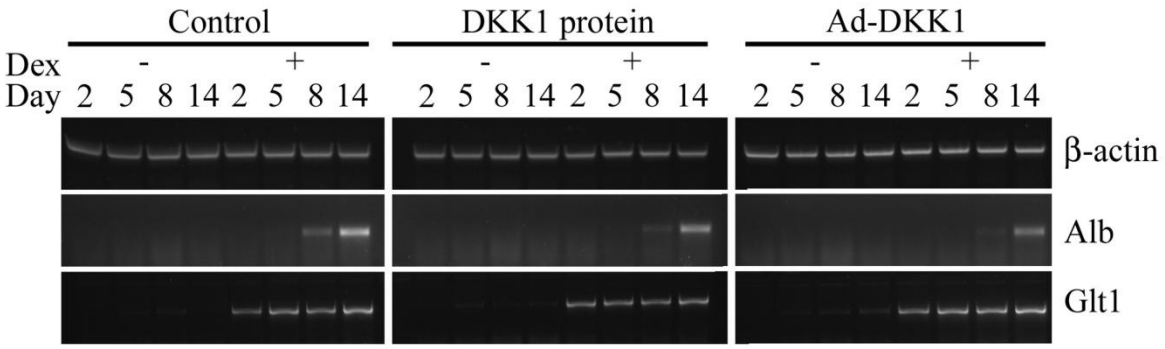

Figure 6.14 Ectopic expression of DKK1 does not stimulate hepatic transdifferentiation of pancreatic B13 cells

Total RNA was purified from B13 cells on Day2, 5, 8 and 14 after cultured in the medium with Ad-DKK1 infection (M.O.I. 100) or addition of DKK1 soluble protein with or without Dex (1μM). RT-PCR analysis was performed using specific primers for hepatic genes including *Alb, Albumin* and *Glt1, Glutamate transporter 1*. Results showed that ectopic DKK1 alone does not induce transdifferentiation.

6.3 Discussion

Previous studies from our laboratory have shown that the synthetic glucocorticoid Dexamethasone (Dex) is able to induce the transdifferentiation of pancreatic B13 cells to hepatocyte-like cells (Shen et al, 2000). While the transfection of the liver-enriched transcription factor C/EBPβ into pancreatic B13 cells can induce a hepatic phenotype, the morphological changes associated with Dex treatment are lacking. This suggests that additional factors were necessary to induce hepatic morphogenesis of the pancreatic B13 cells. One candidate transcription factor that might be involved in this process is HNF4α.

HNF-4a is a transcription factor of the nuclear hormone receptor family that is expressed in the hepatic diverticulum at the onset of liver development. Examination of the mouse complementation of HNF4a (-/-) embryos with a tetraploid embryo-derived wild-type visceral endoderm revealed that HNF4α is dispensable for specification of the hepatic lineage. However HNF4α is essential for the expression of genes that define a fully differentiated hepatocyte phenotype (Li et al., 2000). The *ex vivo* morphogenetic potential of HNF4α has been analysed using HNF4α-null embryonic hepatic cells and livers (Hayhurst et al., 2008). Using mice floxed for HNF4α, hepatic cells lacking HNF4α were isolated placed into primary culture and subsequently derived into cell lines. HNF4α-null cells show no difference with control cells in regeneration ability and expression of major cell lineages. However loss of HNF4α *in vivo* may induce stress response that interferes with liver morphogenesis.

Our results demonstrated that ectopic expressed of HNF4α could induce hepatic morphological changes of B13 cells to a more flattened phenotype. However either HNF4α or C/EBPβ alone is not

sufficient to induce hepatic differentiation of B13. Only co-expressed of C/EBPβ and HNF4α could induce morphological changes of B13 cells reminiscent of hepatocytes and induction of hepatic specific gene expression.

The maximal infectious rate of Ad-GFP-C/EBPβ was about 50%. To enhance the hepatic phenotype higher infection rates could be achieved by addition of diethylaminoethyl dextran (Sambrook et al, 1989) or alternatively a lentivirus system may be applied for further evaluation. Other strategies such as culturing in the lower concentration of serum may be an option. However if lowering the serum would lead to low cell viability need further examination. Ectopic expression of other liver enriched transcription factors may also improve the hepatic phenotype. For example, Hnf4α plus Foxa1, Foxa2 or Foxa3 have been demonstrated that can convert mouse embryonic and adult fibroblasts into cells that closely resemble hepatocytes in vitro (Sekiya and Suzuki, 2011).The phenotype of C/EBPβ/HNF4α co-expressing cells could be examined in more detail for example the study of liver function, such as albumin secretion, bioconjugation of xenobiotics and ammonia removal.

The flavonol-type flavonoid Quercetin has increased in popularity because it is a highly studied, multidimensional bioactive compound that possesses both antioxidant properties and the ability to modulate many signal transduction pathways including canonical Wnt, phosphatidylinositol 3 (PI3)-kinase (Giuliani et al., 2008) and extracellular signal-regulated kinese (ERK) (Li et al., 2012) mediated signalling pathways. Previous studies had shown that Quercetin could rapidly induce UDP-glucuronosyltransferase (UGT) in the human intestinal cell line Caco-2. The induction of UGT by Quercetin pretreatment was studied both in the intact cells and cell homogenates, measured as the glucuronidation of Quercetin, and by immunoblot analysis of the UGT 1A protein (Galijatovic et al., 2000). The complexity and rapid metabolism of Quercetin make it a challenge to repeat the previous

published results. Wright and colleagues showed that transient suppression of Wnt signalling is necessary for glucocorticoid-dependent transdifferentiation of B13 cells into hepatocytes is dependent (Wallace et al, 2010). I have tried to further investigate this phenomenon by adding two compounds, Quercetin and TD114-2, and one recombinant protein, DKK1 into our Dex induced B13 transdifferentiation model. However I failed to reproduce the same result described previously. The reason could be due to the difference between cell clones or other unknown factors which might need further investigation.

CHAPTER 7 FINAL DISCUSSION AND FUTURE PROSPECTS

Liver is the largest internal organ and it provides many essential metabolic, exocrine and endocrine functions. Embryonic liver development has been substantially studied for many years (Zaret and Grompe, 2008). Originating from the ventral foregut endoderm, embryonic liver receives induction cues from adjacent developing heart at E9.0. At E9.5, the hepatic endoderm cells, known as hepatoblasts delaminate from the epithelium and invade the adjacent septum transversum mesenchyme to form the liver bud. Between E10-15 the liver bud undergoes a period of accelerated growth as it is vascularized and colonized by hematopoietic cells to become the major fetal hematopoietic organ. Establishment of the lobular liver architecture during the perinatal period is accompanied by zonal gene regulation. Some liver enzymes are expressed in periportal regions while other enzymes are expressed in perivenous regions. The compartmentalization of function determined by the position of hepatocytes within the lobule makes it possible for liver to carry many different metabolic pathways effectively and efficiently. Although hepatic zonation is critical for its normal function, the molecular mechanism underlying the phenomenon were poorly understood until studies demonstrating the role of the Wnt/β-catenin signalling pathway in the maintenance of zonation in the adult liver. Benhamouche et al and our lab have established a role for the Wnt pathway in maintenance the zonation of ammonia detoxification in adult mice (Benhamouche et al, 2006; Burke et al, 2009). In this thesis, we uncover the role of Wnt/β-catenin signalling pathway in regulating zonation in embryonic liver.

The motivation of this work was driven by mainly two scientific questions: 1.) when and where are members of the Wnt/β-catenin pathway expressed during embryonic liver development? Then based on the spatiotemporal expression profile of Wnt/β-catenin pathway we asked the second question which was 2.) can we switch the hepatic zonal phenotype by modulating Wnt/β-catenin pathway during development?

In this thesis I have demonstrated a comprehensive expression profile of members in Wnt/β-catenin pathway using *in situ* hybridization. The temporal expression of both Wnt ligands and β-catenin suggested they may exert diverse effects on hepatic differentiation. Additionally I have shown detailed expression of the perivenous marker, GS, and the periportal marker, CPS using immunohistochemistry and western blotting. β-catenin has been reported to be declined after E14.5 and remained undetectable at perinatal stages (Micsenyi et al, 2004). However both cytoplasmic/nuclear fractionation data and immunohistochemical analysis showed clear nuclear accumulation of β-catenin between E17.5 and E18.5. This β-catenin activation at perinatal stage is also suggested to correlate with the induction of GS expression. There are 19 *Wnt* genes and 10 *Frizzled* genes identified so far in the mice. The dynamic expression patterns of these *Wnt* genes during development strongly suggest their heterogenic functions to regulate growth and differentiation. Here we have established the *in situ* hybridization technique however only demonstrated 4 *Wnt* genes and 2 *Frizzled* genes due to the limited time. More riboprobes for the rest of the members in Wnt pathway including the inhibitors should be generated and detected to provide a full circle of how Wnts signalling pathway regulated the mouse liver development.

Based on the observation of expression profile of β-catenin, CPS and GS, We went on to answer the second question: can we switch the hepatic zonation phenotype by modulating Wnt/β-catenin

pathway during development? We attempted the question from two strategies including *in vivo* by generating conditional deletion mouse of *Apc* and *β-catenin* and *in vitro* by establishing E11.5 liver buds culture system and then subsequently altering the Wnt/β-catenin pathway. The conditional deletion strategy was designed for deletion of *Apc* or *β-catenin* by AhCre-mediated recombination. In the AhCre transgenic line, Cre expression is under the control of the Cyp1A1 promoter element that is normally transcriptional silent but can be up-regulated in response to lipophilic xenobiotics such as β-napthoflavone (β–NF) (Matsushita et al., 1993). We successfully delete Apc at different embryonic stages and for the first time, we demonstrate that *Apc* deletion during mouse embryonic development would perturbs the establishment of liver zonation. Additionally, we showed *Apc* deletion will lead to liver proliferation and an increase of ductal-like structures. The canonical Wnt pathway has been shown to regulate the Notch pathway genes in intestinal adenomas (Ungerback et al, 2011). Notching signalling has been implicated in the formation of bile ducts composed of cholangiocytes by altering the expression of liver-enriched transcription factor, HNF1β (Tanimizu and Miyajima, 2004). Here we showed *Apc* deletion induced ductal phenotype during mouse development indicated by up regulation of Sox9 protein expression. We also showed the activation of Notch downstream target genes including Hes1, Hey1 and manic fringe after *Apc* gene deletion. Based on the previous studies and our result, we suggested that Wnt/β-catenin pathway induces ductal formation through activating Notching signalling pathway. However more experiments are needed to prove the hypothesis such as the analysis of ductal formation in embryonic livers dissected from *Apc/Notch* double deletion animals.

The second strategy to prove Wnt/β-catenin pathway plays critical role in regulating embryonic liver zonation is by manipulating the culture environment of dissected E11.5 liver buds. Ectopic

expression of transgene was been found to be difficult due to the nature that the nascent liver cells or hepatoblasts are surrounded by the mesenchymal cells which are notoriously easy to transfect in the culture. Here we took advantage of a well-established system in our lab of amplification and purification of high titre of adenoviral vectors to carry the genes of interest into the culture buds. The paracrine property of Wnt ligands also makes it suitable to more efficiently manipulate the Wnt/β-catenin pathway in liver culture. Here we show GS increased and CPS decreased in liver buds cultured for 5 days with the supplement of ITS and then infected with adenovirus carrying Wnt1 gene. Infection with adenovirus carrying Wnt antagonist DKK1 leads to decrease of GS and increase of CPS. This model provides us a feasible tool to investigate more detail mechanism of zonation regulation during mouse development. To further improve the *in vitro* culture systems, the effects of addition of soluble factors such as nicotinamide (Sato et al., 1999), hepatic growth factors and cytokines or cultured with extracellular proteins including type I collagen and type IV collagen should be further evaluated in the future.

The last part of my thesis was to characterize the molecular mechanism of conversion of pancreatic AR42J-B13 cells to the hepatocyte-like cells. Transdifferentiation is the conversion of one differentiated cell type to another and may occur either with or without cell division. Our lab has established a model of transdifferentiation by culturing AR42J-B13 cells with synthetic glucocorticoid dexamethasone (Dex) for 2 weeks. The pancreatic cells can then transdifferentiate into hepatocytes and start expressing hepatocyte markers such as glucose-6-phosphatase, transferrin (TFN) and albumin. The C/EBP-β has also been identified as the molecular basis of the switch. Although transfection of C/EBPβ caused a similar hepatic transdifferentiation programme to treatment of Dex, it did not cause the same degree of morphological flattening suggesting that

additional factors may be required to produce a more differentiated hepatic phenotype from pancreatic cells. HNF4α became a potential candidate due to transdifferentiated cells induced by Dex also showed nuclear expression of HNF4α. To test the role of the liver-enriched transcription factor HNF4α we co-expressed C/EBPβ and HNF4α in B13 cells by using adenoviral infection. From morphology changing and immunostaining for hepatic markers we showed that ectopic expressed HNF4α and C/EBPβ could induce a more differentiated hepatic phenotype of B13 cells.

The disadvantages of RT-PCR include its complexity and problems associated with its sensitivity, reproducibility, and specificity. Moreover, it suffers from the problems inherent in traditional PCR when it is used as a quantitative method (Bustin, 2000). However, the introduction of real-time RT-PCR and the availability of modern equipment provide extended possibilities for the accurate quantification of mRNA species. Real-time RT-PCR allows the determination of the initial template concentration and, therefore, an accurate estimation of cell number. Real-time RT-PCR has several advantages over other PCR-based quantification approaches, including elimination of post amplification handling, easier automation, and processing of large numbers of samples. In addition, it has a very large dynamic range of template determination (around 6 orders of magnitude) (Heid et al., 1996). Therefore, as the real-time PCR assay provides more accurate and precise data it should be considered as a potential technique to apply in future experiments.

Confocal microscopy is an optical imaging technique used to increase the optical resolution and contrast of a micrograph by using point illumination and a spatial pinhole to eliminate out-of-focus light in specimens that are thicker than the focal plane. It enables the reconstruction of three-dimensional structures from the obtained images. This technique has gained popularity in the scientific and industrial communities and should be considered in the future experiments.

REFERENCE

Al-Adsani, A., Burke, Z.D., Eberhard, D., Lawrence, K.L., Shen, C.N., Rustgi, A.K., Sakaue, H., Farrant, J.M., and Tosh, D. (2010). Dexamethasone treatment induces the reprogramming of pancreatic acinar cells to hepatocytes and ductal cells. PLoS One *5*, e13650.

Artavanis-Tsakonas, S., Rand, M.D., and Lake, R.J. (1999). Notch signaling: cell fate control and signal integration in development. Science *284*, 770-776.

Atkinson, S., and Armstrong, L. (2008). Epigenetics in embryonic stem cells: regulation of pluripotency and differentiation. Cell Tissue Res *331*, 23-29.

Austin, T.W., Solar, G.P., Ziegler, F.C., Liem, L., and Matthews, W. (1997). A role for the Wnt gene family in hematopoiesis: expansion of multilineage progenitor cells. Blood *89*, 3624-3635.

Barker, J.E. (1968). Development of the mouse hematopoietic system. I. Types of hemoglobin produced in embryonic yolk sac and liver. Dev Biol *18*, 14-29.

Benhamouche, S., Decaens, T., Godard, C., Chambrey, R., Rickman, D.S., Moinard, C., Vasseur-Cognet, M., Kuo, C.J., Kahn, A., Perret, C., *et al.* (2006). Apc tumor suppressor gene is the "zonation-keeper" of mouse liver. Dev Cell *10*, 759-770.

Beresford, W.A. (1990). Direct transdifferentiation: can cells change their phenotype without dividing? Cell Differ Dev *29*, 81-93.

Berkowitz, C.M., Shen, C.S., Bilir, B.M., Guibert, E., and Gumucio, J.J. (1995). Different hepatocytes express the cholesterol 7 alpha-hydroxylase gene during its circadian modulation in vivo. Hepatology *21*, 1658-1667.

Bernal, W., Hall, C., Karvellas, C.J., Auzinger, G., Sizer, E., and Wendon, J. (2007). Arterial ammonia and clinical risk factors for encephalopathy and intracranial hypertension in acute liver failure. Hepatology *46*, 1844-1852.

Bhatia, A.S., and Mihas, A.A. (2006). Cholestatic liver disease. Recognizing the clinical signs. Postgrad Med *119*, 67-75, 82.

Bi, Y., Huang, J., He, Y., Zhu, G.H., Su, Y., He, B.C., Luo, J., Wang, Y., Kang, Q., Luo, Q., *et al.* (2009). Wnt antagonist SFRP3 inhibits the differentiation of mouse hepatic progenitor cells. J Cell Biochem *108*, 295-303.

Birkenmeier, E.H., Gwynn, B., Howard, S., Jerry, J., Gordon, J.I., Landschulz, W.H., and McKnight, S.L. (1989). Tissue-specific expression, developmental regulation, and genetic mapping of the gene encoding CCAAT/enhancer binding protein. Genes Dev *3*, 1146-1156.

Block, T.M., Mehta, A.S., Fimmel, C.J., and Jordan, R. (2003). Molecular viral oncology of hepatocellular carcinoma. Oncogene *22*, 5093-5107.

Blouin, A., Bolender, R.P., and Weibel, E.R. (1977). Distribution of organelles and membranes between hepatocytes and nonhepatocytes in the rat liver parenchyma. A stereological study. J Cell Biol *72*, 441-455.

Bone, H.K., Damiano, T., Bartlett, S., Perry, A., Letchford, J., Ripoll, Y.S., Nelson, A.S., and Welham, M.J. (2009). Involvement of GSK-3 in regulation of murine embryonic stem cell self-renewal revealed by a series of bisindolylmaleimides. Chem Biol *16*, 15-27.

Bone, H.K., Nelson, A.S., Goldring, C.E., Tosh, D., and Welham, M.J. (2011). A novel chemically directed route for the generation of definitive endoderm from human embryonic stem cells based on inhibition of GSK-3. J Cell Sci *124*, 1992-2000.

Borlak, J., Dangers, M., and Thum, T. (2002). Aroclor 1254 modulates gene expression of nuclear transcription factors: implications for albumin gene transcription and protein synthesis in rat hepatocyte cultures. Toxicol Appl Pharmacol *181*, 79-88.

Borlak, J., and Thum, T. (2001). Induction of nuclear transcription factors, cytochrome P450 monooxygenases, and glutathione S-transferase alpha gene expression in Aroclor 1254-treated rat hepatocyte cultures. Biochem Pharmacol *61*, 145-153.

Bossard, P., McPherson, C.E., and Zaret, K.S. (1997). In vivo footprinting with limiting amounts of embryo tissues: a role for C/EBP beta in early hepatic development. Methods *11*, 180-188.

Bossard, P., and Zaret, K.S. (1998). GATA transcription factors as potentiators of gut endoderm differentiation. Development *125*, 4909-4917.

Braeuning, A., Ittrich, C., Kohle, C., Hailfinger, S., Bonin, M., Buchmann, A., and Schwarz, M. (2006). Differential gene expression in periportal and perivenous mouse hepatocytes. FEBS J *273*, 5051-5061.

Bralet, M.P., Branchereau, S., Brechot, C., and Ferry, N. (1994). Cell lineage study in the liver using retroviral mediated gene transfer. Evidence against the streaming of hepatocytes in normal liver. Am J Pathol *144*, 896-905.

Brameld, J.M., Weller, P.A., Saunders, J.C., Buttery, P.J., and Gilmour, R.S. (1995). Hormonal control of insulin-like growth factor-I and growth hormone receptor mRNA expression by porcine hepatocytes in culture. J Endocrinol *146*, 239-245.

Buhler, R., Lindros, K.O., Nordling, A., Johansson, I., and Ingelman-Sundberg, M. (1992). Zonation of cytochrome P450 isozyme expression and induction in rat liver. Eur J Biochem *204*, 407-412.

Burke, Z.D., Reed, K.R., Phesse, T.J., Sansom, O.J., Clarke, A.R., and Tosh, D. (2009). Liver zonation occurs through a beta-catenin-dependent, c-Myc-independent mechanism. Gastroenterology *136*, 2316-2324 e2311-2313.

Burke, Z.D., Shen, C.N., Ralphs, K.L., and Tosh, D. (2006a). Characterization of liver function in transdifferentiated hepatocytes. J Cell Physiol *206*, 147-159.

Burke, Z.D., Thowfeequ, S., and Tosh, D. (2006b). Liver specification: a new role for Wnts in liver development. Curr Biol *16*, R688-690.

Bustin, S.A. (2000). Absolute quantification of mRNA using real-time reverse transcription polymerase chain reaction assays. J Mol Endocrinol *25*, 169-193.

Cadigan, K.M., and Nusse, R. (1997). Wnt meeting 1996. Biochim Biophys Acta *1332*, R1-5.

Cadoret, A., Ovejero, C., Terris, B., Souil, E., Levy, L., Lamers, W.H., Kitajewski, J., Kahn, A., and Perret, C. (2002). New targets of beta-catenin signaling in the liver are involved in the glutamine metabolism. Oncogene *21*, 8293-8301.

Callikan, S., and Girard, J. (1979). Perinatal development of glucoeneogenic enzymes in rabbit liver. Biol Neonate *36*, 78-84.

Carraro, G., del Moral, P.M., and Warburton, D. (2010). Mouse embryonic lung culture, a system to evaluate the molecular mechanisms of branching. J Vis Exp.

Chen, J.R., Tsao, M.S., and Duguid, W.P. (1995). Hepatocytic differentiation of cultured rat pancreatic ductal epithelial cells after in vivo implantation. Am J Pathol *147*, 707-717.

Chivu, M., Dima, S.O., Stancu, C.I., Dobrea, C., Uscatescu, V., Necula, L.G., Bleotu, C., Tanase, C., Albulescu, R., Ardeleanu, C., *et al.* (2009). In vitro hepatic differentiation of human bone marrow mesenchymal stem cells under differential exposure to liver-specific factors. Transl Res *154*, 122-132.

Christoffels, V.M., Sassi, H., Ruijter, J.M., Moorman, A.F., Grange, T., and Lamers, W.H. (1999). A mechanistic model for the development and maintenance of portocentral gradients in gene expression in the liver. Hepatology *29*, 1180-1192.

Cirillo, L.A., Lin, F.R., Cuesta, I., Friedman, D., Jarnik, M., and Zaret, K.S. (2002). Opening of compacted chromatin by early developmental transcription factors HNF3 (FoxA) and GATA-4. Mol Cell *9*, 279-289.

Cooper, A.J., and Plum, F. (1987). Biochemistry and physiology of brain ammonia. Physiol Rev *67*, 440-519.

Coultas, L., Chawengsaksophak, K., and Rossant, J. (2005). Endothelial cells and VEGF in vascular development. Nature *438*, 937-945.

Cunha, G.R. (1976). Epithelial-stromal interactions in development of the urogenital tract. Int Rev Cytol *47*, 137-194.

Dabeva, M.D., Hwang, S.G., Vasa, S.R., Hurston, E., Novikoff, P.M., Hixson, D.C., Gupta, S., and Shafritz, D.A. (1997). Differentiation of pancreatic epithelial progenitor cells into hepatocytes following transplantation into rat liver. Proc Natl Acad Sci U S A *94*, 7356-7361.

Decaens, T., Godard, C., de Reynies, A., Rickman, D.S., Tronche, F., Couty, J.P., Perret, C., and Colnot, S. (2008). Stabilization of beta-catenin affects mouse embryonic liver growth and hepatoblast fate. Hepatology *47*, 247-258.

Descombes, P., Chojkier, M., Lichtsteiner, S., Falvey, E., and Schibler, U. (1990). LAP, a novel member of the C/EBP gene family, encodes a liver-enriched transcriptional activator protein. Genes Dev *4*, 1541-1551.

Diehl, A.M., Michaelson, P., and Yang, S.Q. (1994). Selective induction of CCAAT/enhancer binding protein isoforms occurs during rat liver development. Gastroenterology *106*, 1625-1637.

Dingemanse, M.A., De Jonge, W.J., De Boer, P.A., Mori, M., Lamers, W.H., and Moorman, A.F. (1996). Development of the ornithine cycle in rat liver: zonation of a metabolic pathway. Hepatology *24*, 407-411.

Dingemanse, M.A., and Lamers, W.H. (1994). Expression patterns of ammonia-metabolizing enzymes in the liver, mesonephros, and gut of human embryos and their possible implications. Anat Rec *238*, 480-490.

Douarin, N.M. (1975). An experimental analysis of liver development. Med Biol *53*, 427-455.

Dufort, D., Schwartz, L., Harpal, K., and Rossant, J. (1998). The transcription factor HNF3beta is required in visceral endoderm for normal primitive streak morphogenesis. Development *125*, 3015-3025.

Eberhard, D., O'Neill, K., Burke, Z.D., and Tosh, D. (2010). In vitro reprogramming of pancreatic cells to hepatocytes. Methods Mol Biol *636*, 285-292.

Evarts, R.P., Nagy, P., Marsden, E., and Thorgeirsson, S.S. (1987). A precursor-product relationship exists between oval cells and hepatocytes in rat liver. Carcinogenesis *8*, 1737-1740.

Finley, K.R., Tennessen, J., and Shawlot, W. (2003). The mouse secreted frizzled-related protein 5 gene is expressed in the anterior visceral endoderm and foregut endoderm during early post-implantation development. Gene Expr Patterns *3*, 681-684.

Furuyama, K., Kawaguchi, Y., Akiyama, H., Horiguchi, M., Kodama, S., Kuhara, T., Hosokawa, S., Elbahrawy, A., Soeda, T., Koizumi, M., *et al.* (2011). Continuous cell supply from a Sox9-expressing progenitor zone in adult liver, exocrine pancreas and intestine. Nat Genet *43*, 34-41.

Gaasbeek Janzen, J.W., Westenend, P.J., Charles, R., Lamers, W.H., and Moorman, A.F. (1988). Gene expression in derivatives of embryonic foregut during prenatal development of the rat. J Histochem Cytochem *36*, 1223-1230.

Galijatovic, A., Walle, U.K., and Walle, T. (2000). Induction of UDP-glucuronosyltransferase by the flavonoids chrysin and quercetin in Caco-2 cells. Pharm Res *17*, 21-26.

Gebhardt, R. (1992). Metabolic zonation of the liver: regulation and implications for liver function. Pharmacol Ther *53*, 275-354.

Geetha-Loganathan, P., Nimmagadda, S., Antoni, L., Fu, K., Whiting, C.J., Francis-West, P., and Richman, J.M. (2009). Expression of WNT signalling pathway genes during chicken craniofacial development. Dev Dyn *238*, 1150-1165.

Giuliani, C., Noguchi, Y., Harii, N., Napolitano, G., Tatone, D., Bucci, I., Piantelli, M., Monaco, F., and Kohn, L.D. (2008). The flavonoid quercetin regulates growth and gene expression in rat FRTL-5 thyroid cells. Endocrinology *149*, 84-92.

Glass, C.K., and Rosenfeld, M.G. (2000). The coregulator exchange in transcriptional functions of nuclear receptors. Genes Dev *14*, 121-141.

Gouysse, G., Couvelard, A., Frachon, S., Bouvier, R., Nejjari, M., Dauge, M.C., Feldmann, G., Henin, D., and Scoazec, J.Y. (2002). Relationship between vascular development and vascular differentiation during liver organogenesis in humans. J Hepatol *37*, 730-740.

Grigoryan, T., Wend, P., Klaus, A., and Birchmeier, W. (2008). Deciphering the function of canonical Wnt signals in development and disease: conditional loss- and gain-of-function mutations of beta-catenin in mice. Genes Dev *22*, 2308-2341.

Gualdi, R., Bossard, P., Zheng, M., Hamada, Y., Coleman, J.R., and Zaret, K.S. (1996). Hepatic specification of the gut endoderm in vitro: cell signaling and transcriptional control. Genes Dev *10*, 1670-1682.

Guo, Y., Zhang, X., Huang, J., Zeng, Y., Liu, W., Geng, C., Li, K.W., Yang, D., Wu, S., Wei, H., *et al.* (2009). Relationships between hematopoiesis and hepatogenesis in the midtrimester fetal liver characterized by dynamic transcriptomic and proteomic profiles. PLoS One *4*, e7641.

Haar, J.L., and Ackerman, G.A. (1971). A phase and electron microscopic study of vasculogenesis and erythropoiesis in the yolk sac of the mouse. Anat Rec *170*, 199-223.

Hahn, E., Wick, G., Pencev, D., and Timpl, R. (1980). Distribution of basement membrane proteins in normal and fibrotic human liver: collagen type IV, laminin, and fibronectin. Gut *21*, 63-71.

Hailfinger, S., Jaworski, M., Braeuning, A., Buchmann, A., and Schwarz, M. (2006). Zonal gene expression in murine liver: lessons from tumors. Hepatology *43*, 407-414.

Haubrich, R.H., Flexner, C., Lederman, M.M., Hirsch, M., Pettinelli, C.P., Ginsberg, R., Lietman, P., Hamzeh, F.M., Spector, S.A., and Richman, D.D. (1995). A randomized trial of the activity and safety of Ro 24-7429 (Tat antagonist) versus nucleoside for human immunodeficiency virus infection. The AIDS Clinical Trials Group 213 Team. J Infect Dis *172*, 1246-1252.

Hayhurst, G.P., Strick-Marchand, H., Mulet, C., Richard, A.F., Morosan, S., Kremsdorf, D., and Weiss, M.C. (2008). Morphogenetic competence of HNF4 alpha-deficient mouse hepatic cells. J Hepatol *49*, 384-395.

Hebrok, M., Kim, S.K., and Melton, D.A. (1998). Notochord repression of endodermal Sonic hedgehog permits pancreas development. Genes Dev *12*, 1705-1713.

Heid, C.A., Stevens, J., Livak, K.J., and Williams, P.M. (1996). Real time quantitative PCR. Genome Res *6*, 986-994.

Heller, R.S., Dichmann, D.S., Jensen, J., Miller, C., Wong, G., Madsen, O.D., and Serup, P. (2002). Expression patterns of Wnts, Frizzleds, sFRPs, and misexpression in transgenic mice suggesting a role for Wnts in pancreas and foregut pattern formation. Dev Dyn *225*, 260-270.

Houssaint, E. (1981). Differentiation of the mouse hepatic primordium. II. Extrinsic origin of the haemopoietic cell line. Cell Differ *10*, 243-252.

Hrebackova, J., Hrabeta, J., and Eckschlager, T. (2010). Valproic acid in the complex therapy of malignant tumors. Curr Drug Targets *11*, 361-379.

Hussain, S.Z., Sneddon, T., Tan, X., Micsenyi, A., Michalopoulos, G.K., and Monga, S.P. (2004). Wnt impacts growth and differentiation in ex vivo liver development. Exp Cell Res *292*, 157-169.

Ireland, H., Kemp, R., Houghton, C., Howard, L., Clarke, A.R., Sansom, O.J., and Winton, D.J. (2004). Inducible Cre-mediated control of gene expression in the murine gastrointestinal tract: effect of loss of beta-catenin. Gastroenterology *126*, 1236-1246.

Ishikawa, T., Tamai, Y., Zorn, A.M., Yoshida, H., Seldin, M.F., Nishikawa, S., and Taketo, M.M. (2001). Mouse Wnt receptor gene Fzd5 is essential for yolk sac and placental angiogenesis. Development *128*, 25-33.

Jiang, J.G., and Zarnegar, R. (1997). A novel transcriptional regulatory region within the core promoter of the hepatocyte growth factor gene is responsible for its inducibility by cytokines via the C/EBP family of transcription factors. Mol Cell Biol *17*, 5758-5770.

Johnson, G.R., and Moore, M.A. (1975). Role of stem cell migration in initiation of mouse foetal liver haemopoiesis. Nature *258*, 726-728.

Jover, R., Rodrigo, R., Felipo, V., Insausti, R., Saez-Valero, J., Garcia-Ayllon, M.S., Suarez, I., Candela, A., Compan, A., Esteban, A., *et al.* (2006). Brain edema and inflammatory activation in bile duct ligated rats with diet-induced hyperammonemia: A model of hepatic encephalopathy in cirrhosis. Hepatology *43*, 1257-1266.

Jung, J., Zheng, M., Goldfarb, M., and Zaret, K.S. (1999). Initiation of mammalian liver development from endoderm by fibroblast growth factors. Science *284*, 1998-2003.

Jungermann, K., and Katz, N. (1989). Functional specialization of different hepatocyte populations. Physiol Rev *69*, 708-764.

Jungermann, K., and Kietzmann, T. (1996). Zonation of parenchymal and nonparenchymal metabolism in liver. Annu Rev Nutr *16*, 179-203.

Kato, A., Bamba, H., Shinohara, M., Yamauchi, A., Ota, S., Kawamoto, C., and Yoshida, Y. (2005). Relationship between expression of cyclin D1 and impaired liver regeneration observed in fibrotic or cirrhotic rats. J Gastroenterol Hepatol *20*, 1198-1205.

Katz, N., Teutsch, H.F., Sasse, D., and Jungermann, K. (1977). Heterogeneous distribution of glucose-6-phosphatase in microdissected periportal and perivenous rat liver tissue. FEBS Lett *76*, 226-230.

Kawakami, Y., Capdevila, J., Buscher, D., Itoh, T., Rodriguez Esteban, C., and Izpisua Belmonte, J.C. (2001). WNT signals control FGF-dependent limb initiation and AER induction in the chick embryo. Cell *104*, 891-900.

Kikuchi, A., Kishida, S., and Yamamoto, H. (2006). Regulation of Wnt signaling by protein-protein interaction and post-translational modifications. Exp Mol Med *38*, 1-10.

Kinzler, K.W., Nilbert, M.C., Su, L.K., Vogelstein, B., Bryan, T.M., Levy, D.B., Smith, K.J., Preisinger, A.C., Hedge, P., McKechnie, D., *et al.* (1991). Identification of FAP locus genes from chromosome 5q21. Science *253*, 661-665.

Kinzler, K.W., and Vogelstein, B. (1996). Lessons from hereditary colorectal cancer. Cell *87*, 159-170.

Kmiec, Z. (2001). Cooperation of liver cells in health and disease. Adv Anat Embryol Cell Biol *161*, III-XIII, 1-151.

Krakowski, M.L., Kritzik, M.R., Jones, E.M., Krahl, T., Lee, J., Arnush, M., Gu, D., and Sarvetnick, N. (1999). Pancreatic expression of keratinocyte growth factor leads to differentiation of islet hepatocytes and proliferation of duct cells. Am J Pathol *154*, 683-691.

Kuo, F.C., and Darnell, J.E., Jr. (1991). Evidence that interaction of hepatocytes with the collecting (hepatic) veins triggers position-specific transcription of the glutamine synthetase and ornithine aminotransferase genes in the mouse liver. Mol Cell Biol *11*, 6050-6058.

Kurash, J.K., Shen, C.N., and Tosh, D. (2004). Induction and regulation of acute phase proteins in transdifferentiated hepatocytes. Exp Cell Res *292*, 342-358.

Lardon, J., Huyens, N., Rooman, I., and Bouwens, L. (2004). Exocrine cell transdifferentiation in dexamethasone-treated rat pancreas. Virchows Arch *444*, 61-65.

Lazaro, C.A., Croager, E.J., Mitchell, C., Campbell, J.S., Yu, C., Foraker, J., Rhim, J.A., Yeoh, G.C., and Fausto, N. (2003). Establishment, characterization, and long-term maintenance of cultures of human fetal hepatocytes. Hepatology *38*, 1095-1106.

Le Douarin, N. (1968). [Synthesis of glycogen in hepatocytes undergoing differentiation: role of homologous and heterologous mesenchyma]. Dev Biol *17*, 101-114.

Li, J., Mottamal, M., Li, H., Liu, K., Zhu, F., Cho, Y.Y., Sosa, C.P., Zhou, K., Bowden, G.T., Bode, A.M., *et al.* (2012). Quercetin-3-methyl ether suppresses proliferation of mouse epidermal JB6 P+ cells by targeting ERKs. Carcinogenesis *33*, 459-465.

Li, J., Ning, G., and Duncan, S.A. (2000). Mammalian hepatocyte differentiation requires the transcription factor HNF-4alpha. Genes Dev *14*, 464-474.

Lickert, H., Kispert, A., Kutsch, S., and Kemler, R. (2001). Expression patterns of Wnt genes in mouse gut development. Mech Dev *105*, 181-184.

Lindros, K.O. (1997). Zonation of cytochrome P450 expression, drug metabolism and toxicity in liver. Gen Pharmacol *28*, 191-196.

Longnecker, D.S. (1994). The quest for preneoplastic lesions in the pancreas. Arch Pathol Lab Med *118*, 226.

Manchado, C., Yubero, P., Vinas, O., Iglesias, R., Villarroya, F., Mampel, T., and Giralt, M. (1994). CCAAT/enhancer-binding proteins alpha and beta in brown adipose tissue: evidence for a tissue-specific pattern of expression during development. Biochem J *302 (Pt 3),* 695-700.

Mao, B., Wu, W., Li, Y., Hoppe, D., Stannek, P., Glinka, A., and Niehrs, C. (2001). LDL-receptor-related protein 6 is a receptor for Dickkopf proteins. Nature *411,* 321-325.

Mashima, H., Shibata, H., Mine, T., and Kojima, I. (1996). Formation of insulin-producing cells from pancreatic acinar AR42J cells by hepatocyte growth factor. Endocrinology *137,* 3969-3976.

Matsumoto, K., Yoshitomi, H., Rossant, J., and Zaret, K.S. (2001). Liver organogenesis promoted by endothelial cells prior to vascular function. Science *294,* 559-563.

Matsushita, N., Sogawa, K., Ema, M., Yoshida, A., and Fujii-Kuriyama, Y. (1993). A factor binding to the xenobiotic responsive element (XRE) of P-4501A1 gene consists of at least two helix-loop-helix proteins, Ah receptor and Arnt. J Biol Chem *268,* 21002-21006.

Medlock, E.S., and Haar, J.L. (1983). The liver hemopoietic environment: I. Developing hepatocytes and their role in fetal hemopoiesis. Anat Rec *207,* 31-41.

Meijer, A.J., Lamers, W.H., and Chamuleau, R.A. (1990). Nitrogen metabolism and ornithine cycle function. Physiol Rev *70,* 701-748.

Meredith, M.J. (1988). Rat hepatocytes prepared without collagenase: prolonged retention of differentiated characteristics in culture. Cell Biol Toxicol *4,* 405-425.

Merkel, C.E., Karner, C.M., and Carroll, T.J. (2007). Molecular regulation of kidney development: is the answer blowing in the Wnt? Pediatr Nephrol *22,* 1825-1838.

Michalopoulos, G.K., Bowen, W.C., Mule, K., and Luo, J. (2003). HGF-, EGF-, and dexamethasone-induced gene expression patterns during formation of tissue in hepatic organoid cultures. Gene Expr *11,* 55-75.

Micsenyi, A., Tan, X., Sneddon, T., Luo, J.H., Michalopoulos, G.K., and Monga, S.P. (2004). Beta-catenin is temporally regulated during normal liver development. Gastroenterology *126*, 1134-1146.

Miller, J.R., Hocking, A.M., Brown, J.D., and Moon, R.T. (1999). Mechanism and function of signal transduction by the Wnt/beta-catenin and Wnt/Ca2+ pathways. Oncogene *18*, 7860-7872.

Miyajima, A., Kinoshita, T., Tanaka, M., Kamiya, A., Mukouyama, Y., and Hara, T. (2000). Role of Oncostatin M in hematopoiesis and liver development. Cytokine Growth Factor Rev *11*, 177-183.

Monga, S.P., Micsenyi, A., Germinaro, M., Apte, U., and Bell, A. (2006). beta-Catenin regulation during matrigel-induced rat hepatocyte differentiation. Cell Tissue Res *323*, 71-79.

Monga, S.P., Monga, H.K., Tan, X., Mule, K., Pediaditakis, P., and Michalopoulos, G.K. (2003). Beta-catenin antisense studies in embryonic liver cultures: role in proliferation, apoptosis, and lineage specification. Gastroenterology *124*, 202-216.

Moore, M.A., and Metcalf, D. (1970). Ontogeny of the haemopoietic system: yolk sac origin of in vivo and in vitro colony forming cells in the developing mouse embryo. Br J Haematol *18*, 279-296.

Moorman, A.F., De Boer, P.A., Das, A.T., Labruyere, W.T., Charles, R., and Lamers, W.H. (1990). Expression patterns of mRNAs for ammonia-metabolizing enzymes in the developing rat: the ontogenesis of hepatocyte heterogeneity. Histochem J *22*, 457-468.

Morris, S.M., Jr., Kepka, D.M., Sweeney, W.E., Jr., and Avner, E.D. (1989). Abundance of mRNAs encoding urea cycle enzymes in fetal and neonatal mouse liver. Arch Biochem Biophys *269*, 175-180.

Nagy, P., Bisgaard, H.C., and Thorgeirsson, S.S. (1994). Expression of hepatic transcription factors during liver development and oval cell differentiation. J Cell Biol *126*, 223-233.

Nebert, D.W., Roe, A.L., Dieter, M.Z., Solis, W.A., Yang, Y., and Dalton, T.P. (2000). Role of the aromatic hydrocarbon receptor and [Ah] gene battery in the oxidative stress response, cell cycle control, and apoptosis. Biochem Pharmacol *59*, 65-85.

Nishisho, I., Nakamura, Y., Miyoshi, Y., Miki, Y., Ando, H., Horii, A., Koyama, K., Utsunomiya, J., Baba, S., and Hedge, P. (1991). Mutations of chromosome 5q21 genes in FAP and colorectal cancer patients. Science *253*, 665-669.

Notenboom, R.G., de Boer, P.A., Moorman, A.F., and Lamers, W.H. (1996). The establishment of the hepatic architecture is a prerequisite for the development of a lobular pattern of gene expression. Development *122*, 321-332.

Notenboom, R.G., Moorman, A.F., and Lamers, W.H. (1997). Developmental appearance of ammonia-metabolizing enzymes in prenatal murine liver. Microsc Res Tech *39*, 413-423.

Ober, E.A., Verkade, H., Field, H.A., and Stainier, D.Y. (2006). Mesodermal Wnt2b signalling positively regulates liver specification. Nature *442*, 688-691.

Oyadomari, S., Matsuno, F., Chowdhury, S., Kimura, T., Iwase, K., Araki, E., Shichiri, M., Mori, M., and Takiguchi, M. (2000). The gene for hepatocyte nuclear factor (HNF)-4alpha is activated by glucocorticoids and glucagon, and repressed by insulin in rat liver. FEBS Lett *478*, 141-146.

Paner, G.P., Gonzalez, M., Al-Masri, H., Smith, D.M., and Husain, A.N. (2002). Parafallopian tube transitional cell carcinoma. Gynecol Oncol *86*, 379-383.

Park, C.H., Chang, J.Y., Hahm, E.R., Park, S., Kim, H.K., and Yang, C.H. (2005). Quercetin, a potent inhibitor against beta-catenin/Tcf signaling in SW480 colon cancer cells. Biochem Biophys Res Commun *328*, 227-234.

Percival, A.C., and Slack, J.M. (1999). Analysis of pancreatic development using a cell lineage label. Exp Cell Res *247*, 123-132.

Perez-Pomares, J.M., Carmona, R., Gonzalez-Iriarte, M., Macias, D., Guadix, J.A., and Munoz-Chapuli, R. (2004). Contribution of mesothelium-derived cells to liver sinusoids in avian embryos. Dev Dyn *229*, 465-474.

Quinlan, J.M., Yu, W.Y., Hornsey, M.A., Tosh, D., and Slack, J.M. (2006). In vitro culture of embryonic mouse intestinal epithelium: cell differentiation and introduction of reporter genes. BMC Dev Biol *6*, 24.

Rao, M.S., Bendayan, M., Kimbrough, R.D., and Reddy, J.K. (1986). Characterization of pancreatic-type tissue in the liver of rat induced by polychlorinated biphenyls. J Histochem Cytochem *34*, 197-201.

Rao, M.S., Dwivedi, R.S., Subbarao, V., Usman, M.I., Scarpelli, D.G., Nemali, M.R., Yeldandi, A., Thangada, S., Kumar, S., and Reddy, J.K. (1988). Almost total conversion of pancreas to liver in the adult rat: a reliable model to study transdifferentiation. Biochem Biophys Res Commun *156*, 131-136.

Rao, M.S., Dwivedi, R.S., Yeldandi, A.V., Subbarao, V., Tan, X.D., Usman, M.I., Thangada, S., Nemali, M.R., Kumar, S., Scarpelli, D.G., *et al.* (1989). Role of periductal and ductular epithelial cells of the adult rat pancreas in pancreatic hepatocyte lineage. A change in the differentiation commitment. Am J Pathol *134*, 1069-1086.

Reya, T., and Clevers, H. (2005). Wnt signalling in stem cells and cancer. Nature *434*, 843-850.

Rossi, J.M., Dunn, N.R., Hogan, B.L., and Zaret, K.S. (2001). Distinct mesodermal signals, including BMPs from the septum transversum mesenchyme, are required in combination for hepatogenesis from the endoderm. Genes Dev *15*, 1998-2009.

Routy, J.P., Tremblay, C.L., Angel, J.B., Trottier, B., Rouleau, D., Baril, J.G., Harris, M., Trottier, S., Singer, J., Chomont, N., *et al.* (2012). Valproic acid in association with highly active antiretroviral therapy for reducing systemic HIV-1 reservoirs: results from a multicentre randomized clinical study. HIV Med *13*, 291-296.

Rubinfeld, B., Albert, I., Porfiri, E., Fiol, C., Munemitsu, S., and Polakis, P. (1996). Binding of GSK3beta to the APC-beta-catenin complex and regulation of complex assembly. Science *272*, 1023-1026.

Sansom, O.J., Reed, K.R., Hayes, A.J., Ireland, H., Brinkmann, H., Newton, I.P., Batlle, E., Simon-Assmann, P., Clevers, H., Nathke, I.S., *et al.* (2004). Loss of Apc in vivo immediately perturbs Wnt signaling, differentiation, and migration. Genes Dev *18*, 1385-1390.

Sato, F., Mitaka, T., Mizuguchi, T., Mochizuki, Y., and Hirata, K. (1999). Effects of nicotinamide-related agents on the growth of primary rat hepatocytes and formation of small hepatocyte colonies. Liver *19*, 481-488.

Scarpelli, D.G., and Rao, M.S. (1981). Early changes in regenerating hamster pancreas following a single dose of N-nitrosobis (2-oxopropyl)amine (NBOP) administered at the peak of DNA synthesis. Cancer *47*, 1552-1561.

Schoneveld, O.J., Gaemers, I.C., Hoogenkamp, M., and Lamers, W.H. (2005). The role of proximal-enhancer elements in the glucocorticoid regulation of carbamoylphosphate synthetase gene transcription from the upstream response unit. Biochimie *87*, 1033-1040.

Sekine, S., Lan, B.Y., Bedolli, M., Feng, S., and Hebrok, M. (2006). Liver-specific loss of beta-catenin blocks glutamine synthesis pathway activity and cytochrome p450 expression in mice. Hepatology *43*, 817-825.

Sekiya, S., and Suzuki, A. (2011). Direct conversion of mouse fibroblasts to hepatocyte-like cells by defined factors. Nature *475*, 390-393.

Semenov, M.V., Tamai, K., Brott, B.K., Kuhl, M., Sokol, S., and He, X. (2001). Head inducer Dickkopf-1 is a ligand for Wnt coreceptor LRP6. Curr Biol *11*, 951-961.

Sen, S., Rose, C., Ytrebo, L.M., Davies, N.A., Nedredal, G.I., Drevland, S.S., Kjonno, M., Prinzen, F.W., Hodges, S.J., Deutz, N.E., *et al.* (2006). Effect of albumin dialysis on intracranial pressure increase in pigs with acute liver failure: a randomized study. Crit Care Med *34*, 158-164.

Shen, C.N., Seckl, J.R., Slack, J.M., and Tosh, D. (2003). Glucocorticoids suppress beta-cell development and induce hepatic metaplasia in embryonic pancreas. Biochem J *375*, 41-50.

Shen, C.N., Slack, J.M., and Tosh, D. (2000). Molecular basis of transdifferentiation of pancreas to liver. Nat Cell Biol *2*, 879-887.

Shen, C.N., and Tosh, D. (2010). Transdifferentiation of pancreatic cells to hepatocytes. Methods Mol Biol *640*, 273-280.

Shibata, H. (1997). Rapid Colorectal Adenoma Formation Initiated by Conditional Targeting of the Apc Gene. Science *278*, 120-123.

Shiojiri, N., and Sugiyama, Y. (2004). Immunolocalization of extracellular matrix components and integrins during mouse liver development. Hepatology *40*, 346-355.

Sigal, S.H., Brill, S., Fiorino, A.S., and Reid, L.M. (1992). The liver as a stem cell and lineage system. Am J Physiol *263*, G139-148.

Slack, J.M. (1986). Epithelial metaplasia and the second anatomy. Lancet *2*, 268-271.

Slack, J.M., and Tosh, D. (2001). Transdifferentiation and metaplasia--switching cell types. Curr Opin Genet Dev *11*, 581-586.

Spear, B.T., Jin, L., Ramasamy, S., and Dobierzewska, A. (2006). Transcriptional control in the mammalian liver: liver development, perinatal repression, and zonal gene regulation. Cell Mol Life Sci *63*, 2922-2938.

Spijkers, J.A., van den Hoff, M.J., Hakvoort, T.B., Vermeulen, J.L., Tesink-Taekema, S., and Lamers, W.H. (2001). Foetal rise in hepatic enzymes follows decline in c-met and hepatocyte growth factor expression. J Hepatol *34*, 699-710.

Spooner, B.S., Bassett, K.E., and Spooner, B.S., Jr. (1989). Embryonic salivary gland epithelial branching activity is experimentally independent of epithelial expansion activity. Dev Biol *133*, 569-575.

Staal, F.J., and Clevers, H.C. (2005). WNT signalling and haematopoiesis: a WNT-WNT situation. Nat Rev Immunol *5*, 21-30.

Steiner, R., and Vogel, H. (1973). On the kinetics of erythroid cell differentiation in fetal mice. I. Microspectrophotometric determination of the hemoglobin content in erythroid cells during gestation. J Cell Physiol *81*, 323-338.

Suksaweang, S., Lin, C.M., Jiang, T.X., Hughes, M.W., Widelitz, R.B., and Chuong, C.M. (2004). Morphogenesis of chicken liver: identification of localized growth zones and the role of beta-catenin/Wnt in size regulation. Dev Biol *266*, 109-122.

Tamai, K., Semenov, M., Kato, Y., Spokony, R., Liu, C., Katsuyama, Y., Hess, F., Saint-Jeannet, J.P., and He, X. (2000). LDL-receptor-related proteins in Wnt signal transduction. Nature *407*, 530-535.

Tan, X., Yuan, Y., Zeng, G., Apte, U., Thompson, M.D., Cieply, B., Stolz, D.B., Michalopoulos, G.K., Kaestner, K.H., and Monga, S.P. (2008). Beta-catenin deletion in hepatoblasts disrupts hepatic morphogenesis and survival during mouse development. Hepatology *47*, 1667-1679.

Tanimizu, N., and Miyajima, A. (2004). Notch signaling controls hepatoblast differentiation by altering the expression of liver-enriched transcription factors. J Cell Sci *117*, 3165-3174.

Tatematsu, M., Kaku, T., Medline, A., and Farber, E. (1985). Intestinal metaplasia as a common option of oval cells in relation to cholangiofibrosis in liver of rats exposed to 2-acetylaminofluorene. Lab Invest *52*, 354-362.

Thompson, M.D., and Monga, S.P. (2007). WNT/beta-catenin signaling in liver health and disease. Hepatology *45*, 1298-1305.

Thowfeequ, S., Ralphs, K.L., Yu, W.Y., Slack, J.M., and Tosh, D. (2007). Betacellulin inhibits amylase and glucagon production and promotes beta cell differentiation in mouse embryonic pancreas. Diabetologia *50*, 1688-1697.

Tosh, D., Borthwick, E.B., Sharp, S., Burchell, A., Burchell, B., and Coughtrie, M.W. (1996). Heterogeneous expression of sulphotransferases in periportal and perivenous hepatocytes prepared from male and female rat liver. Biochem Pharmacol *51*, 369-374.

Tosh, D., and Slack, J.M. (2002). How cells change their phenotype. Nat Rev Mol Cell Biol *3*, 187-194.

Tremblay, K.D., and Zaret, K.S. (2005). Distinct populations of endoderm cells converge to generate the embryonic liver bud and ventral foregut tissues. Dev Biol *280*, 87-99.

van Roon, M.A., Zonneveld, D., de Boer, P.A., Moorman, A.F., Charles, R., and Lamers, W.H. (1990). Regulation of hepatocyte-specific gene expression in cultures of human embryonic hepatocytes. Biol Neonate *58*, 152-159.

Vinken, M., Papeleu, P., Snykers, S., De Rop, E., Henkens, T., Chipman, J.K., Rogiers, V., and Vanhaecke, T. (2006). Involvement of cell junctions in hepatocyte culture functionality. Crit Rev Toxicol *36*, 299-318.

Waalkes, M.P., Cherian, M.G., Ward, J.M., and Goyer, R.A. (1992). Immunohistochemical evidence of high concentrations of metallothionein in pancreatic hepatocytes induced by cadmium in rats. Toxicol Pathol *20*, 323-326.

Wallace, K., Long, Q., Fairhall, E.A., Charlton, K.A., and Wright, M.C. (2011). Serine/threonine protein kinase SGK1 in glucocorticoid-dependent transdifferentiation of pancreatic acinar cells to hepatocytes. J Cell Sci *124*, 405-413.

Wallace, K., Marek, C.J., Currie, R.A., and Wright, M.C. (2009). Exocrine pancreas trans-differentiation to hepatocytes--a physiological response to elevated glucocorticoid in vivo. J Steroid Biochem Mol Biol *116*, 76-85.

Wallace, K., Marek, C.J., Hoppler, S., and Wright, M.C. (2010). Glucocorticoid-dependent transdifferentiation of pancreatic progenitor cells into hepatocytes is dependent on transient suppression of WNT signalling. J Cell Sci *123*, 2103-2110.

Wan, Y.J., An, D., Cai, Y., Repa, J.J., Hung-Po Chen, T., Flores, M., Postic, C., Magnuson, M.A., Chen, J., Chien, K.R., *et al.* (2000). Hepatocyte-specific mutation establishes retinoid X receptor alpha as a heterodimeric integrator of multiple physiological processes in the liver. Mol Cell Biol *20*, 4436-4444.

Wandzioch, E., and Zaret, K.S. (2009). Dynamic signaling network for the specification of embryonic pancreas and liver progenitors. Science *324*, 1707-1710.

Wang, R.Y., Shen, C.N., Lin, M.H., Tosh, D., and Shih, C. (2005). Hepatocyte-like cells transdifferentiated from a pancreatic origin can support replication of hepatitis B virus. J Virol *79*, 13116-13128.

Wells, J.M., and Melton, D.A. (1999). Vertebrate endoderm development. Annu Rev Cell Dev Biol *15*, 393-410.

Yamashita, Y., Shimada, M., Harimoto, N., Rikimaru, T., Shirabe, K., Tanaka, S., and Sugimachi, K. (2003). Histone deacetylase inhibitor trichostatin A induces cell-cycle arrest/apoptosis and hepatocyte differentiation in human hepatoma cells. Int J Cancer *103*, 572-576.

Yang, L., Yamasaki, K., Shirakata, Y., Dai, X., Tokumaru, S., Yahata, Y., Tohyama, M., Hanakawa, Y., Sayama, K., and Hashimoto, K. (2006). Bone morphogenetic protein-2 modulates Wnt and frizzled expression and enhances the canonical pathway of Wnt signaling in normal keratinocytes. J Dermatol Sci *42*, 111-119.

Yost, C., Torres, M., Miller, J.R., Huang, E., Kimelman, D., and Moon, R.T. (1996). The axis-inducing activity, stability, and subcellular distribution of beta-catenin is regulated in Xenopus embryos by glycogen synthase kinase 3. Genes Dev *10*, 1443-1454.

Yu, W.Y., Slack, J.M., and Tosh, D. (2005). Conversion of columnar to stratified squamous epithelium in the developing mouse oesophagus. Dev Biol *284*, 157-170.

Zajicek, G., Oren, R., and Weinreb, M., Jr. (1985). The streaming liver. Liver *5*, 293-300.

Zakim, D., and Dannenberg, A. (1990). Thermal stability of microsomal glucose-6-phosphatase. J Biol Chem *265*, 201-208.

Zaret, K. (1998). Early liver differentiation: genetic potentiation and multilevel growth control. Curr Opin Genet Dev *8*, 526-531.

Zaret, K. (1999). Developmental competence of the gut endoderm: genetic potentiation by GATA and HNF3/fork head proteins. Dev Biol *209*, 1-10.

Zaret, K.S. (2002). Regulatory phases of early liver development: paradigms of organogenesis. Nat Rev Genet *3*, 499-512.

Zaret, K.S., and Grompe, M. (2008). Generation and regeneration of cells of the liver and pancreas. Science *322*, 1490-1494.

Zeng, G., Awan, F., Otruba, W., Muller, P., Apte, U., Tan, X., Gandhi, C., Demetris, A.J., and Monga, S.P. (2007). Wnt'er in liver: expression of Wnt and frizzled genes in mouse. Hepatology *45*, 195-204.

Zhang, X., Bush, K.T., and Nigam, S.K. (2012). In vitro culture of embryonic kidney rudiments and isolated ureteric buds. Methods Mol Biol *886*, 13-21.

Zhou, J., Montrose-Rafizadeh, C., Janczewski, A.M., Pineyro, M.A., Sollott, S.J., Wang, Y., and Egan, J.M. (1999). Glucagon-like peptide-1 does not mediate amylase release from AR42J cells. J Cell Physiol *181*, 470-478.